The Analysis of Solar - Fuel Cell Hybrid Systems

by

Justin Lonchar

A Thesis Presented in Partial Fulfillment
of the Requirements for the Degree
Master of Science

Approved April 2017 by the
Graduate Supervisory Committee:

Arunachala Mada Kannan, Chair
Keng Hsu
John Robertson

ARIZONA STATE UNIVERSITY

May 2017

ABSTRACT

As the demand for renewable and alternative energy continues to increase with both large industrial companies and average homeowners, there continues to be a challenge of efficient energy storage. Several main alternative energy producers such as wind turbines, hydroelectric dams, and solar photovoltaic arrays have become more commonly used over the past decade for generating energy. One of the most common issues with these alternative energy producers is the intermittent production and supply of energy due to fluctuations in weather conditions, peak loads, and instantaneous power draw. To counteract these issues, storage units such as battery banks and proton exchange membrane fuel cells are introduced to provide electricity for the unmet energy demands. In this study, a solar photovoltaic array and fuel cell hybrid system has been set up to provide the energy needs for an average Arizona residential household. A bench test setup has revealed that a solar photovoltaic array and the fuel cell hybrid system can produce enough energy to power an Arizona household that on average consumes 37.7 kWh/d. Additionally, a Mathworks MATLAB/Simulink model of the hybrid system has been created to simulate specific scenarios which provide insight into the system's reaction to various conditions such as varying solar irradiance and temperature variables and poor weather conditions. Finally, the economic impact of the hybrid system was simulated using HOMER Legacy to analyze the cost effectiveness of a 25-year project.

i

DEDICATION

To my family and friends, thank you so much for your support and guidance over the

years of my education. Without you all in my life, guiding me through the ups and the

downs, I would not be here at this point. Thank you so much, and I will always be forever

grateful.

ACKNOWLEDGMENTS

TABLE OF CONTENTS

iv

LIST OF TABLES

LIST OF FIGURES

LIST OF SYMBOLS

CHAPTER 1

INTRODUCTION

1.1 PEMFC Definition

A fuel cell can be defined as a device that generates electricity or an electric charge through the process of a chemical reaction. The electricity is generated by sending hydrogen molecules through the anode, a positive electrode, side of an electrolyte where an electron is stripped from the hydrogen molecule to power a load. The electron is then returned to bond with the hydrogen ion that is passing through the cathode, negative electrode, of the electrolyte and an oxygen molecule to form water. There is a total of five main types of fuel cells that have been used in various fields of industry; alkali fuel cell (AFC), phosphoric acid fuel cell (PAFC), molten carbonate fuel cell (MCFC), solid oxide (SOFC) and the proton exchange membrane fuel cell (PEMFC). The five types of fuel cells are classified by the type of electrolyte used because each electrolyte requires a slightly different process to generate electricity. The first three types listed above are classified as liquid electrolytes because the electrolyte is comprised of a liquid solution such as potassium hydroxide, magnesium carbonate, and phosphoric acid. The remaining two fuel cell types use a solid electrolyte such as a polymer. Another key feature of the fuel cell system is the operating temperature. The AFC, SPFC, and the PEMFC systems operate at low temperatures between 40 and 80 °C, which makes these systems more suitable for small applications such as providing energy for average homes (El-Sharkh et al. 199). The PAFC operates at medium temperatures between 150 and 200 °C, and the MCFC and the SOFC operate at higher temperatures between 500 and 600 °C. The focus

of this study is on PEMFCs because these fuel cells are more commonly used in both the automotive and home industries. As defined by the Smithsonian Institution,

> PEMFCs work with a polymer electrolyte in the form of a thin, permeable sheet. Efficiency is about 40 to 50 percent, and operating temperature is about 80 degrees Celsius. Generally, cell outputs range from 50 to 250 kW. The solid, flexible electrolyte will not leak or crack, and these cells operate at low enough temperature to make them suitable for homes and cars. (1)

1.2 PEMFC History

When reviewing the history of the fuel cell, the first working prototype of the fuel cell stack was made in the early 19th century. However, there is some controversy as to who discovered or built the first fuel cell. Per the United States Department of Energy (DOE), a German chemist, Friedrich Schonbein, was the first person to conduct and publish his scientific findings on the development of the fuel cell (Andujar and Segura 2310). But in most other scientific organizations, the scientist Sir William Robert Grove first discovered the inner workings of the hydrogen fuel cell, but Grove did not publish his work until after Schonbein. These two men during the 19th century were both scientific rivals, which led to two separate and competitive avenues of research on the fuel cell topic. In either case, Grove could provide full evidence in 1838 that, "immersing two platinum electrodes on one end in a solution of sulphuric acid and the other two ends separately sealed in containers of oxygen and hydrogen, a constant current was found to be flowing between the electrodes" (Andujar and Segura 2310). After Grove and Schonbein had made the first discoveries of fuel cells, the next major technological advancement came in 1921 as the first MCFC and SOFC were built by Emil Baur and

William Jacques. Jacques and Baur were able to produce a fuel cell of 1.5 kW with a stack of 100 tubular units, which as a result was the first high power fuel cell system (Andujar and Segura 2311). However, the extensive use of fuel cell technology was not considered until 1959 with the research conducted by Francis Bacon. Bacon was able to develop the first fully operational fuel cell with his research covering the PEMFC and AFC systems. After Bacon had completed his experiments proving the usefulness of the fuel cell technology, the National Aeronautics and Space Administration (NASA) adopted both the PEMFC and AFC technologies to provide the onboard spacecraft energy needs for the Gemini and Apollo manned space programs (Sharaf and Orphan 812). The fuel cell devices were used to serve two purposes where the first purpose was to provide energy to the cabin electronics, and the second purpose was to provide drinking water for the astronauts. "The NASA fuel cells were customized, non-commercial, experienced several malfunctions and used pure oxygen and hydrogen as an oxidant and fuel" (Sharaf and Orphan 813). NASA would continue to use the experimental fuel cells for the next few decades even with some of the malfunctions that were experienced, which caused research and development on fuel cell technology to expand tremendously. In a completely different industry, fuel cells were first introduced into the transportation industry by General Motors (GM) in 1966, but the first passenger fuel cell vehicle that was developed by GM did not enter the market (O'Malley et al. 419). For the next several decades, the transportation industry kept fuel cell technology in the research and development sector.

In recent history, the fuel cell has been used in several applications such as the transportation, stationary, portable, and micro power sectors. In the transportation field,

the fuel cell is to this day primarily experimental as the typical gasoline and diesel engines are preferred over the expensive fuel cell technology. However, in 2007 the car manufacturing company, Honda, produced the first fuel cell powered vehicle, called the FCX Clarity, that was released to the public consumer. Since then, other transportation vehicles have been equipped with a fuel cell system such as city buses, specialty vehicles, forklifts, and motorcycles. The primary draw for switching to the fuel cell systems over the traditional gasoline engines is the lack of toxic emissions and the higher efficiency ratings (Spakovsky and Olsommer 1249). In traditional internal combustion engines (ICE) and electric power plants, the common byproduct of generating energy through these technologies is the harmful emission of carbon dioxide (CO_2). In fact, the most advanced fossil-fired system still produces around 900 g CO_2-eg./kWh which is significant when compared to a fuel cell that produces near zero emissions (Viebahn et al. 4420). With the fuel cell system, the only byproduct is water. The efficiency of the PEMFC is also more reliable than the traditional ICE engine as the fuel cell's efficiency is on average 50%, but the ICE engine is only 25-30% efficient (U.S. Department of Energy, "Fuel Cell Technologies"). Efficiency ratings in both cases are established primarily due to the loss of energy through heat.

1.3 PEMFC Market

The market for PEMFC changes from year to year. The two main applications that the PEMFC is found in is the transportation and home industries, but the primary application is transportation. The PEMFC is relatively compact and lightweight when compared to other fuel cells, and has a fast start up process which makes the system ideal for the transportation industry. Another key factor that makes the PEMFC more

4

marketable is the cost of maintenance, which is considerably cheaper due to no moving parts in the system. Common uses of the PEMFC in distributed generation or stationary applications can be found in peak shaving, combined heat and power, grid support, standby power, and remote/standalone systems ("Fuel Cell Handbook" 1-21). However, factors such as durability, storage, transport, and cost are still the major barriers to fuel cell commercialization (Andrews and Shabani 1186, Ho et al. 67). This is due to both the lifecycle of the fuel cell and the actual material of the catalyst, which in most cases for the PEMFC is platinum (Lucia 165).

Fuel cells in today's transportation market can be seen in several pre-production vehicles such as the GM Hydrogen 1, Ford Demo IIA, Daimler Chrysler NeCar4a, the Honda FCX-V3, Toyota FCHV, and the Nissan XTERRA FCV (Wang et al. 982). However, there are several factors that are preventing mass production of the fuel cell powered vehicles, and these factors include the cost of the fuel cell, refueling hydrogen stations, and fuel cell durability. The overall fuel cell system is comparatively more expensive than the traditional ICE as the fuel cell is about 61 $/kW and the ICE is 25 $/kW (Wang et al. 982). These expenses are upfront costs to the consumer which has in the past changed the perspective on buying a fuel cell powered vehicle. The upfront costs of fuel cell powered vehicles when compared to traditional ICE vehicles may be more expensive, but the operational costs over the vehicle's lifetime are relatively minimal compared to the ICE due to the lack of moving parts. The ICE has many mechanical moving parts that break down over time and require service, whereas the fuel cell operates by a chemical reaction and no mechanical parts. Another challenge to overcome is the hydrogen fuel source as the infrastructure for hydrogen refueling stations has not

been established yet. However, there is an effort underway to establish a hydrogen

fueling network where 364 new hydrogen stations will be constructed starting in 2018

across the United States and Canada by Nikola (Nikola, "Hydrogen Stations"). Nikola's

main objective is to promote the commercialization of fuel cell vehicles, and the

company will lead the way by introducing a new fleet of hydrogen-fueled semi trucks

with new hydrogen stations to keep the fleet moving. If the Nikola Company can succeed

in building a hydrogen station infrastructure in the United States and Canada, the reality

of fuel cell powered vehicles entering the market is optimistic as the cost of the

technology should decrease. The last major hurdle that the fuel cell technology must

overcome to become more marketable is the durability of the fuel cell stack. Fuel cell

stacks experience degradation over time primarily due to the repeated cycles of the

chemical reaction that occurs where contaminants can build up. There are many factors

that can lead to degradation in a PEMFC such as lack of hydration, too much hydration or

flooding of the membrane, and corrosion, but eventually all PEMFCs experience

degradation (Stumper and Stone 470). The goal or target as defined by the DOE is to

reach 5000 hours of operational use from PEMFCs in transportation before degradation

begins, which at that point will make the fuel cell more competitive to the ICE in

transportation (Schmittinger and Vahidi 2). Currently, the average operating hours before

signs of degradation is about 1500 hours. If the unit cost, hydrogen refueling stations, and

durability is improved in the transportation industry, the fuel cell will become more

competitive with regards to the traditional ICE vehicle.

Current stationary applications of fuel cell systems have been developed for

primarily water heaters, emergency backup systems, and small-scale power generation.

Within the past few years, several PEM fuel cells have been developed for residential applications of 3-7 kW, building electricity and hot water applications of 50 kW, and the largest power generation application manufactured by Ballard Power Systems of 250 kW (Kirubakaran et al. 2432). However, fuel cells in the stationary application industry are experiencing the same issues or hurdles as in the transportation industry for commercialization. As described by the DOE, the challenge with stationary fuel cells is both cost and operational durability and predicts that fuel cells will become more marketable if a 40,000 hour of operation rating or a life expectancy of five years is achieved. The PEMFC has been demonstrated to reach 30,000 hours, but the average lifetime for stationary applications is 20,000 hours (Simbolotti 3). For there to be an increase in commercialization of the fuel cell, cost of the stack components and increased operating hours must be achieved to compete with the grid energy in the stationary application industry.

1.4 Hybrid Systems

Alternative energy systems over the past few decades have started to experience a boom as the market for these clean energy systems are expanding. More than 80% of the world's energy is generated from fossil fuels. However, industries have started to use alternative energy systems more as the supply of fossil fuels decrease (Kajikawa et al. 771). With each new technological advance in solar, wind, etc., the method of creating energy has become more reliable and efficient, however, alternative energy systems do have some drawbacks that still need to be resolved. One of those main problems is the variations in production of power in respect to the hour of the day, the period of the year, and the various weather conditions imposed (Belmonte et al. 21428). For example, a

wind turbine can only produce a limited amount of power during a windy day. What happens to the generation of power when there is no wind? Similarly, a solar PV array is very effective at generating energy during a sunny day, but what happens to the generation of energy if the skies become cloudy or if the sun has set for the day? The answer to maintaining a consistent energy flow even when the production of power has decreased below the peak power demand is a hybrid system. Hybrid alternative energy systems can be defined as a main power producer such as wind, solar, or hydroelectric combined with an energy storage unit which could be a battery bank or combustible gas such as hydrogen and methane. For this case study, the hybrid system selected for analysis is the solar PV array and hydrogen PEMFC system. The solar PV array was selected for analysis because this energy is used extensively in the residential industry due to the high-energy potential (Cooper and Sovacool 628). An example of how an energy storage system could be used to support the alternative energy system is shown in *Figure 1*. The solar power output is greater during the middle of the day, but not all the power generated is consumed by the load. The home's electric demand or the peak load demand occurs after the peak period of solar PV power generation, which means the solar PV array alone will not supply enough energy for the load. Therefore, the extra power generated during peak power generation by the solar PV array could be stored for later use when the alternative energy system is unable to supply enough energy for the load.
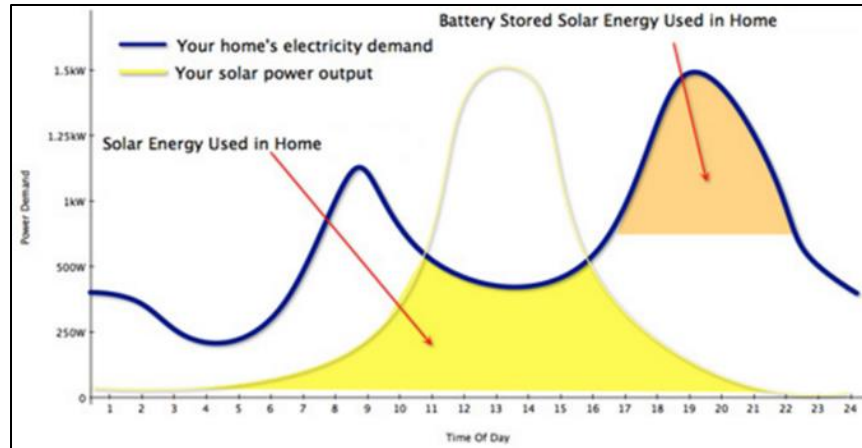
Figure 1: Solar PV Array Power Output vs. Load (FNQ, "Hybrid Systems").

By introducing hybrid systems that incorporate a storage system, many helpful functions are added to the renewable energy systems. Examples of these benefits are meeting a peak electric load at any given time, time varying energy management, management of distributed or standby power generation, or even supporting the use of smart grids (Belmonte et al. 21433). The problem with electricity is storage, and the most effective method of storing electricity is to convert that energy into another form using a chemical energy. The battery and hydrogen gas are the more common forms of chemical energy, but there are advantages and disadvantages to both. The battery storage system is used for short term storage for various reasons such as the low energy density of 0.5 Wh/kg and severe operating conditions of repeated overcharging, discharging, and insufficient charging (Yilanci et al. 232). The battery storage is susceptible to harsh operating conditions for little energy yield, therefore, the system requires high maintenance to keep the system operating. The typical operating range of the battery storage system is five to ten years depending on both the battery chemistry and the operating conditions. The hydrogen storage method allows for long term storage as the hydrogen gas does not degrade rapidly over time as does the stored chemical energy in

9

batteries. Because hydrogen can be stored for longer periods of time and the chemical reaction for producing energy is controlled, the fuel cell technology is more efficient than the battery storage system.

1.5 Research Objectives

When thinking about the typical alternative energy provider for small residential homes, the solar PV system is the alternative energy system of choice, with occasionally the help from either the grid or battery storage system. After reviewing recent literature on the solar/fuel cell hybrid systems, the insight was made that other countries from different areas of the world are performing feasibility tests on the hydrogen storage system. Based on the countries research, the solar/fuel cell system is a feasible system to use in different applications. However, there has been little research conducted in the United States when compared to these other countries to determine if the solar/fuel cell system can be used to provide energy for residential homes. In this study, the solar PV array in combination with a PEMFC system is evaluated for the effectiveness of providing the energy needs for an average Arizona homeowner without the use of grid energy. Therefore, the hypothesis tested was to determine if the solar/fuel cell system is feasible to use in the Arizona environment to provide energy for residential use. The Solar-H2 Cycle (SH2C) project is the hybrid system that tested the hypothesis where a solar PV array provides the energy needed for an Arizona home during the day and a PEM fuel cell system provides energy at night or during hours the PV array cannot meet the energy demand. The SH2C project is a three-year project sponsored by the Salt River Project (SRP) where the first year provides insight into the system requirements and constraints, modeling and simulation, and an economic impact analysis report.

The system requirements and constraints objective determined what components were needed for building a functional prototype of the SH2C system in Arizona. Components that were needed on the fuel cell side of the system include a PEMFC, electrolyzer, DC/DC converter, metal hydride (MH) storage tank or hydrogen gas cylinder, circulator, and a hydrogen sensor, which was used for monitoring hydrogen leaks. In the first year or phase one of the project, building a prototype system with the fuel cell components was completed by using equipment in the lab that had already been acquired such as the PEMFC, electrolyzer, DC/DC converter, and the circulator. However, the MH storage tank was purchased during the first phase of the project, and both the hydrogen gas cylinder and the MH storage tank were used for testing. The two hydrogen storage tanks were analyzed to determine which storage method would be more efficient for the proposed SH2C system. The basic fuel cell system tests were conducted to provide insight into two areas of research. The first objective determined how various components within the fuel cell system interacted with each other, which ties into the second objective. The second objective was to analyze the bench test data and decide where plausible areas of the system needed to be upgraded. For example, if the electrolyzer is unable to fill the MH storage tank during the daylight hours of operation from the solar PV array, then the electrolyzer would need to be upgraded to fulfill this requirement. Performing the basic tests through the bench test setup only provided information on general sizes of the equipment needed for the SH2C system to work. Basic functionality tests and analysis provided insight as to the reaction the system has in the Arizona environment. Further testing was conducted through modeling and

11

simulation where the data collected from the bench tests helped direct the model's flow from one component to the next.

Modeling and simulation of the SH2C system was the second main research objective, and the simulations were completed by using the Mathworks MATLAB and Simulink simulation programs. The models provided an accurate prediction and assessment of the scalability of the SH2C system, and the simulations were used to predict several potential system reactions to different scenarios such as a lack of power generated by the PV array for a period of time due to weather conditions. The model is separated into three main systems; the solar PV array, the fuel cell system, and the load, which in the case of this study is the average hourly energy load from an Arizona home of 37.7 kilo-watt hour per day (kWh/d). The solar PV array operates under a set of input parameters based on several conditions such as:

- Ambient Temperature (monthly Arizona averages)

- Dust Composition

- Weather Conditions

- Module Power Rating

- Module Efficiency

The power output of this system is used in both the load system and the fuel cell system. The energy generated from the solar PV array supplies energy to the fuel cell system, more specifically the electrolyzer for generating hydrogen and the circulator for temperature control, and to the energy demand from the house during the daylight hours. The second part or subsystem of the model is the fuel cell system. The fuel cell system accommodates the MH storage tank, the circulator, and the PEMFC. The circulator is a

12

variable that changes only during the operational state of the PEMFC whereas the

PEMFC and the MH tank have fluctuating input and output variables. The fluctuating

variables include the following:

- Operating Hydrogen Pressure

- PEMFC Stack Temperature

- PEMFC Voltage and Current

- Ambient Temperature

- Hydrogen Flow Rate

The third subsystem of the model is the load. The load is a constant variable or is a

variable that does not change over a period of time. This method of using a constant

variable at first was done to verify that both the solar PV array and PEMFC subsystems

work and work together based on the amount of solar radiation available. Once the

overall model worked and had been validated, a fluctuating load and weather pattern

based on the Arizona residential averages was applied to provide more accurate analysis

of the system's reaction to peak loads, system energy generation, transition from day to

nighttime, instantaneous power changes, and energy storage capacity.

An economic analysis of the SH2C system was the third and final main objective,

and the analysis was completed by using the HOMER Legacy program. HOMER is an

economic and energy production simulation tool that enables users to model a desired

system such as a grid/alternative energy hybrid system, and determine the behavior of the

project over a simulated time frame. There are three core steps that are used in the

HOMER program, which is simulation, optimization, and sensitivity analysis. The model

starts with the simulation where HOMER simulates a viable system for all possible

combinations of the equipment that is to be considered. The simulation may include

several different loads and power sources such as generators, batteries, wind power, solar

power, biomass, and the grid power. After simulating the proposed system model,

optimization occurs where HOMER examines all possible combinations of the system

types, and if desired by the user, sorting through the simulated systems by the

optimization variable such as lowest net present cost or highest energy production per

year. By sorting through all the plausible system combinations using the optimization

variable of choice, an ideal system solution was presented based on the desired

constraints of the project. Sensitivity analysis gives insight into areas of the system that

could otherwise be improved. The analysis provides answers to questions within the

system. For example, if a component's base unit cost can be reduced by a factor of 25%

to 75%, will the equipment be used more within the system? For the SH2C project,

HOMER provided insight into the economic impact and energy production patterns over

a period of 25 years that represents the Arizona environment and resident load demand.

CHAPTER 2

LITERATURE REVIEW

2.1 Hybrid On/Off Grid System Examples

With the decreasing supply of fossil fuels and the increasingly negative environmental impact of using coal to produce power, the energy market has started to turn to alternative energy systems. In some cases where the traditional grid infrastructure has already been established in the home, small residential home owners in various places around the world have decided to add the solar/fuel cell system to reduce dependency on the grid energy. For example, what started out to be a field test study in Sapporo, Japan, residents of the installed solar/fuel cell system saw a reduction in energy consumption from the grid of about 66% annually (Hamada et al. 3684). By further reducing the need of the grid energy, off grid solutions using a solar/fuel cell system are becoming more common. On the other end of the extreme where situations are direr, communities are switching to alternative energy systems because the traditional fossil fuel powered plants are generating less electricity due to the depleting supply of the fossil fuel. Egypt is facing this scenario and has turned to solar/hydrogen systems to compensate for the losses of energy production (Abdallah et al. 505). The common areas where off-grid applications are seen in is telecommunication sites, water pumping installation, farms, and small communities where grid connection is expensive or infeasible (Gray et al. 654). In the United States, there has been an increase in combining the use of grid energy and alternative energy systems to meet the demands of both residential and industrial applications. In Arizona, the solar PV array coupled with the grid infrastructure for residential use has become more popular over the past decade, but there have been few

studies conducted to determine why residents are switching to a solar/grid system versus a solar/fuel cell system. However, in other regions around the world who have similar residential communities and environments as Arizona have switched to either a grid/renewable energy system or a renewable energy/storage system. The studies reviewed would provide insight as to why other countries are switching to a grid/renewable energy system, and how these systems perform within the given environment. The analysis of these studies helped guide the decision as to the feasibility of implementing these systems in Arizona. The literature also provided insight into the alternative energy system's challenges such as dust covered PV modules producing less power than clean modules. Reviewing the challenges of these systems as well provided a better understanding of what challenges may be expected and planned for in the SH2C system.

A prime example of feasible off grid applications can be seen in Australia where about 25% of the population live in remote areas, which results in expensive measures to extend the grid to these locations. In fact, Northern Australia has more than 100 communities that are not connected to the grid, and the energy demand on average is hundreds of kW (Gray et al. 655). These communities receive energy from a Solar/Metal Hydride/Fuel Cell system where the solar PV array provides energy for the homes during the day, and the fuel cell system provides the energy needed during the night through the stored energy that was produced through electrolysis. A solar/hydrogen hybrid system has become the most ideal technology in these conditions, where the grid energy is hard to get to, because of the simple operation, high efficiency, and ability to provide power quickly from a standby condition (Galli and Stefanoni 453). Additionally, a wind turbine

16

may be added to the solar/fuel cell system depending on the region. In Canada, a 10 kW wind turbine coupled with a 1 kW solar PV array and 5 kW fuel cell system was used to meet the energy needs of a 12 kW load (Agbossou et al. 168). By introducing the wind turbine, the size of the PV array was reduced, and another alternative energy source was added. Using solar radiation and the wind to provide energy, the system was better equipped to handle various weather conditions.

In some cases, a battery pack or storage system may also be included in the Solar PV array and fuel cell system. The purpose of the battery storage system is to provide energy during instantaneous power draws. The PEMFC requires more time to provide rated power to the energy load, and the power output of the fuel cell should only be increased slowly after initial startup procedures (Rekioua et al. 1605). However, the battery storage system could discharge the available energy that the system contains in a matter of seconds. An example of a solar/fuel cell/battery system configuration is shown in *Figure 2*, where this system has been constructed and used in Elazig, Turkey. The batteries within the system are primarily used in the startup process of the system to allow the fuel cell to warm up essentially. Once the fuel cell has finished the warm-up cycle, the fuel cell takes over and provides the energy needed in the system. A similar system is used in Morelos Mexico, however, the energy from the battery storage system is used first before the PEMFC is used (Torres et al. 1005).
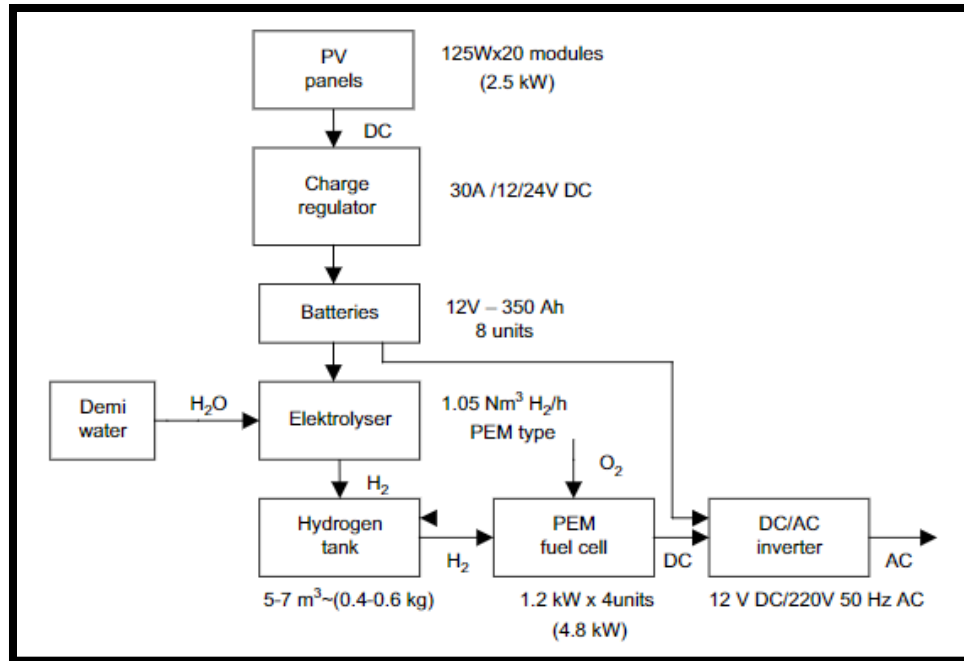
Figure 2: Solar PV/Fuel Cell/Battery System Configuration (Gencoglu and Ural 5246).

In some cases, alternative energy devices have been added to the current grid powered system. An example of adding a fuel cell backup system is seen in several telecommunication sites located throughout Europe. At these telecommunication sites, the grid is used as the primary power source, however, the grid does not always provide constant energy to these sites, which is problematic as the telecommunication sites require an uninterrupted supply of energy. The solution to the random grid outages is a 5 kW PEMFC system for each site that will provide enough energy to continue working for an additional five hours with no grid support. Currently, each site experiences a grid interruption every 48 hours, but the PEMFC systems cover more than 99.6% of the possible grid power failures (Varkaraki et al. 15). In these situations presented, the initial investment cost of the fuel cell backup system is negligible as failure to keep the telecommunication sites operational is very expensive and the cost to establish a more reliable grid source is substantially larger.

18

Telecommunication sites in Arizona experience some of the same issues of connectivity to the grid infrastructure. In some cases, the telecommunication sites in Arizona are in remote areas where the grid infrastructure does not exist and would be expensive to expand to. These sites in Arizona require the use of alternative energy systems to keep the site functional throughout the year. However, with residential applications in Arizona, the grid infrastructure has been thoroughly developed throughout the state, but the population within Arizona is continuing to grow which means the energy demand will increase. To meet the increasing need for energy and to reduce the load stress on the grid infrastructure, Arizona could incorporate alternative energy systems like the other regional communities have.

2.2 Hybrid System Case Study Examples

In Arizona where the climate is a very hot and dry environment, the average homeowner, who is looking to meet the energy needs of their home by using alternative and clean energy, relies on a solar PV array to generate energy during the day. However, the solar PV array does have limitations. The primary limitation of the solar PV array is the time of day and weather conditions for generating energy. Once the sun has set for the day or if the weather conditions are poor such as cloudy skies, the solar PV array stops generating power, which leaves the homeowner without a supply of energy. In most cases in Arizona, the homeowner has installed a solar PV system to provide energy during the days with perfect weather conditions and then rely on the grid power to supply energy during nighttime hours or days with poor weather conditions. Traditionally, a solar/grid energy system has dominated the market, but this type of system requires the homeowner to be dependent on the grid. Furthermore, the PV module is the preferred technology to

19

be integrated into the PV array for residential use. Other solar devices such as the solar dish or tower solar power technology are not used in a residential environment due to the required space claim for the mirror field and the low possibility for hybridization with other systems (Baharoon et al. 1017).

In the case study conducted in Turin, Italy, the comparison between a solar PV array and battery system and a solar PV array and fuel cell system presented a unique perspective on the effectiveness and scalability of the two alternative energy production systems (Belmonte et al. 21430). The two systems were set up to accomplish the same goal of providing enough power to a 3 kW load or small house in Turin. However, the only differences in the two systems were the actual components or hardware needed to generate power. The solar PV array with the battery storage system was constructed of twenty 250 W modules, and there was a total of twelve 12 V 75 Ah Li-ion batteries arranged in series to provide 48 V at 75 Ah. The solar PV array with the fuel cell system was constructed of thirty-two 250 W modules, and the PEM fuel cell used was a 3 kW system with a 5 kW Alkaline Electrolyzer and twelve 50 L hydrogen MH tanks. The results of the experiment showed a close comparison between the two systems. Both systems could provide the appropriate energy needed by the house, however, the solar/fuel cell system was much more expensive to build than the solar/battery system. The total price of the solar/battery system came out to about €24,000 whereas the solar/fuel cell system was about €50,000, which is about $25,500 and $53,000 respectively.

Similarly, a study was conducted in Valle dell'Eugio-Locana, Italy, to analyze the efficiency in three methods of power generation; the solar PV array, micro hydro, and

wind turbine coupled with a PEMFC in each scenario. The experiment was conducted to provide energy for a 1.5 kW load, which was a small house located in a remote area in the mountains. In all three cases, the three power generation methods perform adequately to keep the house powered throughout the simulated year.

There were pros and cons to all three methods. However, the method that produced a steady stream of power to meet the energy needs of the house was the solar PV array and fuel cell system. One of the important lessons learned in this study was the change in hydrogen production during different months of the year. During the winter months, the average generation of hydrogen was 25 m³/month whereas, during the summer months, the production was 225 m³/month (Santarelli et al. 1583). The increase in hydrogen production is due to the exposure time of the solar irradiation. The daylight hours are longer during the summer months than during the winter months thus more solar irradiance is captured by the solar PV array. This outcome should also be expected in the SH2C system in Arizona. However, due to the excessive heat of the Arizona environment, an analysis comparing the effects of hydrogen generation with respect to the changing levels of solar radiance and temperature throughout a year was considered. Determining the effects of hydrogen generation rates also provided insight into the appropriate sizing of the fuel cell components especially for worse case scenarios such as high thermal resistance and peak load conditions.

In the southern part of Australia, a solar/fuel cell hybrid system is used to power residential homes with less than a 3 kW load (Shabani 5442). The objective of this study is to determine how to improve the overall efficiency of the system as the current efficiency is set between 20 and 40%. One of the unique aspects of this hybrid system

21

setup is the use of the water heater within the home. The water heater currently is powered by either the 500 W fuel cell system or the PV array depending on the hour of the day. The hypothesis tested in this scenario was to determine if recapturing the heat produced by the fuel cell can be redirected towards heating the water heater to increase the overall efficiency of the power generation system. Using the heat produced from the fuel cell would help reduce the amount of energy required for generation by the fuel cell, which results in less hydrogen consumption. In *Figure 3*, the four pie charts show the predicted correlation between an increase in power generation and the results of increased heat generation by the fuel cell. If a 500 W power generation is required to provide power for the load within the house, 58% of the power generated will be wasted through heat which as a result the fuel cell will need to generate more power than what is requested to meet the demand of the load.
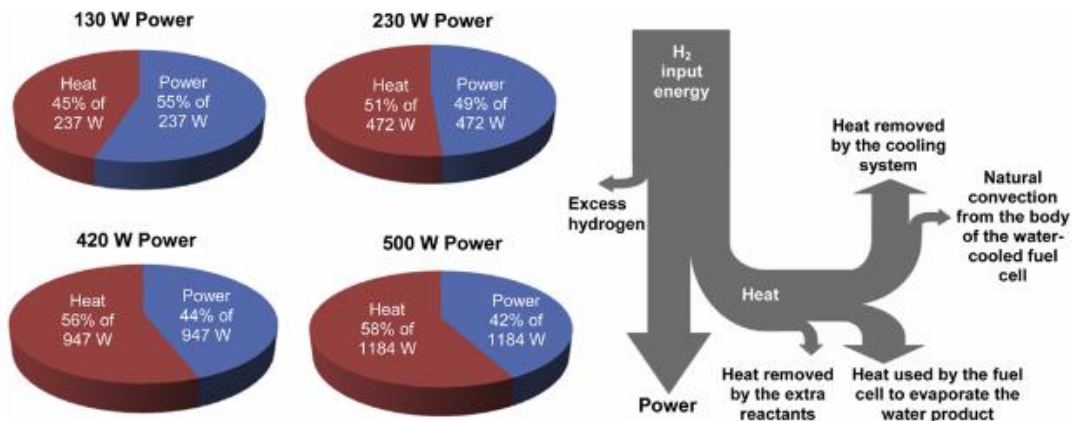

Figure 3: Theoretical Analysis of Power/Heat Generation (Shabani 5443).

The Sankey diagram, on the right side of the figure, represents the flow of the hydrogen energy within the fuel cell and represents how there is wasted energy within the system. The researchers at RMIT University in Melbourne, Australia have developed an experimental setup where the heat of the fuel cell is recaptured and used for heating the

22

water heater. After several tests have been conducted, on average the overall efficiency of the system has increased by 30-50%, which is a 70% efficiency rating for the entire system (Shabani 5442). From this analysis, the conclusion is made that heating and cooling sources such as water heaters require large amounts of energy. Adding a larger load to the fuel cell system only increases the amount of energy that is wasted through heat, which in return reduces the overall efficiency of the system. However, recapturing the energy wasted through heat can be utilized in the operation of the heating/cooling devices, thus increasing the overall efficiency of the system. This analysis is an added advantage to the SH2C system in the Arizona environment. The anticipated loss of energy for the SH2C system is through heat. Considering the system must operate within a high temperature environment of 30 to 45 °C for an extended duration of time throughout the year compared to the rest of the United States, more energy will be spent due to the added thermal resistance within the system, and the energy wasted through heat exponentially grows as the load increases. Recapturing the energy lost through heat would prove beneficial within the Arizona system.

2.3 PEMFC Transportation Examples

Other applications of fuel cell technology besides the stationary application is transportation using commercial and personal application. One of the leading uses of fuel cell technology in the transportation industry is seen in forklifts. The forklift is a heavy transportation equipment used primarily in storage facilities. The purpose of the forklift is primarily to lift heavy objects up or down to store supplies that would normally be too heavy for an average person to lift. Traditionally, battery powered forklifts have dominated the market because of the zero-emission factor which than allows forklifts to

be used indoors (Elgowainy et al. 3557). However, battery powered forklifts do have limitations such as battery charging time, heat produced from charging, and service length before next charge. Fuel cells have the advantage over the battery powered forklifts as the fuel cells do not require long periods for charging, and can be used almost constantly if a steady supply of hydrogen is available.

In today's market, there are three types of forklifts that can be purchased for use that does not consume fossil fuels, which is the fuel cell, fast charging battery, and the conventionally charged battery powered forklifts (Renquist et al. 12054). A recent study was conducted at the Colorado State University to analyze the economic impact of the three main alternative energy types of forklifts. The analysis was conducted for a company that was seeking to invest in a new fleet of fuel cell powered forklifts. However, the company wanted to determine if the investment in the fuel cell powered forklifts would be more beneficial and economically viable than the battery storage system. The research proceeded by determining the modeling parameters that would be associated with the three main types of forklifts. Parameters such as unit cost, replacement cost, durability, costs associated with storage, maintenance, and refueling/charging time were considered to determine the best-suited forklift for the company's needs. The determination was made that the fuel cell powered forklift did, in fact, have a higher durability than the battery-powered forklift, but the cost of maintenance, the cost of hydrogen storage, and cost of storage installation was far greater by several thousand dollars than the battery-powered forklifts. Thus, the research team proposed that the fast-charged battery powered system was the best solution for the company's current investment. However, the fuel cell powered forklift was recommended

for use if the company's battery storage space or the workload required was increased. Similarly, the alternative energy system for the Arizona residential home will need to be compact so that less space is claimed by the system components. The fuel cell system components when compared to a battery storage system can be more compact which would prove more beneficial for the residential home application as well. A representation of both the net present costs of the three different types of forklifts when compared to the forklift load is shown in *Figure 4*.
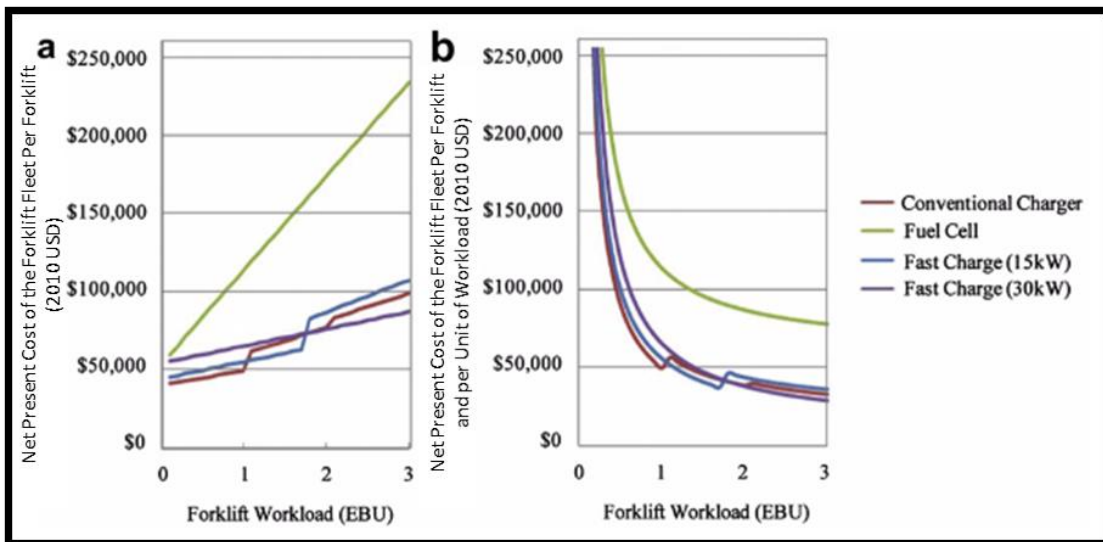
Figure 4: Cost Analysis of the Different Types of Forklifts (Renquist et al. 12058).

At Argonne National Laboratories (ANL), the ICE, battery storage, and fuel cell powered forklifts were compared to analyze the effectiveness of each power generation device. The ICE powered forklifts were used more for loads of 6,000 lbs. or greater, but the fuel cell and the battery powered forklifts are more commonly used for lifting maximum loads between 3,000 and 6000 lbs. (Elgowainy et al. 3558). The ICE engine can lift the heavier loads than that of the battery and fuel cell powered forklifts, however, the greenhouse gasses produced from the ICE is substantial as represented in *Figure 5*.
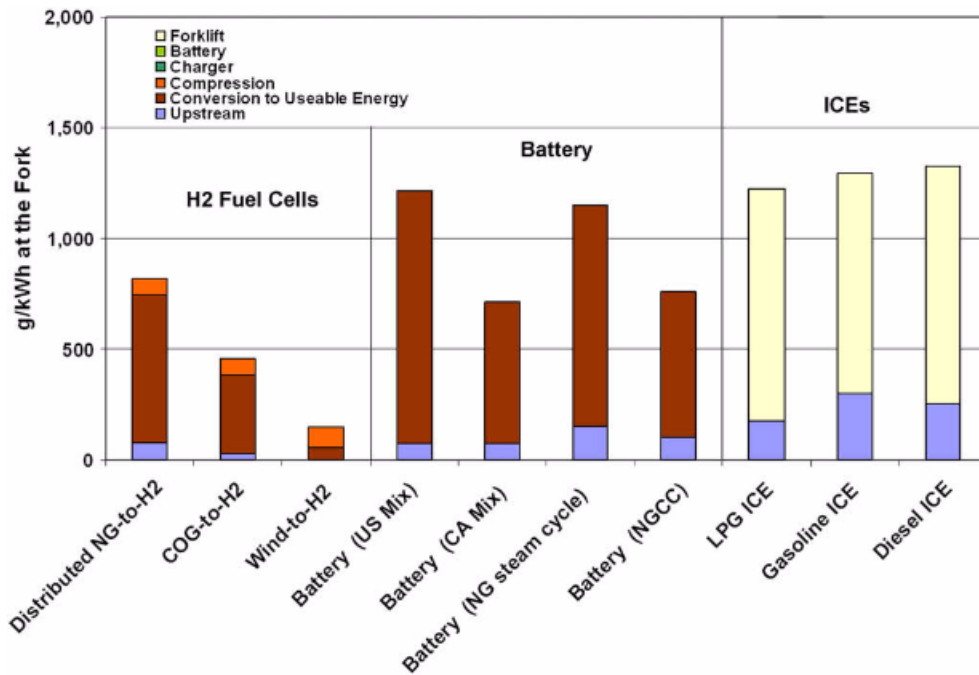
Figure 5: Green House Gases Emitted (Elgowainy et al. 3564).

As shown in *Figure 5*, the fuel cell system produces the least amount of greenhouse gasses, and in fact, most of the emissions come from the power generator used to store hydrogen such as natural gas (NG) and coke oven gas (COG). Some companies have started moving towards fuel cell powered forklifts for these reasons. For example, a company in South Africa called Impala Platinum Refineries, has managed to use the energy wasted through the heat of the manufacturing plant to generate hydrogen (Tolj et al. 13841). The plant has introduced a hydrogen refilling station and has upgraded all the current forklifts to a fuel cell generator. The company has managed to conserve energy and reduce emissions significantly.

2.4 Hybrid System Desert Application Examples

Since the Solar-H2 Cycle project will be used in a desert environment, the effects of desert climate and terrain should be researched to monitor the potential threats to the

26

proposed system. The desert climate is a very harsh environment for power producers. The factors that could affect power production are high ambient temperature, solar radiation, and even dust. For this study and presented research, the desert environmental effects on the solar PV array were researched and analyzed based on the assumption was made that the fuel cell and all the power electronics would be housed in a climate-controlled room of the Arizona household, leaving only the PV modules exposed to the elements. Fuel cell contamination was briefly reviewed in the case that a climate controlled room was not accessible for the housing of the electronics. In general, the main factors that do affect the PEMFC are temperature, pressure, oxygen concentration, and humidity (Mann et al. 174). If the PEMFC system is kept within a cooled, ventilated room of a house, the only true factor that could affect the fuel cell in a desert environment is humidity, but the Arizona climate is accustomed to dry air when compared to much of the world.

Over the past seventy years, extensive research has been conducted to monitor the effects of dust particles on solar PV modules, and research shows there are four main parameters to measure for: current short circuit, power output, reduction in solar intensity, and fill factor (Sarver et al. 700). A current short circuit and power output measurement are not greatly affected by the dust particle unless the module is completely covered in dust and blocking all light. However, the reduction in solar intensity and fill factor are greatly affected by the dust particle. The size of the particle matters as a smaller or fine particle has a greater impact on these two parameters (Sarver et al. 700). To further examine this point, a field test study was conducted in Abu Dhabi where two solar collector fields were examined for a reduction in solar intensity based on the

cleaning cycle of the panels. The region in which the Abu Dhabi collectors are

established experiences a little over one inch of rainfall throughout the year and is

accustomed to dust storms. Due to the regular buildup of dust, the panels are reguarly

cleaned two to three times per week. However, in this case study, field collectors A and F

were left uncleaned for an entire year while the remaining field collectors were regularly

cleaned as prior to the experiment (El-Nashar 105). The results showed that the collector

efficiency dropped for collector A and F while the efficiency of the rest of the field

collectors remained the same as seen in *Figure 6*.
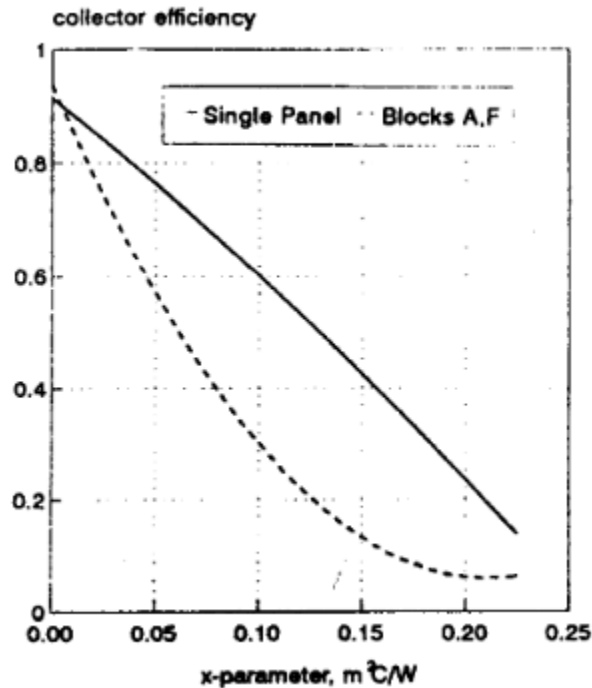
Figure 6: Dusty Panel versus a Clean Panel (El-Nashar 111).

To mitigate the loss of energy production due to dust, a thin film or "preventive coating"

is recommended for preventing both dry and moist dust from sticking to the PV modules.

In addition to the preventive coating applied to the lens of the collectors, an automated

cleaning system that washes the panels when needed is recommended for optimal efficiency in preventing dust from affecting the system.

After analyzing the effect of dust particles on the solar PV modules, the next problem to analyze is the ambient temperature conditions of the desert climate. A recent analysis was conducted on the PV modules performance in desert environments by a team called UREMS in Algeria. This region was chosen for study due to the following characteristics (Bouraiou et al. 1346):

- High ambient temperature in the summer

- High solar irradiance

- Low humidity

- Large number of clear and semi-clear days in the year

- Small number of dust storms

These characteristics can be used to generalize the desert environment for most regions around the world, including the Arizona desert environment. The research team's objectives were to evaluate the performance effects of the ISOFOTON 100 PV module under shading conditions, and the degradation of UDTS 50 PV modules after long-term deployment by comparing the I-V characteristics of the module's manufacturer specifications with the actual I-V characteristics recorded over time. In *Figure 7*, the current (I) versus voltage (V) graph provides insight to the efficiency losses when cells of the module are shaded. The shading effect in this experiment was done using a fine dust spread over one cell at a time. As the results show, the shading effect has a negative impact on the amount of energy produced.
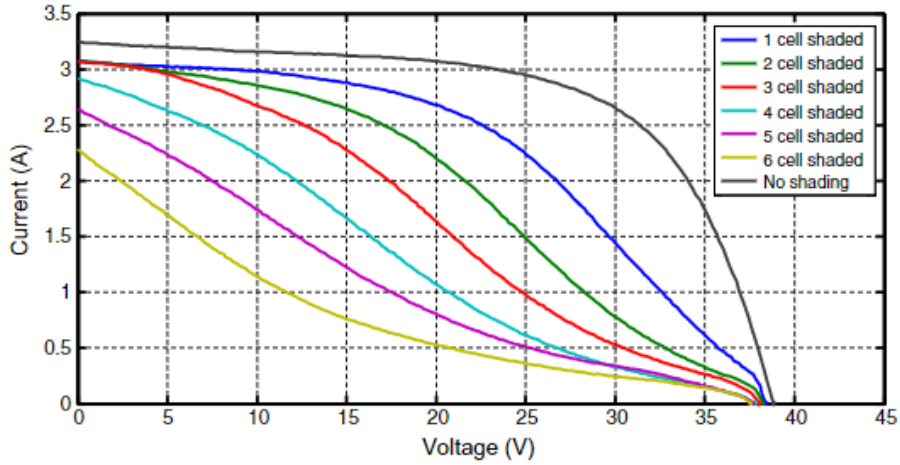
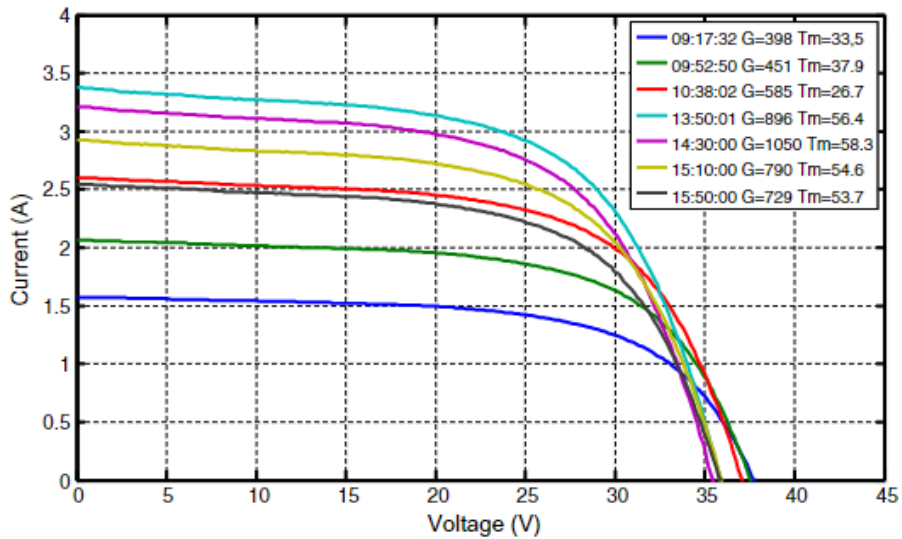*Figure 7: I-V of Modules under Partial Shading (Bouraiou et al. 1352).*

Figure 8: I-V with Solar Irradiation and Temperatures (Bouraiou et al. 1353).

In *Figure 8*, the current versus voltage was measured under different solar irradiation and temperature effects on the PV modules. To determine the efficiency of the PV modules under these conditions, several parameters need to be recorded such as maximum power (Pmax), maximum current (Imax), maximum voltage (Vmax), short circuit current (Isc), open circuit voltage (Voc) and fill factor (FF). To calculate the fill factor, the equation below is used:

$$FF = \frac{Vmax * Imax}{Voc * Isc}$$

To calculate the efficiency of the solar PV module, the following equation is used:

$$\eta = \frac{Pmax}{G * A}$$

The solar irradiation (G) varies and is the deciding factor for the efficiency of the PV module if both the Pmax and the area of the collector (A) remain constant. Under these conditions, the efficiency of the solar panel will decrease as the solar radiation increases.

The effects of fuel cell contamination can be detrimental to the durability of the system. There are three main containments that will cause the fuel cell to enter the degradation process which are fuel cell impurities, air pollutants, and cationic ions. "Contamination affects three major elements of fuel cell performance: Electrode kinetics, conductivity, and mass transfer" (Cheng et al. 739). Contaminates with the residential atmosphere could pose a potential threat to the fuel cell system in regards to durability. The Arizona residential home will contain some amounts of contaminates which would need to be tested for before installing the fuel cell system in a residential setting. To prolong the life of the fuel cell, the system needs to be installed in a cleaner, well ventilated room of the home. Since this system is used in the Arizona environment, dust contaminates poses the largest threat.

2.5 PEMFC System Modeling

When simulating the energy generation of the PEMFC, several variables are to be considered and calculated for. Variables such as number of cells, PEMFC efficiency, consumption of hydrogen, and the output signal conversion and adjustment are to be

included in the models. The following equations are used in determining the variables of

a PEMFC system (Contreras et al. 1379):

$$N_C = \frac{P_{OA}}{D_C V_C A_C}$$

For calculating the number of cells N_C required for a fuel cell stack, the ratio between the

maximum theoretical power P_{OA} and the real output power is taken.

$$\eta = \frac{\Delta G}{\Delta H}$$

To determine the overall efficiency rating η of the PEMFC that is to be used, the ratio

between the useful energy available ΔG and the enthalpy change between the reactants

ΔH is taken.

$$C_{H2} = \frac{E_{EA}}{\eta HHV}$$

To calculate the total consumption of hydrogen that is required to operate any given

system scenario, the ratio between the total annual electrical energy required and the fuel

cell efficiency at the higher heating value (HHV) of hydrogen is taken.

2.6 Economic Analysis Examples

      For analyzing the economic impact of a proposed system, the HOMER Legacy

simulation program provides an accurate prediction of both energy production and

consumption, and net present costs (NPC) of a proposed system configuration. By

simulating the economics of the proposed SH2C system, the analysis was made as to how

much a SH2C system would cost in the Arizona economy, and how the generation of

energy affected the individual costs associated with each subsystem such as the solar PV

array or the fuel cell system. For instance, a case study was conducted to model and

compare two proposed energy production systems that would provide power for the

Bozcaada Island in Turkey (Kalinci et al. 7652). The purpose of the research was to

determine how an alternative energy system could aid in power generation during the

unusual load demand of the island. The average yearly load demands of the island vary

due to the influx of tourists to the island during the summer months. The population of

the island increases from 1500 inhabitants during the winter months to 5000 with an

average energy consumption rate of 5 kWh per day for each residence (Kalinci et al.

7653). Since the change in population is substantial over the summer months, the total

energy consumption increases, which as a result requires the island populace to search for

other reliable means of energy generation. The HOMER model produced evaluates two

separate hybrid systems: a wind turbine system and a wind turbine/PV hybrid system.

The wind turbine system is a standalone system with no other methods of energy

generation added to the system. The wind turbine/PV system contains three methods of

energy generation, which are wind turbines, a PV array, and a fuel cell system with an

electrolyzer and metal hydride storage system. The component configuration of the

proposed hybrid system is represented in *Figure 9*. The wind turbine system has a simple

equipment configuration since both the wind turbines of the system and the primary load

are directly connected to the AC bus.
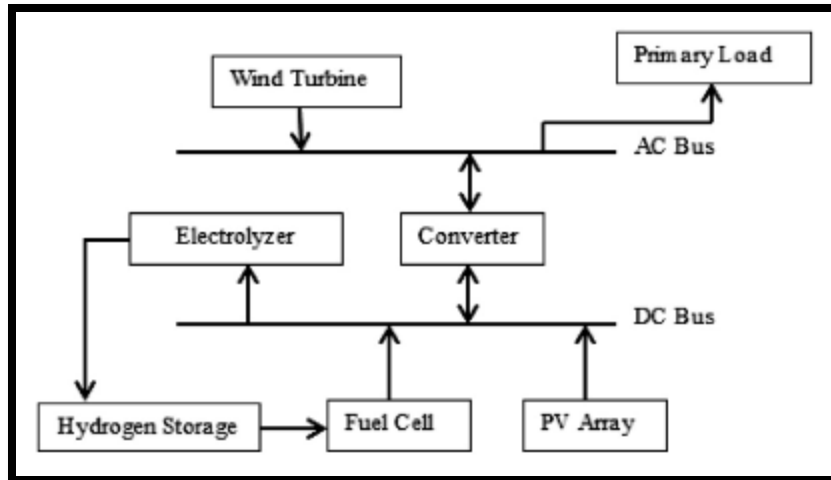
Figure 9: Wind/PV/FC System Schematic (Kalinci et al. 7654).

In both simulated systems, the same load and wind turbine design were applied. In the wind/PV hybrid system, the research team selected solar PV modules, a fuel cell, and the appropriate power electronics that best suit the conditions of the island. After factoring all equipment specifications and costs, the simulations were conducted and compared. The results showed that the wind turbine/PV hybrid system overall had a lower NPC and cost of energy (COE) than the wind turbine system. The projected NPC for a 25-year project of the wind turbine system was approximately $14.6 million with a COE of 1.016 $/kWh. However, the hybrid system's NPC and COE came out to $11.9 million and 0.93 $/kWh respectively (Kalinci et al. 7652). The major advantage of the simulated hybrid system is the use of multiple energy generators. The wind turbine system would only produce power when the wind was present whereas the hybrid system would generate energy if the wind or solar irradiance or both were present. The excess energy that was produced in the hybrid system from either the wind turbines or the solar PV array would be used for powering the electrolyzer to store hydrogen energy for use by the fuel cell.

Another example of an economic analysis study can be seen in the pre-feasibility study conducted for a hybrid energy system using hydrogen for applications in Newfoundland, Canada. The goal of the research project was to determine which hybrid system combination would be most feasible for providing 25 kW/day of energy, which is energy required for powering a home in St. Johns in Newfoundland. A 5 kW diesel generator, 1 kW PV array, 7.5 kW wind turbine, 9,645 kWh battery system, and a 0, 1.5, 3.5, and 5 kW fuel cell system were used for determining the most optimal hybrid system combination. In total, 43,200 system combinations were simulated and compared to determine the optimal system. The wind/battery/diesel system was the optimal and cost-effective system configuration as the COE of the system came out to 0.497 $/kWh. "With a reduction in fuel cell cost of 65%, a wind/diesel/battery/fuel cell system would be feasible" (Khan and Iqbal 853). If the cost of the fuel cell is reduced to 15% of the original cost, the wind/fuel cell system would be the option of choice as the COE would be 0.427 $/kWh (Khan and Iqbal 853). In another system setup with similar conditions only with a diesel generator instead of a wind turbine, the results of the proposed economic system were similar as a reduction in the initial cost of the fuel cell would be needed to compete with the solar/diesel generator system (Zoulias and Lymberopoules 695).

In a similar study conducted in Peninsular Malaysia, about 19% or 14,365 GWh of the electrical energy produced is used for powering residential homes with 100% reliability on grid energy. The purpose of the study was to use HOMER to analyze the potential viability of introducing either a fuel cell/thermal management system or a fuel cell/battery/thermal management system. In scenario A, the fuel cell system coupled with

a thermal management system was used to provide the energy needs of the residential

home which includes domestic water heating, space cooling, and lighting and appliances

(Mahlia and Chan 418). Scenario B uses the same fuel cell and thermal management

system as in scenario A, however, a battery system is also introduced. Because the

electrochemical reactions taking place in the fuel cell are exothermic, the thermal

management system in both scenarios is used to collect wasted energy, and the energy is

then used for operating the water heater. Heat removal is a critical design issue with fuel

cells, which is why researchers recently have been developing methods to re-channel the

heat produced from the fuel cell into energy to be used in thermal applications that

require heat (Cheddie and Munroe 76). The simulation is conducted for a 20-year project

lifetime, and the projected costs of the project are shown in *Figure 10*.
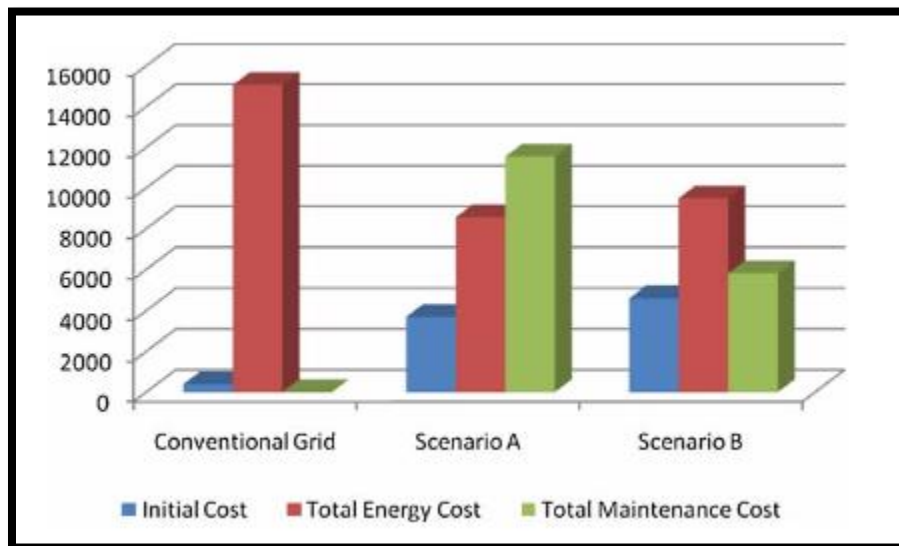
Figure 10: Life Cycle Costs (Mahlia and Chen 425).

The results of the simulation show that scenario B is, in fact, more cost effective

than scenario A. Scenario B has a higher initial investment cost of MYR4100 whereas

scenario A had an investment cost of MYR3700, which is about $920 and $830

respectively. However, the fuel cell throughout the simulated system is used less in scenario B due to the battery storage system (Mahlia and Chan 426). By using the fuel cell less, the equipment does not have to be replaced as often thus scenario B is the cheaper system in the long run. Based on the current costs for the alternative energy production equipment, the grid energy was cheaper to use than the presented two scenarios. Ultimately, the limiting factor for switching to alternative energy systems in this region of the world is the costs associated with the equipment for initial investment and maintenance. When simulating the economic impact of the SH2C system, the grid energy is not considered. For the economic simulation, the analysis is made as to the actual size of the system components, and how the sizes when compared to the costs associated with each of the components affected the operational hours of both the solar PV array and the fuel cell system.

CHAPTER 3

METHODOLOGY

3.1 SH2C Component Selection

When selecting the components that were used during the bench test setup, there were two subsystems that needed to be built, the solar PV array and the fuel cell system. The solar PV array during the first phase of the project was not critical as the PV system would be sourced after determining what the actual size of the fuel cell system would be. Therefore, the fuel cell system took priority for testing. The fuel cell components needed for performing the bench tests were as follows:

- A PEMFC

- Electrolyzer for collecting hydrogen

- DC/DC converter for regulating power fluctuation of the load

- A circulator for temperature control of the MH storage tank

- MH storage tank

- Hydrogen gas cylinder

- Hydrogen Sensor for detecting leaks in the system

- Stainless steel connection lines with valves and regulators

Several of the components were available for use in the fuel cell laboratory before the start of the project. The Nexa 1200 PEMFC, Hogen GC 600 electrolyzer, Nexa 1200 DC/DC converter, and Haake F3 circulator were used in previous experiments by the lab, and for this project's objectives, these components were reused. The Hydrogen gas cylinder was acquired through local means. However, while tests were to be conducted with the gas cylinder, the MH storage tank was sourced and purchased through Pragma

Industries located in France. The MH tank of choice called the MH7000 was purchased

for several reasons: water bath temperature control, 7000 standard liter (sl) capacity of

hydrogen, and the container's physical size as the tank is smaller than the compressed

hydrogen gas cylinder with about the same hydrogen volume content. Another added

device to the fuel cell system was the SBS-H2 hydrogen sensor which was primarily used

for detecting leaks in the system. The sensor is designed to detect volumes of hydrogen

gas within a specific area. At 1% hydrogen concentration within the air, a warning light is

triggered, and at 2% or more hydrogen content, and the alarm is sounded. In *Figure 11*,

the bench test setup the incorporated the tests with the hydrogen gas cylinder and DC/DC

converter is shown. In *Figure 12*, the bench test setup that incorporated the tests with the

MH tank, electrolyzer, and the circulator is shown.

Figure 11: Bench Test Setup with the Hydrogen Gas Cylinder.

Figure 12: Bench Test Setup with the MH7000 tank.

For the PEMFC located in the bottom left corner in *Figure 11*, a Nexa 1200 W fuel cell manufactured by Heliocentris was used for basic testing. The Nexa 1200 is a fully integrated fuel cell system with all the necessary components packaged in one unit including the fuel cell stack, air filtration system, and cooling fan. The fuel cell stack that has been integrated into the Nexa 1200 is the FCgen 1020 stack from Ballard. Each cell within the FCgen stack can produce 43 W, thus the Nexa 1200 stack contains 28 cells to produce 1200 W. An example of how cells are collectively added together to form a fuel cell stack is shown in *Figure 13*. Like a battery system, the cells of the stack are connected in series.
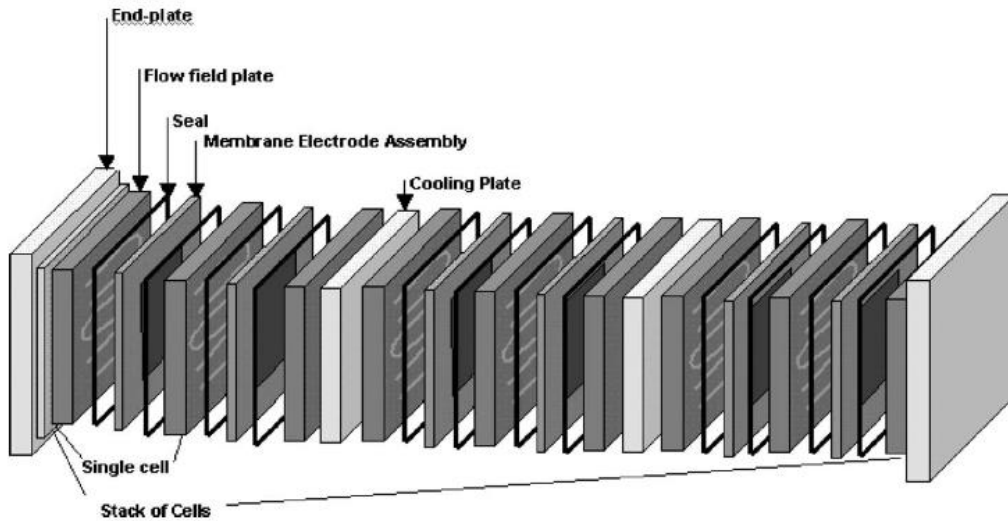
Figure 13: Example of Stack Configuration with Single Cells (Mehta and Cooper 33).

The cooling fan has multiple purposes as the fan is used for cooling the stack, providing

oxygen through the air for the reaction process, and evaporating the only byproduct,

water, that is produced. The stack service life for this unit is guaranteed for 15,000 hours

or two years if used under nominal operating conditions. The following represents the

chemical reactions occurring in the stack of the PEMFC (Mekhilef et al. 984):

The Anode Reaction:

$$2H_2(g) \rightarrow 2H^+ + 2e^-$$

The Cathode Reaction:

$$\frac{1}{2}O_2(g) + 2H^+ + 2e^- \rightarrow 2H_2O(l)$$

Overall Reaction:

$$\frac{1}{2}O_2(g) + H_2(g) \rightarrow 2H_2O(l)$$
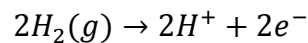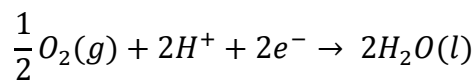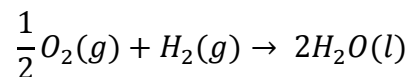
The overall reaction rate occurs with a hydrogen consumption rate of 15 sl/min, and the

net efficiency of the fuel cell is about 50%.

41

The Hogen GC 600 electrolyzer, located on the right side of *Figure 11*, was used during the first phase of the project for testing. This electrolyzer uses a PEM solid electrolyte to separate distilled water into pure oxygen and pure hydrogen (6.0 or 99.9999% purity). The oxygen is vented to atmosphere, and the hydrogen is directed to an output port on the back of the unit. The flow rate of the hydrogen gas varies as the user selects the output pressure between 45 and 200 PSI. The maximum hydrogen output rate is 600 cc/min. The maximum amount hydrogen that can be produced in an hour is calculated by the below equation (Air Products, "Hydrogen Weight").

$$1cc = 0.001l \rightarrow \frac{600cc}{min} * \frac{0.001l}{1cc} * \frac{60min}{hour} = \frac{36l}{hour}$$

$$1m^3 = 1000l \rightarrow \frac{36l}{hour} * \frac{m^3}{1000l} = \frac{0.036m^3}{hour}$$

$$\frac{0.036m^3}{hour} * \frac{0.083kg}{m^3} = \frac{0.003kg}{hour} \; of \; hydrogen$$

The power consumption rating for the electrolyzer is less than 1200 W, and the life expectancy is 15 years at a 100% duty cycle under nominal operating conditions. The following represents the chemical reactions within the electrolyte (Mekhilef et al. 982): The anode reaction is:

$$2H_2O \rightarrow O_2 + 4H^+ + 4e^-$$
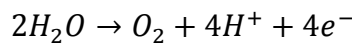
The cathode reaction is:

$$4H^+ + 4e^- \rightarrow 2H_2$$
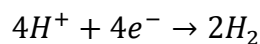
The MH7000 storage tank, located in the middle of *Figure 12*, was purchased from Pragma Industries and is the second largest tank by volume sold by the company. The MH storage tank, unlike the compressed hydrogen gas cylinder, operates under

precise temperature and pressure variables for both the absorption and desorption process. The operating pressure range is from 2 to 12 bar, approximately 29 PSI to 174 PSI at 25°C. Reaching a pressure within the tank of 12 bar at 25°C also indicates that the tank is full. The maximum charging temperature for the tank is 20 to 25°C, and the maximum discharging temperature is 40°C. The temperature and pressure ratings for the tank are very specific because as the temperature surrounding the tank increases, the pressure starts to increase since the rate of desorption has increased. If the temperature is increased too much, the pressure within the tank will reach a critical point, and permanent damage could result. The MH tank if run under nominal conditions is rated for over 5000 cycles, which each cycle includes both the discharging and charging processes.

A question is raised at this point, why use an MH storage tank over a compressed gas cylinder tank? There are several main reasons as to why an MH storage tank is preferred over a gas cylinder tank for stationary applications. The first reason is the low operating pressure that the MH tank can operate at. If the crystalline material is appropriately selected, the MH tank can be charged from traditionally 5-10 bar or 72.5-155 PSI (Vanhanen et al. 269). However, there are several factors that present issues with the metal hydride storage tank, which includes thermal stability of the hydride, the kinetics of hydrogenation and dehydrogenation, thermophysical properties and crystal structures (Gkanas et al. 10796). The most challenging factor with regards to the MH tank is the charging and discharging of hydrogen through the process of a heat transfer. In the case of the MH7000, a circulator is needed to pump water or a coolant depending on the desired temperature range through the tank to achieve temperature control. The MH7000 tank has been designed to have eight cylinders constructed out of stainless steel

43

where seven of the containers hold 1,000 sl of hydrogen and the eighth cylinder, which encases the hydrogen cylinders, is used for the water bath. "The pressure-temperature dependency in equilibrium is dependent on the thermodynamic properties enthalpy of reaction $\Delta^R h$ and entropy of reaction $\Delta^R s$ based off the Van't Hoff equation," shown below (Adametz et al. 1821).

$$\ln\left(\frac{P_{H2}}{P_{H2,ref}}\right) = \frac{\Delta^R h}{RT} - \frac{\Delta^R s}{R}$$

The crystalline structure that is used in the MH7000 tank is composed of $LaNi_5$, which is used for storing the hydrogen gas molecules. "The $LaNi_5$ has wide applications because of high absorption capacity, easy activation, moderate hysteresis, stable performance, and rapid absorption and desorption rates" (Darzi et al. 78). The enthalpy of reaction $\Delta^R h$ for $LaNi_5$ is 28,500 J/mol and entropy of reaction $\Delta^R s$ for $LaNi_5$ is 103.2 J/molK (Makridis et al. 382). The activation energy for $LaNi_5$ is 32,000 J/mol which is achieved in the MH tank through means of temperature change. Equilibrium pressure within the tank is another key point to analyze. Shown in the below equation, the equilibrium pressure P_{eq} is given as a function of both temperature and the hydrogen to metal atomic ratio $\left(\frac{H}{M}\right)$ (Askri et al. 902).

$$P_{eq} = f\left(\frac{H}{M}\right)\exp\left(\frac{\Delta H}{R_g}\left(\frac{1}{T} - \frac{1}{T_{ref}}\right)\right)$$

The variable that changes the equilibrium pressure the most in the MH tank is the change in temperature. As the temperature increases from the reference temperature, the pressure increases.
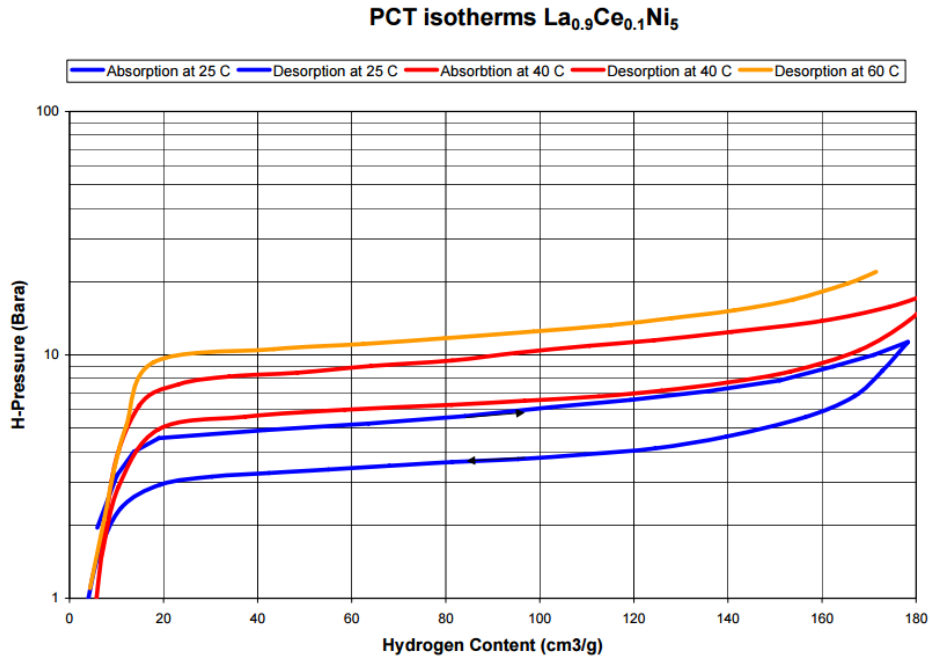
Figure 14: MH7000 Absorption and Desorption Rates.

The absorption and desorption rates that are specific to the MH7000 tank manufactured by Pragma Industries is illustrated in *Figure 14*. The absorption process requires lower temperature and pressure than the desorption process. At higher temperatures for the desorption process, the changes in pressure due to the release of hydrogen gas is sudden when compared to the desorption process at lower temperatures. The analysis is made during the bench tests as to the reaction time of the desorption process, which is critical for determining when a load can be applied to the fuel cell system. The reaction time that is determined from the desorption process of the MH tank is also used in modeling the SH2C system. Based on the required "warm up" period where hydrogen gas is released from the $LaNi_5$ compound, the MATLAB simulation models will reflect the warm up period of the MH tank to determine when the fuel cell will be turned on. For example, the fuel cell system must start generating power before

the solar PV array has ceased generating power to ensure that there is enough energy provided for the load. The warm up period within the model represents a blended mode such that as the power generation of the solar PV array starts to decrease, the fuel cell system will start to generate more power to supply the load.
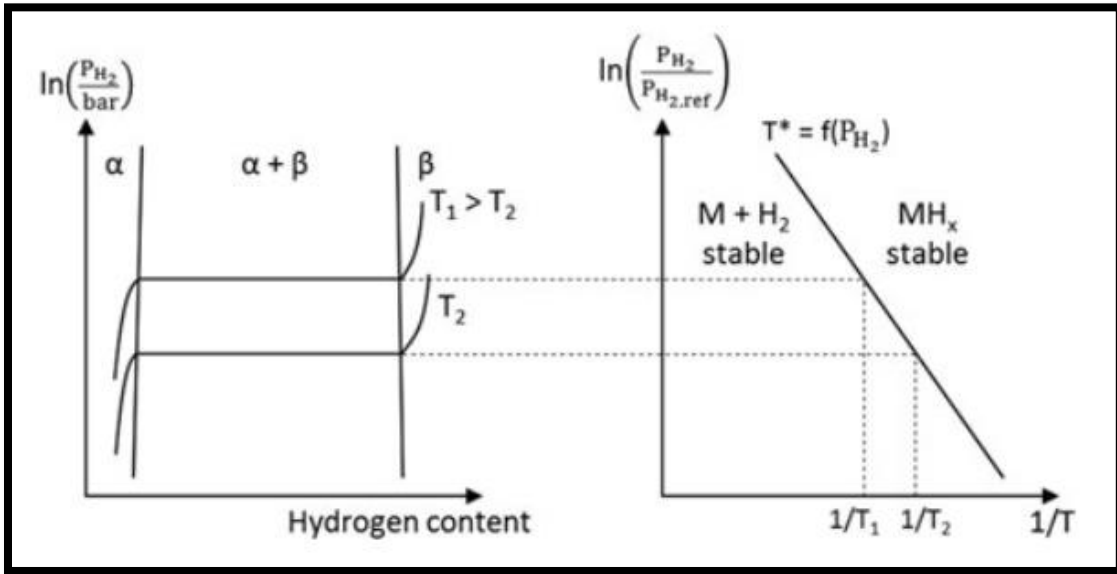
Figure 15: PCI Curve (Left) and Van't Hoff Plot (Right) (Adametz et al. 1821).

The circulator selected for the project is the Haake F3 circulator, which is in the top middle section of *Figure 12*. This circulator performs two functions for the SH2C project which is to provide controlled heating and cooling of the MH tank. As shown in *Figure 15*, the MH tank temperature characteristics play a primary role in the absorption and desorption process of hydrogen as absorption of hydrogen requires a decrease in temperature and desorption requires an increase in temperature. The Haake F3 circulator can circulate water or coolant through the MH tank. If water is to be used, the temperature of the MH tank can be chilled to 5°C and heated to 80°C, which is sufficient for the operation of the MH tank. Temperature control is key in regulating the pressure throughout both the absorption and desorption process as an increase or decrease in

temperature during either process will affect the hydrogen flow that is released into the system (Ni and Liu 2568).

3.2 MATLAB System Simulation Setup

After developing the bench test setup from the components selected for use in the SH2C project, the next step was to simulate the outcomes of the project. The bench test of the project would be able to provide a rough idea of what components within the system needed to be upgraded, but a simulated model based on the component specifications and potential load conditions would provide a new level of accuracy. By predicting the exact production rates from the system based on simulated scenarios, exact equipment required to operate the system efficiently in Arizona would be identified. The model developed was constructed from four subsystems which simulate each of the main physical components. The four subsystems include the solar PV array, electrolyzer, hydrogen storage tank, and the PEMFC. Each subsystem was built and validated before being combined into the main system model. After combining the four subsystems into one model, the model would essentially run each subsystem based off initial starting conditions such as PV generation and weather inputs. To understand the transition process between each subsystem based on the status of the system, the flowchart in *Figure 16* represents how the model reacts to specific scenarios regarding power generation from the PV subsystem.
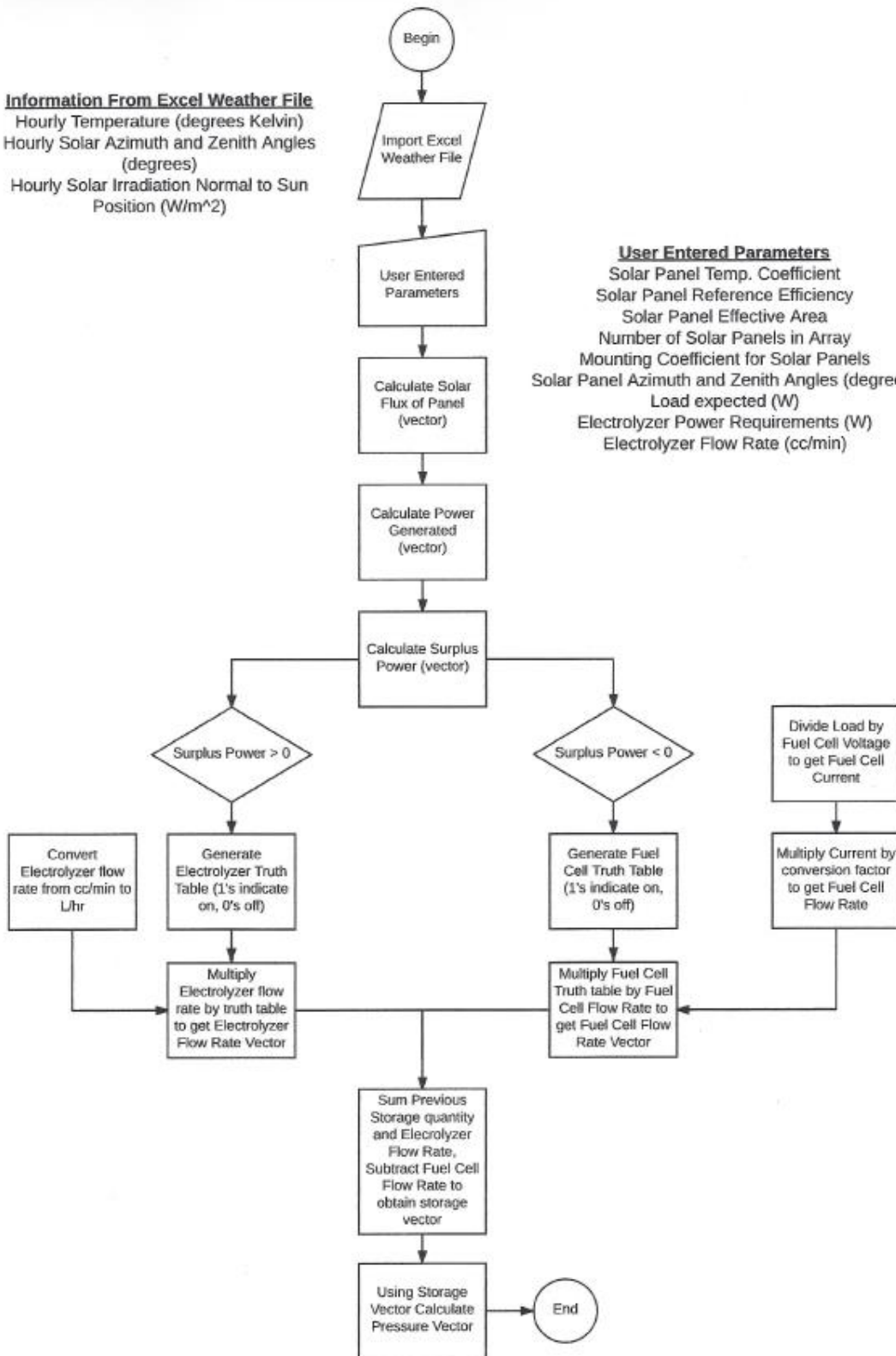
Figure 16: SH2C Project Model Flowchart.

48

The overall flow of the process starts with the solar PV subsystem. The first question that is answered in the model is, "is the solar PV system producing energy"? If the solar PV array is producing energy, the next question that is answered is how much energy? When the solar PV system is producing energy to meet the demand of the load and has a surplus supply of energy, the electrolyzer subsystem is turned on, and the generation of hydrogen is started. The generated hydrogen from the electrolyzer subsystem is sent to the hydrogen storage system, which is then used when the fuel cell system is activated. The fuel cell system is activated whenever the solar PV system cannot produce enough energy to meet the demand of the load which may arise during a sudden spike in load demand or when there is an absence of solar radiation.

The first subsystem that was built was the solar PV model, which out of the four models built, the PV model contained the most input parameters. The subsystem starts by entering in a set of input parameters which includes the following:

- Number of proposed solar panels

- Panel efficiency

- Rated power output per module

- Weather data (specifically hourly data)

    o Ambient temperature

    o Solar radiance/flux

- Mounting orientation of the solar panels

- Dust factor (shading effect)

The general equation for modeling the solar PV model is provided in the equation below (Motalleb et al. 16002).

$$I_{PV} - I_{ph} - I_s \left(\exp \left(\frac{U_{PV} + I_{PV} R_s}{mU_t} \right) - 1 \right)$$

The variable I_{PV} represents the PV module operating current, I_{ph} is the photo current, I_s is the saturation dark current, U_{PV} is the PV module's operating voltage, R_s is the series resistance and mU_t is the ideality factor multiplied by the thermal voltage of the module's cell. Other factors such as rated efficiency of the modules used and the efficiency losses of temperature and dust were included in the model. In the equations listed below, the potential reduction in efficiency due to temperature and the reduction in efficiency due to dust accumulation on the solar module is listed.

$$\eta t = 1 - \beta ref * (Ta + k * Gt - Tref)$$

$$\eta d = e^{-Aj * \Delta D}$$

To determine the total efficiency of the solar PV model, the efficiency rating due to temperature, dust accumulation, and the module efficiency are multiplied together, and the efficiency result that is then produced is the total efficiency.

As for the electrolyzer model, the energy output of the solar PV model is used to power the electrolyzer only when there is an excess of power produced. There are an additional two input parameters for the electrolyzer which involves hydrogen flow rate and the pressure output. Both variables were provided as constants by the Hogen GC 600 electrolyzer datasheet and were used for basic testing and validation of the electrolyzer model. However, to make the output variables more accurate, bench test results that were recorded of these two parameters were added to the model. The bench test results provide the relationship between the actual hydrogen flow rate with respect to the pressure output changes. For example, at a higher pressure setting, the hydrogen flow rate output of the

electrolyzer is reduced. This ratio between the flow rate of hydrogen gas and the pressure provides a better analysis of the continuous outputs from the electrolyzer.

As for the hydrogen storage model, the hydrogen stored inside the MH tank at equilibrium temperature and pressure is given by the following equations. The power balance in the MH tank is:

$$\frac{\Delta P_{H2}}{\Delta t} = P_{el} - P_{FC}$$

The total energy available in the tank in the form of hydrogen is ΔP_{H2}. P_{el} represents the potential energy production of the electrolyzer related to the H_2 production rate and P_{FC} represents the potential energy consumption of the fuel cell related to the H_2 consumption rate. Using the total energy available equation, the model is able to predict how long the fuel cell will be able to run based on the input of hydrogen from the electrolyzer. For example, if the electrolyzer produces 1kg of hydrogen and the fuel cell has not consumed any hydrogen yet, then the total energy available that has been stored in the tank is 1kg of hydrogen energy.

As for the PEMFC model, an initial static (steady-state) model that accounts for the electrochemical energy produced and the environmental losses associated with the system was produced. The model provides a base template for a dynamic model that can predict transient responses of cell voltage, temperature of the stack, hydrogen/oxygen flow rates, and cathode and anode channel temperatures/pressures under a sudden change in load current. The PEMFC is one of the main power sources for the load and dictates the amount of solar power needed. To determine how much energy the fuel cell can produce, the Nernst equation along with the hydrogen consumption rate were used. The Nernst equation, derived from Gibbs free energy, is an electrochemical equation that is

used to evaluate the effects of changing reactant/product activity, temperature and voltage. These factors contribute to the cell voltage potential without considering the losses of the system. The Nernst equation for finding the cell voltage is shown below (Mohamed et al. 20792):

$$V_{FC} = E_{Nernst} - V_{act} - V_{diff} - V_{mem}$$

Three types of losses were also taken into consideration with the model which were activation voltage, membrane voltage, and concentration voltage losses. The activation overvoltage V_{act} is caused by the slowness of the reactions on the surface of the anode and the cathode, and is derived from the Tafel equation:

$$V_{act} = \frac{RT}{anF} \ln\left(\frac{I}{I_o}\right)$$

The variable a represents the charge transfer coefficient, R represents electrode resistance, T represents the temperature, and I_o represents the exchange current. The membrane voltage V_{mem} is described as the resistance observed within the actual membrane of the cell, and is described as:

$$V_{mem} = R_{mem} * I$$

R_{mem} represents the actual membrane resistance. The concentration loss is represented as V_{diff} and the euqtion takes into consideration the change in the concentration of reactants on the electrode surface. The concentration equation can be described as:

$$V_{diff} = \frac{RT}{2F}\left[\ln\left(1 - \left(\frac{I}{I_{limit}}\right)\right)\right]$$

The variable I_{limit} is the limit current of diffusion. A list of the constant variables that are used in the PEMFC for the Nernst equations is shown in table.

3.3 HOMER Economic Analysis Setup

One of the main research objectives of this project is the economic impact

analysis of the system. The underlining question remains, and that question is how much

will this cost? To answer this question, a thorough analysis must be made that includes all

factors that pertain to the system. Factors included in an economic analysis are location,

time, initial capital cost, maintenance and operational costs, and environmental

conditions. The economic analysis modeling tool used for the SH2C project was

HOMER Legacy. To perform the analysis, a model of the SH2C system was constructed

that included all the components of the fuel cell system, an appropriately sized solar PV

array that would accommodate both the fuel cell system and the load, and lastly the

Arizona average household load. In Homer, the first step is to add or remove equipment

from the desired system into the "Equipment to Consider" block. In the case of the SH2C

project, *Figure 17* shows the system layout with each component assigned to the

appropriate bus bar of either alternating current (AC) or direct current (DC).
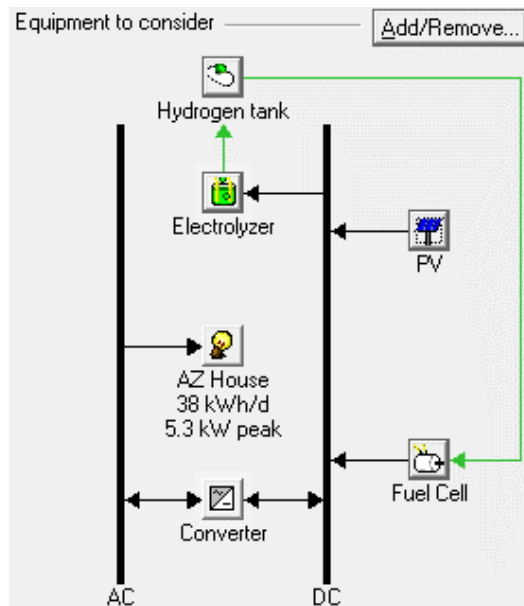
Figure 17: Proposed System Layout and Equipment Used.
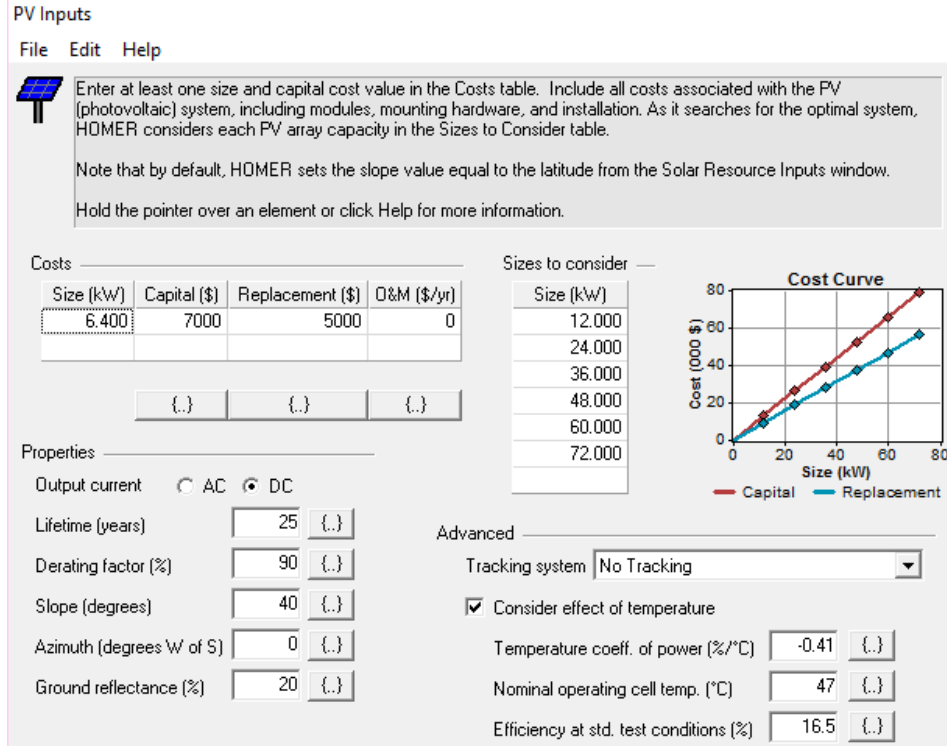
Figure 18: Solar PV Array Inputs.

The PV array for the simulated system was selected based off two constraints:

cost and efficiency. For the PV array analysis performed in the HOMER model, the

Thaisun TSG72-320W panel was selected for use, and input parameters matching the

module specifications were entered as shown in Figure 18. This solar PV module is rated

for 320 W as the maximum power output with a module efficiency of 16.5% which is

about the same as the average efficiency rating compared to other PV modules currently

sold for residential use (Go Green Solar, "Thaisum TSG72-320P Poly"). The cost per

module is about $200. For selecting the input parameters within the PV block of the

model, a solar PV array size of 6.4 kW was entered, which represents a twenty-module

setup. The capital cost for the selected size of the PV array includes all twenty modules,

the mounting hardware for the modules, and the power electronics to run/monitor the

system. The total capital cost after factoring in the costs for hardware and labor comes

out to about $6,000. Another part of the analysis that is incorporated into the simulation

is the sizes to consider column which aids the scalability of the optimal system. HOMER

uses the sizes to be considered input to model different sized systems. The program then

determines which component size will meet the needs of the system, and is selected

based on worst case scenario. For example, if a 12 kW solar PV array provides enough

energy to power the load for 90% of the year, the program will reject the system as 10%

of the energy needs were not met. Therefore, the program over sizes the "optimal" system

to meet about 99.9% of the energy needs.
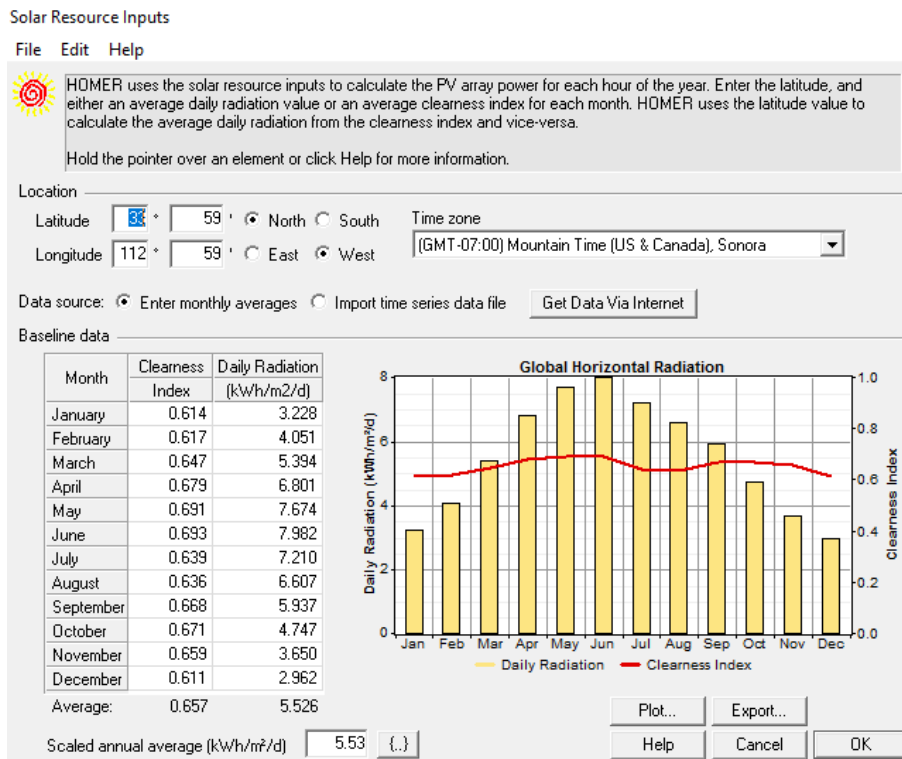
Figure 19: Solar Resource Inputs for Arizona's Daily Radiation.

Within the HOMER Legacy package, the program has a built-in feature that

allows users to select solar radiation averages based on the location from latitude and

longitude values, as shown in *Figure 19*. HOMER has gathered weather data over the

past several decades such as the solar resource so that users of the program can analyze

the effects of the solar radiation potential on a system like a solar PV array. Since the SH2C system uses a solar PV array, the effects of temperature have been included for analysis. Both the electrical efficiency and the power output of the PV modules react to the effects of temperature (Dubey et al. 319). Based on the desired location, the solar radiation averages can change, which affects the simulated system that the user has designed. For this directed research, the Mountain Time solar radiation monthly averages were selected since the SH2C project is to be constructed and operated in the Arizona environment. Based on the selected location, the clearness index and the daily radiation data for monthly averages was listed. This data has been gathered by HOMER, and reflects averages recorded during the previous years. For example, the clearness index and solar radiation data sets listed are the Arizona monthly averages recorded over a decade. The two data sets are then plotted on the right side of *Figure 19*, which visually represents the changes in the data over a period of a year.
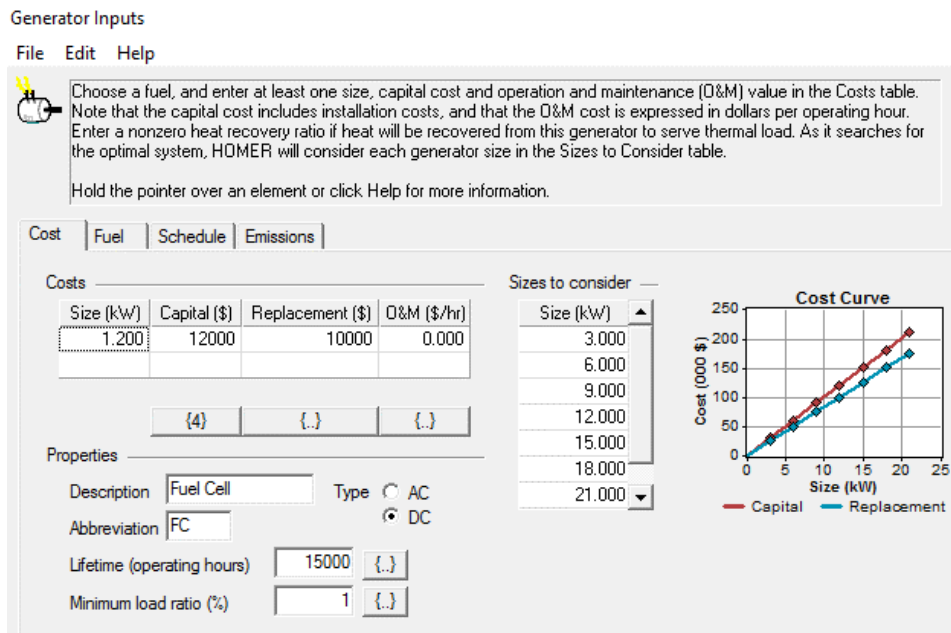
Figure 20: Nexus 1200 PEM Fuel Cell Inputs.

The PEMFC from Heliocentris is the main generator of the SH2C system, and inputs for the generator are shown in *Figure 20*. Two main factors affect the system, which is size and lifetime/durability. The Size of the fuel cell is straight forward as the input was provided by the specifications of the Nexa 1200 unit. The size does take into consideration the efficiency of the fuel cell which is also added as an input under the "Fuel" selection tab. The efficiency input as specified by the Nexa 1200 datasheet is 50%. The second factor that was considered is the lifetime of the fuel cell through operating hours. If the fuel cell were to operate at a 100% duty cycle, the PEMFC would operate for 1.7 years. Realistically, the fuel cell on average throughout the year will operate 16 hours per day assuming the solar PV array will provide power for the load during the remaining time. The PEMFC would then operate for 2.6 years before having to be replaced if operated at 16 hours per day. The calculations predicting the lifetime of the fuel cell is shown below:

$$15000 hours * \frac{1 day}{24 hours} * \frac{1 year}{365 days} = 1.7\ years$$

$$15000 hours * \frac{1 day}{16 hours} * \frac{1 year}{365 days} = 2.6\ years$$
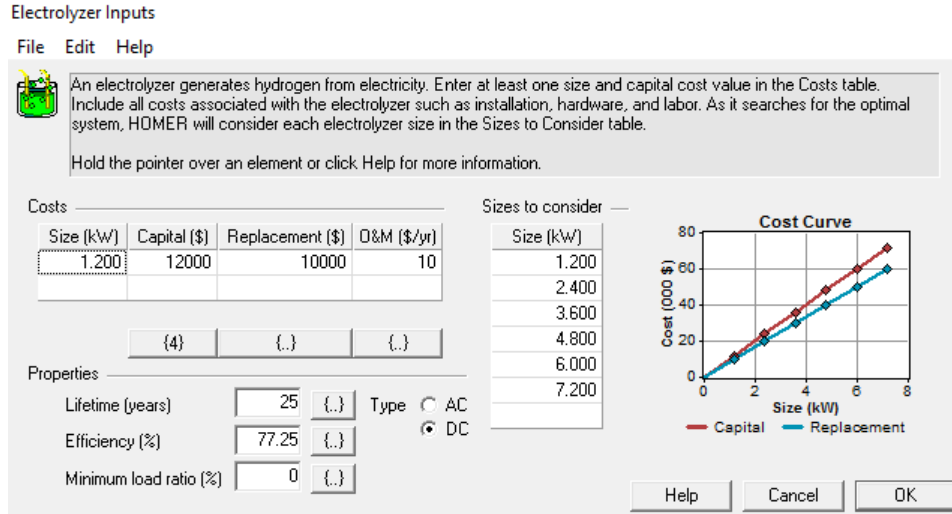
Figure 21: Hogen GC 600 Electrolyzer Inputs.

The electrolyzer plays a major role in the system set up as two main factors affect the outcome of the system significantly. The size of the PEM inside the electrolyzer and the efficiency inputs have been selected to match the values provided by the Hogen GC 600, as shown in *Figure 21*. The electrical power output of the Electrolyzer in an ideal situation is rated for 1200 W, however, some of that energy is lost due to heat. The other factor to consider is the efficiency rating of the electrolyzer, which is found by using the following equation, which uses the lower heating value for a kilogram of hydrogen:

$$\eta = \frac{\frac{39.4 kWh}{kg}}{\frac{51 kWh}{kg}} = 0.77 \ or \ 77\%$$

The HHV of hydrogen is 142 MJ/kg, which is equal to 39.4 kWh/kg (Varkaraki et al. 20). The power that is contained in hydrogen flow represents the potential of hydrogen to release energy which is the higher heating value (Vosen and Keller 1144). To calculate the Hogen GC 600 efficiency, the amount of energy consumed to produce one kilogram of hydrogen is calculated, and the efficiency is determined by dividing the energy content of hydrogen by the electricity consumed. The expected lifetime of the electrolyzer as

58

mentioned before in component selection is 15 years at 100% duty cycle which means the electrolyzer is running 24 hours per day, seven days per week. Since the flow rate of hydrogen is small, the electrolyzer will be running at all times during the operation of the solar PV array. An issue has already been discovered in the size of the electrolyzer based on the flow rate of the hydrogen. The calculations that demonstrate this error is shown below as the amount of time required to completely fill the MH tank with hydrogen is:

$$7m^3 * \frac{1hour}{0.036m^3} * \frac{1day}{24hour} = 8.1 \ days$$

The problem with the current electrolyzer is that in the time the PV array is generating energy throughout the day, the electrolyzer would have only filled 180 sl of hydrogen into the 7000 sl MH tank assuming on average the solar PV array is generating energy for five hours per day. In HOMER, there is a "Sizes to Consider" column which enables the simulation to consider different sizes of electrolyzers. In the optimization stage of the simulation, HOMER decided how large of an electrolyzer is needed based on the Hogen GC 600 specification inputs that have been provided to operate the system efficiently. Based on the known error, sizes to consider range from 10 kW to 100 kW.
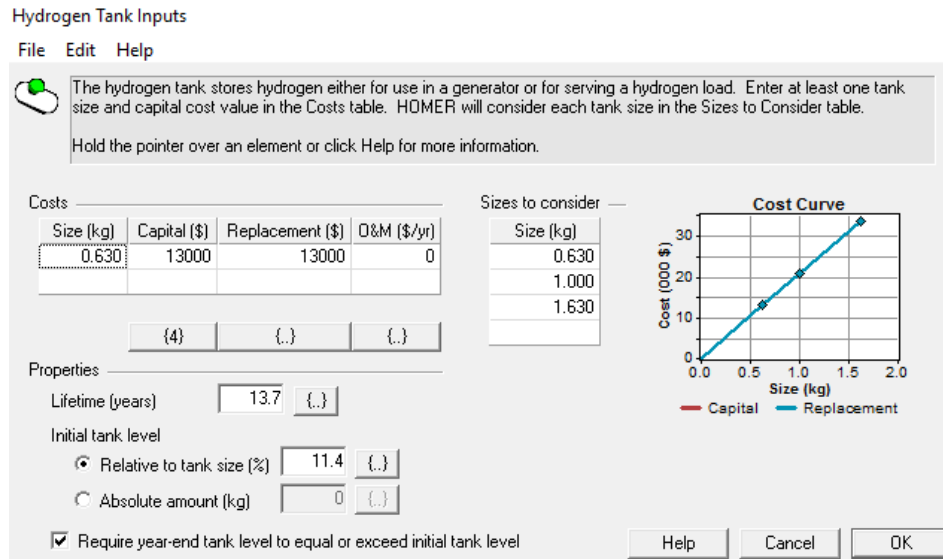
Figure 22: The MH7000 Storage Tank Inputs.

The MH tank specifications followed that of the Pragma Industries MH7000 tank

and were used in the creation of the hydrogen tank inputs, shown in *Figure 22*. The actual

size of the container is important to note as the measurement is in kg of hydrogen in the

tank. Hydrogen as at normal conditions is a low-density gas of 0.09 kg/m³ (Lototskyy and

Yartys 365). Since the maximum size of the container is 7000 sl of hydrogen, the

following equations were used to calculate the amount of hydrogen within the tank.

$$1000l = 1m^3 \rightarrow 7000l = 7m^3$$

$$7m^3 * \frac{0.09kg}{m^3} = 0.63kg \; of \; hydrogen$$

Some other property inputs considered for the hydrogen tank conditions were the

"Lifetime of the Tank" and the "Relative to Tank Size" inputs. The "Relative to Tank

Size" input specifies how much of the tanks volume or capacity of hydrogen can be used

before the tank is considered empty. As specified by the Pragma Industries MH7000

specifications, a minimum of 20 PSI of pressure must be maintained within the tank. If

60

the tank is full at 175 PSI at 25°C, the following equation was performed to determine the

minimum capacity needed:

$$\frac{20PSI}{175PSI} * 100\% = 11.4\% \; Capacity$$

As for the "Lifetime of the Tank," the assumption was made that the tank would undergo

1 cycle per day which includes both the absorption and desorption cycles. As per the

Pragma Industries specifications for the MH7000, the tank is rated for a minimum of

5000 cycles. The following equation was then used for determining the minimum lifetime

of the tank:

$$\frac{1cycle}{day} * \frac{365days}{year} = 365 \frac{cycles}{year} \rightarrow \frac{5000cycles}{365cycles/year} = 13.7 \; years$$
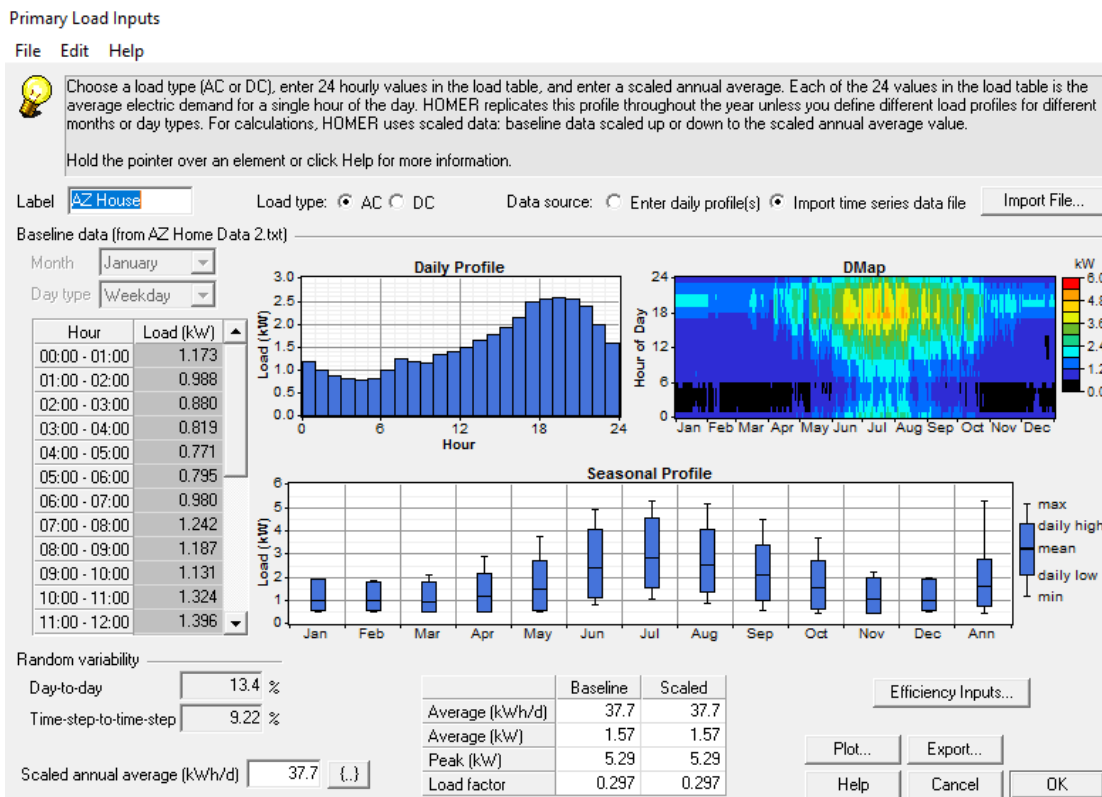
Figure 23: Arizona Primary Load Inputs (EIA, "Household Energy Use").

The Arizona load data was provided by the U.S. Energy Information Administration (EIA) (EIA, "Household Energy Use"), and the average hourly data represents the data collect in 2016. The data for the AZ load curve as seen in the Daily Profile in Figure 23 represents what industry is calling "The Duck Chart," which is displayed in the energy production graph in Figure 24. Essentially, the power plants that produce grid energy are having to predict when to either reduce energy production or ramp up the production of energy to meet the load demand at specific hours of the day. By introducing alternative energy producers into the system, the grid and renewable generators are working together to provide consistent energy even with the sudden spikes in the load demand. For the proposed SH2C system, HOMER analyzed the effectiveness that the system has when reacting to the "Duck Chart."
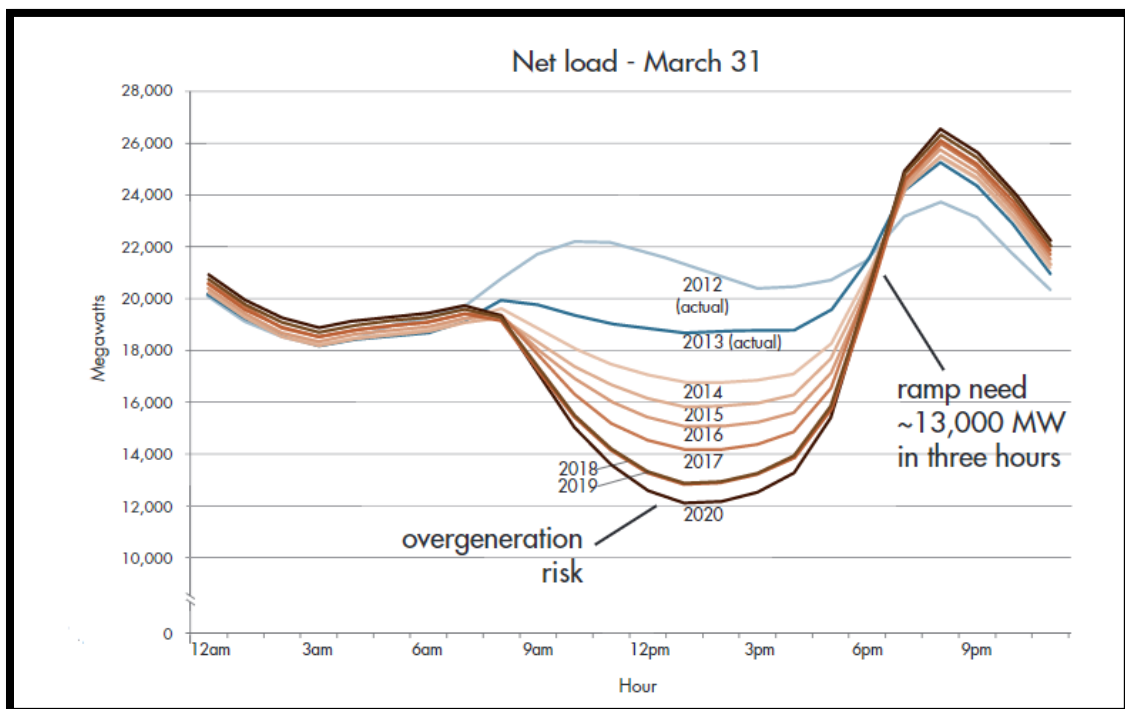
Figure 24: The Duck Chart (California ISO, "What the Duck").

Another Factor to consider in the analysis of the economic model is the DMap located on the right side of *Figure 23*. The DMap demonstrates the level of energy demand by the Arizona residential load, and shows the changing power consumption over time. The graph represents hourly power consumption for the entire simulated year. The scale of power consumption ranges from 0 kW to 6 kW. Based on the data provided, the DMap reveals that the system needs to generate the most power during the evening hours of the summer months, right around 6 PM during the months of July and August. The load of the residential home reaches the peak demand of about 5 kW. Based on this analysis, the program sized the optimal system for the critical load demand which occurs during this period of the summer.
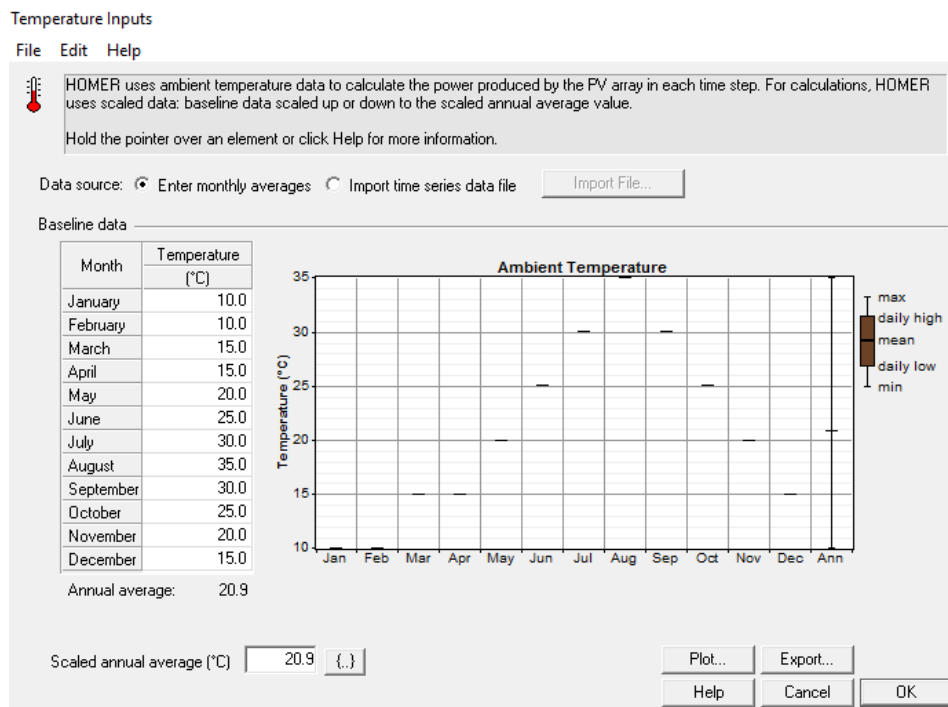
Figure 25: Average Monthly Temperature Inputs for Arizona.

The average monthly temperature data for the Phoenix metropolitan area of Arizona was added as inputs for the monthly temperature conditions, which is shown in

Figure 25 (RSS Weather, "Climate for Phoenix"). The average monthly temperatures do not reflect the absolute high and low temperatures experienced during the year. Because of this fact, the effect of temperature on the simulated system reflects only the predicted system reaction for the averages, not the absolute maximum or minimum effects of the system. HOMER does take this into consideration when calculating the optimal solution to the desired system by adjusting the size of the equipment accordingly.

CHAPTER 4

DATA ANALYSIS

4.1 PEMFC Bench Test Results

  The PEMFC bench test was comprised of two set ups: one with the hydrogen gas cylinder and one with the MH7000 hydrogen tank. For the first half of the research, the hydrogen gas cylinder was used to analyze two components within the system which was the Nexa 1200 PEMFC and the Nexa DC/DC converter. The MH tank setup was used to analyze three components within the system which was the MH tank, electrolyzer, and the circulator. The purpose of analyzing these components was to compare the actual data recorded with the theoretical equations that predict how the system should perform. The fuel cell system with all the accompanying components is a unique system where similar bench tests have been conducted before, but not with the current components that have been selected for use. An 800 W electronic load was used throughout both bench tests to simulate or represent the Arizona residential load.

  In the first bench test setup, the gas cylinder was connected directly to the fuel cell unit. The first test conducted was performed to analyze the actual power curve produced by the PEMFC by applying a 500 W electronic load to the system. In theory, the power curve of the fuel cell should increase as the current is increased of the system. Likewise, system voltage should decrease as the current within the system is increased. The ideal theoretical representation of the behavior of voltage, current, and power is shown in *Figure 26*.
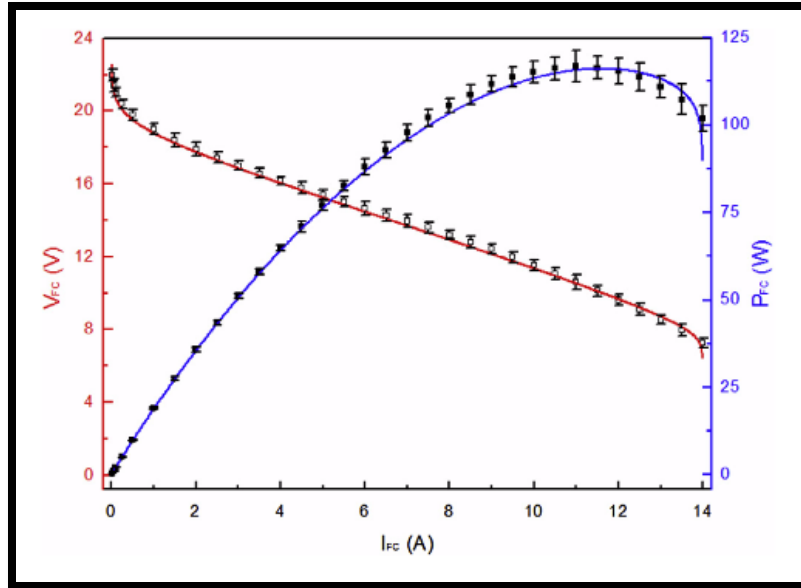
Figure 26: Theoretical PEMFC Polarization and Power Curve (Ou et al. 11716).

When reviewing the theoretical PEMFC power curve, the actual power curve achieved by

the Nexa 1200 PEMFC was compared. When comparing the two graphs from *Figure 26*

and *Figure 27*, the two power curves are almost identical as there are very little

fluctuations in the actual power output of the fuel cell.
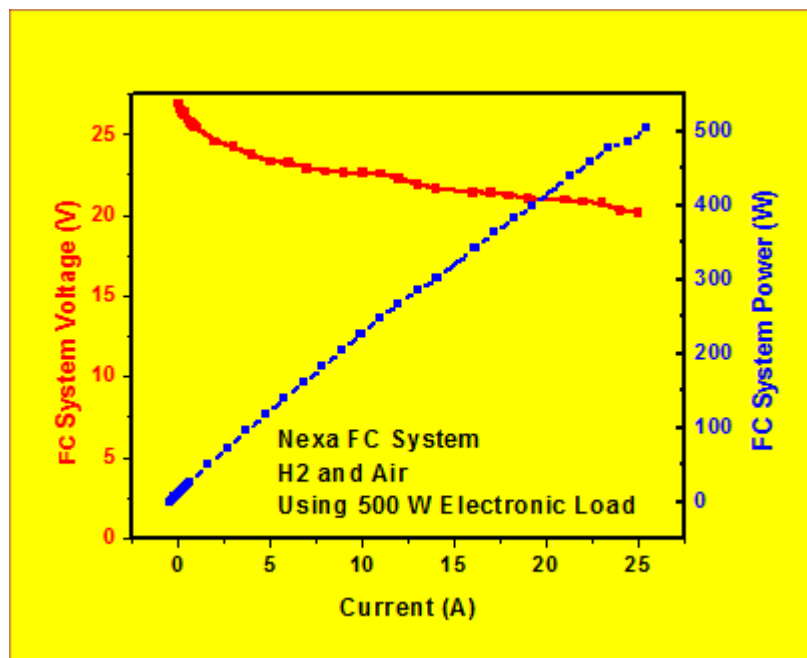
Figure 27: Actual PEMFC Polarization and Power Curve.

66

After performing the first bench test with the PEMFC and the hydrogen gas

cylinder and producing accurate results, the next bench test conducted was with the

DC/DC converter. The converter is used to regulate the DC voltage output from the

PEMFC since the fuel cell produces unregulated voltage. The unregulated voltage that is

produced from the fuel cell could cause a potential failure in powering the load. The load

is expecting a constant supply of energy, and if that supply of energy is fluctuating, the

load may not stay powered on. The DC/DC converter is designed to smooth out the

voltage of the fuel cell and ultimately provide a steady stream of energy for the load. This

bench test was conducted to analyze the behavior of the Nexa 1200 DC/DC converter

while a gradual load up to 125 W was applied. The results of placing the converter

between the power output of the fuel cell and the load is shown in *Figure 28*.
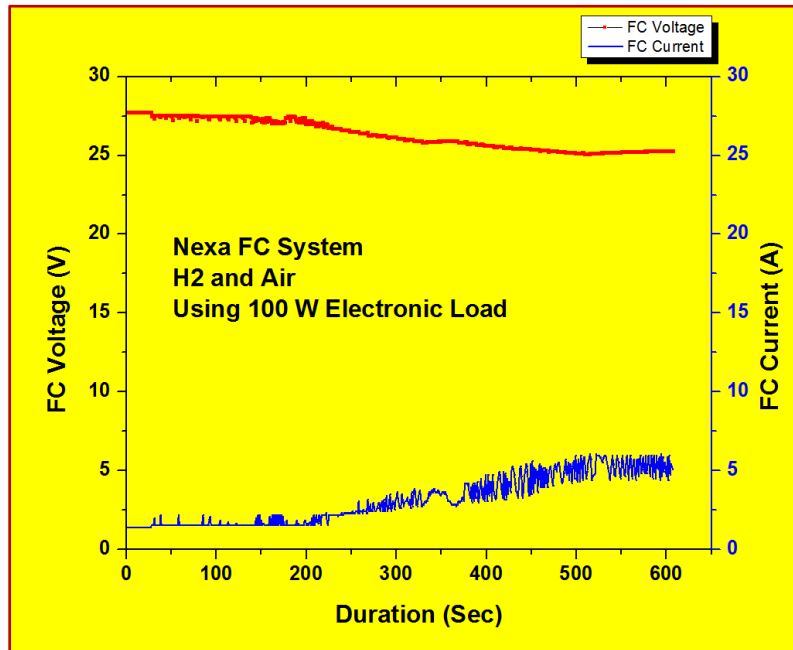
Figure 28: Fuel Cell Test Results with DC/DC Converter.

After using the DC/DC converter with the PEMFC system, the next step was to

compare the data collected with data obtained from not using the DC/DC converter

within the system. In *Figure 29*, the converter was removed from the system and the results collected are presented.
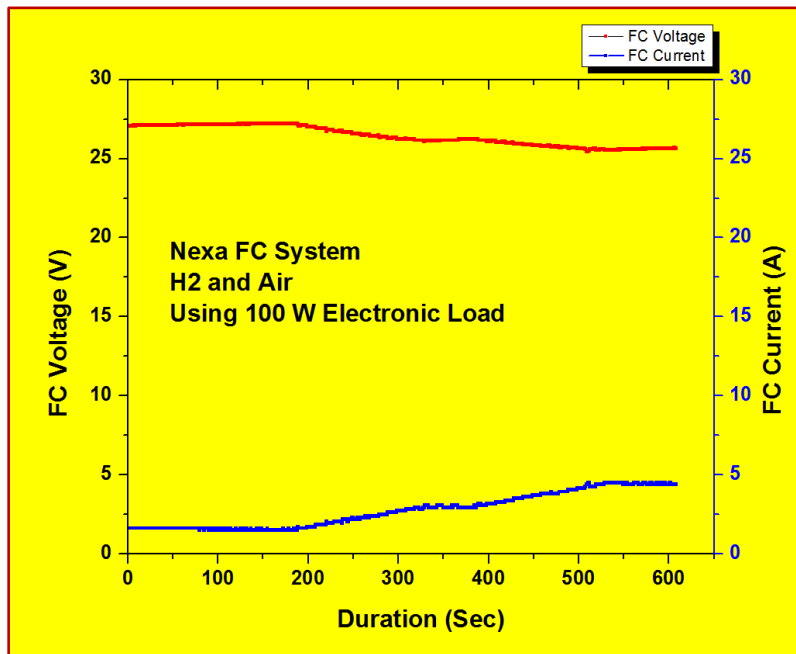
Figure 29: Fuel Cell Test Results without DC/DC Converter.

When comparing the two sets of data recorded, the DC/DC converter does, in fact, affect the system. However, the power output of the fuel cell fluctuates more with the converter than without. The voltage output in both cases remains smooth with no sudden spikes or drops in the voltage. The current of the system changes significantly with the converter incorporated in the system. The current draw of the converter oscillates which in return causes the power output of the fuel cell fluctuate. Since there are oscillations in the power output of the system when a constant load is applied, the converter was removed from the system and was not used in further testing while applying a steady load. The converter was not tested with a fluctuating load, and further testing should be conducted with the converter when an oscillating load is applied.

The third bench test was conducted with the MH tank instead of the hydrogen gas cylinder, and the goal was to determine the electrolyzer characteristics. Two primary variables, pressure output, and hydrogen flow rate, were tested and the data collected would be used in the MATLAB simulations. In preparation for the test, the initial pressure within the MH tank was recorded, and the temperature of the tank was reduced to and kept at a constant 20°C. Once the tank was fully prepared for absorbing the hydrogen gas, the electrolyzer was started with an initial pressure output rating of 100 PSI. For every half hour during the test, the pressure within the tank was recorded. Once the pressure within the tank reached 5 PSI below the output pressure of the electrolyzer, the pressure was increased, which in return decreased the flow rate of hydrogen. During the experiment, the output pressure was changed twice with the initial pressure being 100 PSI, the second pressure setting being 130 PSI, and the last setting being 175 PSI. At 170 PSI within the tank at 20°C, the MH tank was full, and the electrolyzer was turned off. The recorded pressure values in the MH tank during the absorption process (charging) are shown in Figure 30.
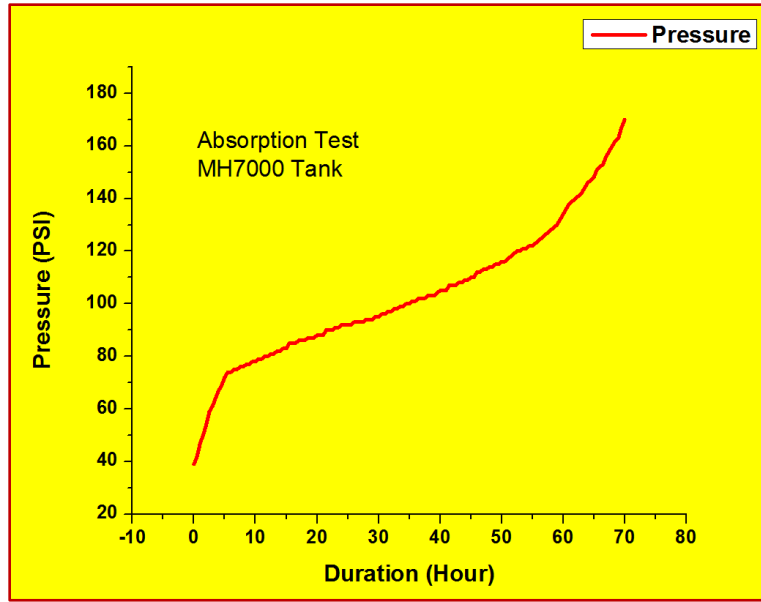
Figure 30: Electrolyzer Pressure Over Time.

Once the MH tank was filled, the fourth bench test was conducted, which was to

determine how the fuel cell reacts to the MH storage tank. The storage tank within the

system required several procedures to be conducted first before the hydrogen gas could

be used. The first procedure that was conducted was the desorption process of the MH

tank. During the time when the MH tank was not being used, the hydrogen within the

cylinder was in a state of absorption where the $LaNi_5$ crystalline compound is storing the

hydrogen molecules within the compound's structure. Since the temperature of the tank

remained at 20°C for storage and no temperature change was experienced, the hydrogen

continued to be absorbed by the $LaNi_5$ slowly over time. A reduction in tank pressure

was observed as the tank's total pressure dropped from 170 PSI to 130 PSI. At this point,

the hydrogen gas has now been condensed into the $LaNi_5$ compound. To start using the

hydrogen within the tank, the ambient temperature was increased from 20°C to 25°C,

which starts the process of desorption. The observation was made that the desorption

process does take time, and hydrogen gas is not directly available to be used by the fuel

70

cell system. After allowing the desorption process to proceed for thirty minutes, the fuel

cell was started, and a load was applied to the system. For initial testing, a load of up to

100 W was applied. The results of the experiment are shown *Figure 31*, which does

follow the ideal pattern of energy production for a PEMFC.
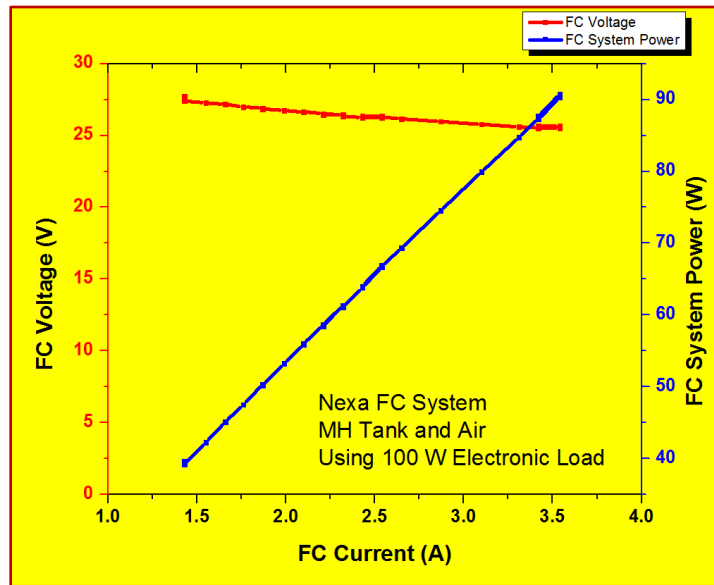
Figure 31: Fuel Cell Test Results with the MH7000.

4.2 MATLAB System Simulation Results

      Once the equations were gathered that govern the overall operation of the system,

the models were built. Both MATLAB and Simulink were used in constructing the

models where the base parameters for each of the models were placed in a MATLAB

script and the formula driven models were constructed in Simulink. The initial prototype

of the Simulink model for the physical system that uses the solar PV array, electrolyzer,

fuel cell, and the storage tank has been completed and is shown in Figure 32. This

prototype calculates the power generated by the solar PV system, the hydrogen generated

by the electrolyzer, and the hydrogen used by the fuel cell. A solar flux calculator has

been added to the solar model along with a truth table to avoid negative power values that

may be calculated due to possible negative solar flux. The negative solar flux can be

generated in two ways: if there is a decrease in solar flux or if there is no solar flux

available. The electrolyzer model has been simplified to an on or off model which

assumes if enough power is generated by the solar PV array to power both the load and

the electrolyzer, then the system will start to generate hydrogen at the flow rate provided

by the user. The fuel cell model has also been simplified to an on or off model which

calculates the flow rate of hydrogen necessary to maintain the load provided by the user.
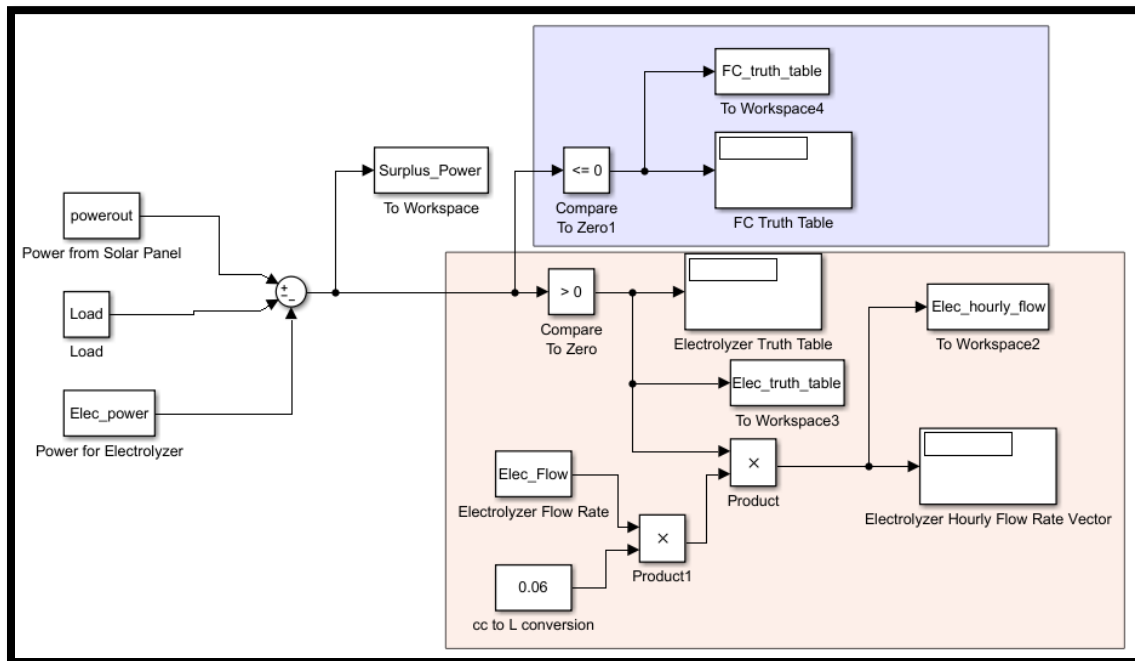
Figure 32: Energy Generation and Consumption Simulation.

As shown in *Figure 32*, the main model has the simple logic that is governed by

how much energy the solar PV array is producing. If the value determined by the amount

of energy generated by the solar PV array is less than or equal to that of the combined

value of the consumed energy from the electrolyzer and the primary residential load, the

fuel cell system engages to provide energy for the system. The model currently has four

sub-models that are linked to the main Simulink model, which includes the solar PV

array model, solar flux calculation model, pressure and hydrogen storage model, and the hydrogen flow rate model. Each sub-model provides critical information to the main model. For example, the solar PV model contains all parameters, efficiencies, and weather condition equations that effect the rated power output of the system. The user must enter the desired parameters such as the specific solar module specifications into the system. Based on the component specifications provided by the user, the model predicts the total energy produced and consumed by the system. Some of the main issues encountered in the models was with the H_2 pressure and flow rate from the electrolyzer and the consumption by the fuel cell system. The pressure and the hydrogen flow rate calculations had to be split into two separate Simulink models to allow the output variables to pass from one model to the next. Essentially, the hydrogen flow rate and pressure from the electolyzer became the input of the hydrogen storage tank model. Once the fuel cell turns on in the model based on the conidtions of the solar PV array, the output of the electrolyzer model became the input of the fuel cell system. The complications within the model were removed once the electrolyzer and the fuel cell system were seperated into two models.

To validate the accuracy of the models, each system was calculated by hand by using an Excel file. The equations that were used for governing each sub-system were placed in an Excel document, and the same simulation with the same parameters was conducted. The Excel file used for calculated the solar flux as the parameters change throughout the day is shown in *Figure 33*. The temperatures that were used for the verification of the solar flux calculations were values recorded in the Phoenix metropolitan area of Arizona during the month of December, 2016.

Time (Hour)	Temp (degrees F)	Sun Zenith	Sun Azimuth	Solar Irradiation
1:00	50	99	-99	0
2:00	50	99	-99	0
3:00	48	99	-99	0
4:00	48	99	-99	0
5:00	46	99	-99	0
6:00	46	99	-99	0
7:00	44	99	-99	0
8:00	46	87.8	119.3	625
9:00	50	80.5	125.8	1415
10:00	53	71.1	136.2	1415
11:00	57	63.5	148.7	1415
12:00	59	58.4	163.4	1415
13:00	61	56.5	179.6	1415
14:00	62	58.2	195.8	1415
15:00	62	63.1	210.6	1415
16:00	64	70.6	223.2	1415
17:00	64	79.9	233.7	1415
18:00	61	87.5	240.5	696
19:00	61	99	-99	0
20:00	57	99	-99	0
21:00	55	99	-99	0
22:00	53	99	-99	0
23:00	52	99	-99	0
0:00	52	99	-99	0

Figure 33: Solar Flux Calculation Verification.

The Simulink model that was used for calculating the solar flux of the system for one day is shown in *Figure 34*. The two systems based on the same input parameters and equations produced the same results. This method of validation was completed for all the models, and the determination was made that the system models work and are accurate. However, the models can be updated further in some aspects of the model such as the absorption and desorption rates of hydrogen in the MH tank system. Currently, the models use constants and do not accurately represent the MH7000 tank that uses the $LaNi_5$ compound. Once data on this process is collected from the bench tests, the model will be updated to better reflect the system dynamics.

74

Ta	SZdeg	+1 SAdeg	+2 Gt
24x1 double	24x1 double	24x1 double	24x1 double
1	1	1	1
1	50	1	99	1	-99	1	0
2	50	2	99	2	-99	2	0
3	48	3	99	3	-99	3	0
4	48	4	99	4	-99	4	0
5	46	5	99	5	-99	5	0
6	46	6	99	6	-99	6	0
7	44	7	99	7	-99	7	0
8	46	8	87.8	8	119.3	8	625
9	50	9	80.5	9	125.8	9	1415
10	53	10	71.1	10	136.2	10	1415
11	57	11	63.5	11	148.7	11	1415
12	59	12	58.4	12	163.4	12	1415
13	61	13	56.5	13	179.6	13	1415
14	62	14	58.2	14	195.8	14	1415
15	62	15	63.1	15	210.6	15	1415
16	64	16	70.6	16	223.2	16	1415
17	64	17	79.9	17	233.7	17	1415
18	61	18	87.5	18	240.5	18	696
19	61	19	99	19	-99	19	0
20	57	20	99	20	-99	20	0
21	55	21	99	21	-99	21	0
22	53	22	99	22	-99	22	0
23	52	23	99	23	-99	23	0
24	52	24	99	24	-99	24	0

Figure 34: Solar Flux Results from the Model.

4.3 HOMER Economic Analysis Results

The HOMER model was set up to analyze several key factors within the proposed

SH2C system. The first factor to consider when running the simulation is the Capital and

Replacement Cost Multiplier. The multiplier is a tool that can be used for projecting the

optimal solution through various cost reductions of the products over time. For example,

the PEMFC used for the economic analysis was priced at $12,000 per unit and $10,000

for a replacement. A multiplier of 0.75, 0.5, and 0.25 was added to both the initial cost

and the replacement cost. Once the simulation is started, HOMER analyzed the optimal

solution to the system by factoring in the adjusted costs, which in the case of the PEMFC

is $9,000 at 0.75, $6,000 at 0.5, and $3,000 at 0.25 for the initial cost. A multiplier was

added to the most expensive components of the system which were the PEMFC, the MH

tank, and the electrolyzer. Another factor that was considered for this model was the

PEMFC scheduling. There is a scheduling tool within HOMER that allows the user to

select an operating schedule for the PEMFC to operate by. For example, the PEMFC

could be forced on during the night hours throughout the entire project lifetime. In the

case of this model, the optimized schedule was selected, which automatically turns

components on or off based on the conditions that are being simulated. For example, if

the solar PV array cannot meet the power demand of the load at 5 PM in the month of

July, the fuel cell will turn on to support the needs. After setting up the initial system and

the appropriate conditions, the simulation was conducted. The results of the suggested

optimized solutions based on the cost multipliers is shown in *Table 1*.

Table 1: Optimization Results for the Proposed SH2C System.

FC Mult.	Elec. Mult.	MH Multi.	PV (kW)	FC (kW)	Elec. (kW)	MH (kg)	Initial Capital	Total NPC	COE ($/kWh)
1.0	1.0	1.0	48	6	4.5	1.0	$181,000	$370,000	2.13
0.75	0.75	0.75	36	6	6.0	1.0	$145,000	$337,000	1.94
0.5	0.5	0.5	36	6	6.0	1.0	$110,000	$301,000	1.74
0.25	0.25	0.25	36	6	6.0	1.0	$75,000	$266,000	1.54

As shown in *Figure 35*, the cash flow summary of the optimized SH2C system is

presented with a breakdown of where the expenditures are for the project. The fuel cell

system is the most expensive component of the project as the initial investment cost of

the system is $60,000, which accounts for five of the Nexa 1200 fuel cell systems, and

the replacement costs of the fuel cell throughout the 25-year project lifetime is about

$180,000. The fuel cell component within the project lifetime was replaced seventy-two

times at $2,500 per replacement. The PV array and the electrolyzer have a onetime initial

investment cost and do not require replacement. Operational and Maintenance Costs

(O&M) are almost negligible with the PV array, fuel cell, converter, and the MH tank. However, the electrolyzer does have a minimal cost associated due to the cost of distilled water. The total cost of the system comes out to $370,000 for the 25-year project timeline. This does consider the discounted rates of the PEMFC, electrolyzer, and MH tank.

Component	Capital ($)	Replacement ($)	O&M ($)	Fuel ($)	Salvage ($)	Total ($)
PV	52,500	0	0	0	0	52,500
Fuel Cell	60,000	179,847	0	0	-447	239,401
Converter	400	167	0	0	-31	536
Electrolyzer	48,000	0	511	0	0	48,511
Hydrogen Tank	20,635	9,288	0	0	-842	29,080
System	181,535	189,302	511	0	-1,320	370,029
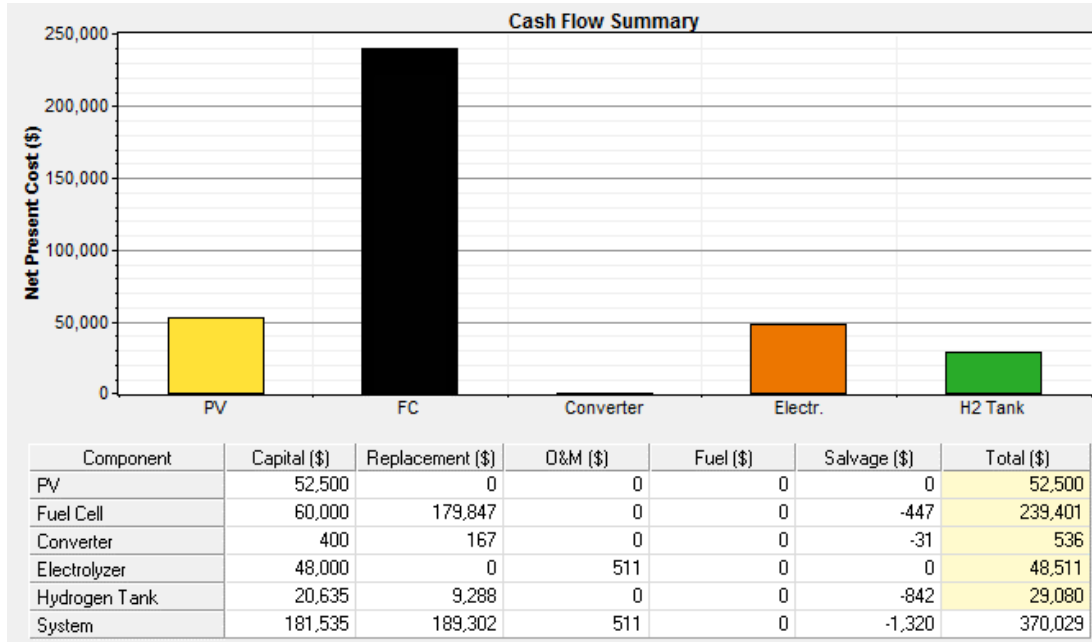
Figure 35: Cash Flow Summary.

The total energy production that was generated from the system was about 100,500 kWh/yr with the solar PV array generating about 92% of the energy or about 93,000 kWh/yr. As shown in *Figure 36*, the maximum production of energy from the solar PV array occurs in the month of April with an average energy production of just over 12.5 kW. The maximum energy production from the fuel cell occurs during the month of July which is about 1.5 kW. As for the energy consumption results, the AC load from the Arizona residential home consumes on average roughly 13,500 kWh/yr and the electrolyzer load consumes 11,600 kWh/yr. Through the consumption analysis, a key

determination was made that the AC load only consumes 54% of the energy that is used

from the system, and the remaining 46% of the consumed energy was used by the

electrolyzer. Since the electrolyzer used almost half of the consumed energy, the sizing of

the PV array was almost doubled to accommodate the amount of energy the electrolyzers

consumes. One of the key findings from this analysis is the comparison between the

production and consumption rates of energy per year. The system generated 100,500

kWh/yr of energy while the two loads only consumed about 25,000 kWh/yr, which

means the system produced an excess of energy of 73%. The system produced more

energy than was consumed to meet the demands of the load almost 100% of the time. For

example, the energy demand during the summer months requires an increase in energy

production, which in return requires the size of the system to be increased. The increased

size of the SH2C system can provide enough energy to meet the demand of the load

during the summer but creates an excess of energy during the winter months. Excess

energy generated that cannot be stored in the already full storage system becomes wasted

energy.
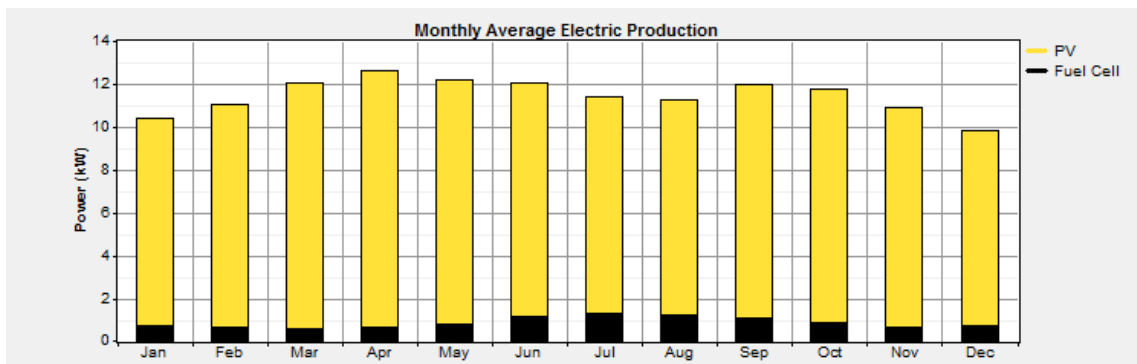
Figure 36: Electrical Production and Consumption Results.

The proposed solar PV array has a rated capacity of 48kW with a mean output of

255 kWh/d. In general, the PV array for the simulated system could produce energy for

78

almost every day of the year with some exceptions due to various weather conditions. On average, the PV array started producing energy for use at 7 AM and stopped producing energy around 6 PM, which is shown in *Figure 37*. The PV array was operated for about 4,400 hours per year, and the levelized cost of the energy produced was 0.044 $/kWh. Based on the power output color key on the right-hand side of *Figure 37*, the PV array produced the most power during the middle of the day of the winter months when used in the Arizona environment. Further analysis shows that the PV array struggles to produce power during the middle of the day during the summer months. Based on the literature reviewed prior to conducting the simulation, the results are expected as the excessive heat acts as a parasitic load on the PV system. The key insight is made that the energy generation during the summer months of Arizona is less when compared to the rest of the simulated year. Because less energy is generated during the summer months in Arizona by the solar PV array, the sizes of both the solar PV array and the fuel cell system must increase to compensate for the loss of energy due to high temperatures. Therefore, the system sizing was adjusted to accommodate for the worst-case scenario of loss of energy during the summer months.
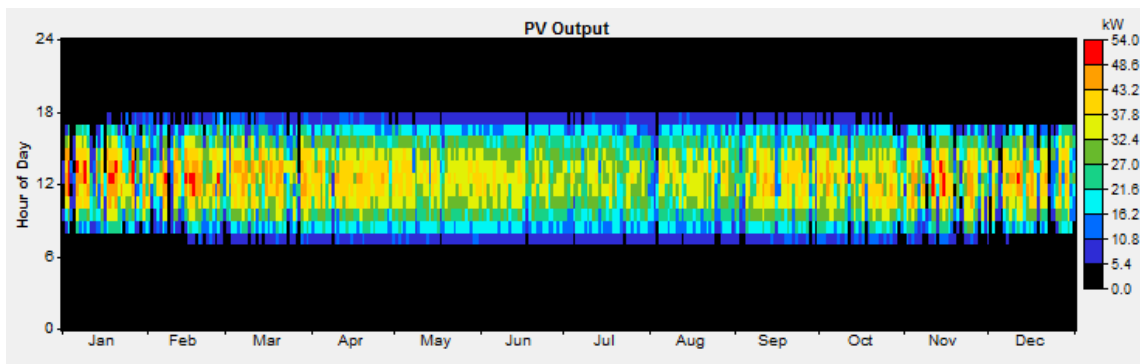
Figure 37: Solar PV Array Output Results.

For the proposed fuel cell system to function and provide enough daily energy for the consumer, the production of hydrogen gas per year came out to 227 kg. The rate of hydrogen production per month varies with respect to the load demand as seen in *Figure 38*. For example, the energy load demand was greater in the month of July than in the month of March thus more hydrogen was produced to provide enough energy for the demand. The analysis was made that the production of hydrogen would need to be greater since the solar PV array is generating less energy during the summer months. The Arizona residential load has the highest peak power demand during the same months, thus the fuel cell system would have to be used more during this period. Based on the amount of energy produced and the operational hours of the fuel cell, the cost per kg of hydrogen produced comes out to 127 $/kg.
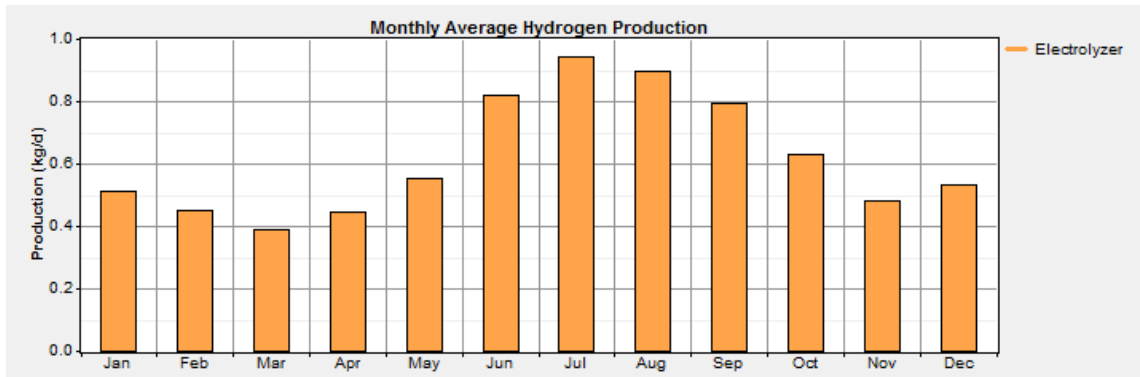
Figure 38: Average Hydrogen Production by the Electrolyzers.

As for the proposed fuel cell system, the optimal system architecture included a 6kW fuel cell system along with a 6 kW electrolyzer and a 1 kg MH storage tank. With this proposed system, the fuel cell generated power for about 4,800 hours per year with just under 400 system startups within each year. When comparing the fuel cell system with the solar PV array, the fuel cell had more operation hours listed than the PV array, which could be the cause of a lack of sufficient solar radiation due to weather or other

unknown factors. However, due to the increased expenditures of the fuel cell system, the cost for running the PEMFC comes out to 3.33 $/hr. Another key insight from the simulation is the time of day and the amount of energy generated throughout the year by the PEMFC. As shown *Figure 39*, the PEMFC is primarily operated during the nighttime hours, and the highest demand for energy comes in the evening hours during the summer months of the year.
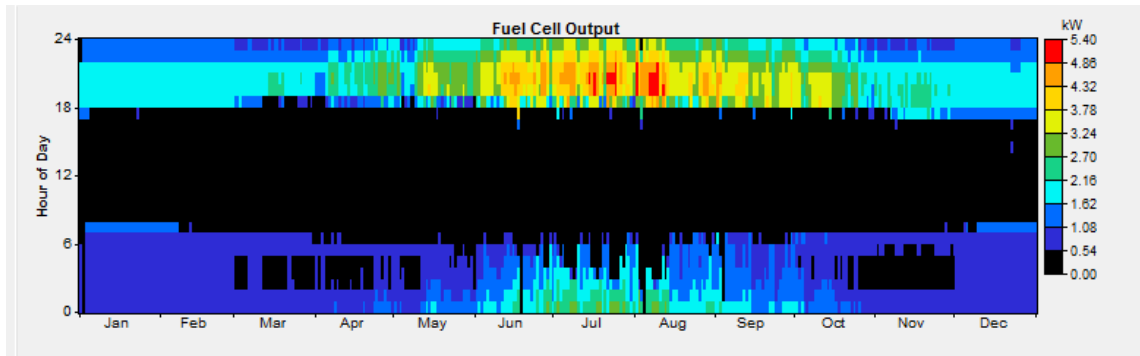
Figure 39: PEMFC Results for the SH2C System.

From the generated reports of the fuel cell and solar PV array energy generation, the next and final process to analyze is the coverage of the load demand. The solar PV array, for the most part, provided energy for the load throughout the daytime hours and the fuel cell system provided the energy needed during the nighttime hours. However, was there enough hydrogen produced from the electrolyzers for the fuel cell to operate throughout the entire year? As shown in *Figure 40*, the hydrogen tank for the most part throughout the year is full by the time the solar PV array stops generating energy and the fuel cell is turned on.
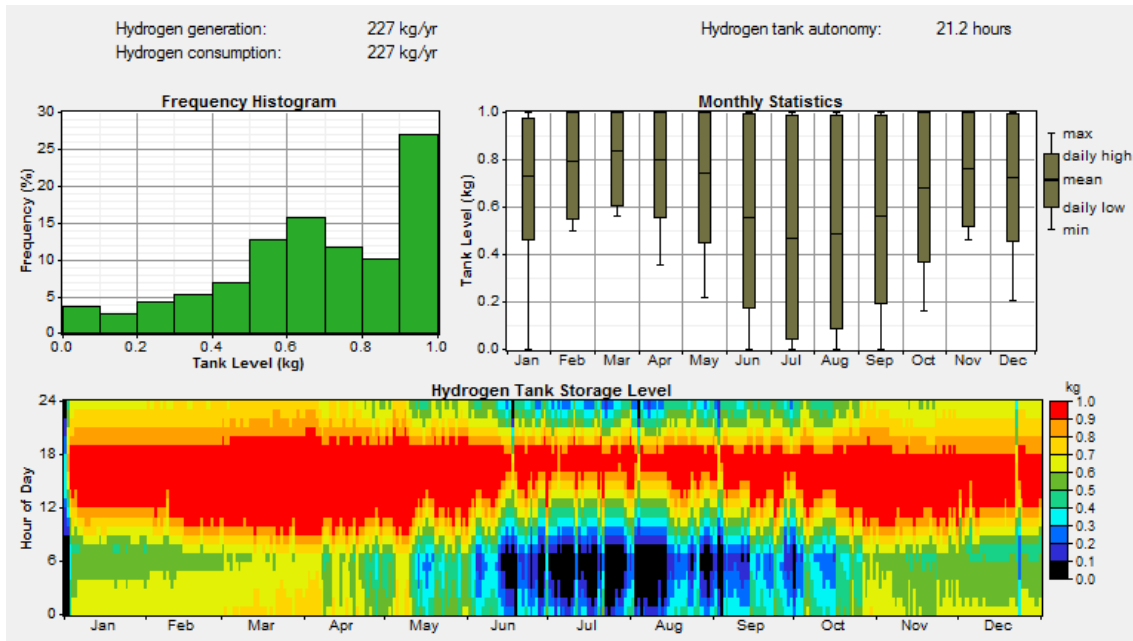
Figure 40: Stored Hydrogen averages for the MH Tank.

However, there are some cases within the year where the 1kg MH tank was not filled completely and not enough energy was generated for the load. The summer months based on the analysis report shown in the Hydrogen Tank Storage Level graph at the bottom of *Figure 40* is the period during the year that this proposed system has the most difficulty in producing enough energy for the Arizona residential home. Since the MH7000 tank can hold up to 0.63 kg of hydrogen, two of the hydrogen storage units would need to be filled to provide enough energy during the peak energy demands during the summer months so that the residential home has power 24/7.

82

CHAPTER 5

DISCUSSION

5.1 Lessons Learned

After completing the primary objectives, several lessons and insights have been gained while accomplishing the three main research objectives. The bench test setup with both the hydrogen gas cylinder and the MH tank has provided insight into different methods of hydrogen storage, filling rates under various temperature and pressure conditions, and operating scenarios with various loads being applied. The MATLAB models provided insight into the various governing equations of the components used within the SH2C system, and how those equations are affected due to the operational and environmental conditions. The HOMER model analysis provided key insight into the distribution of the energy generation, and what the exact expenditures are within the project.

While discovering these key insights from the three research objectives, several lessons were learned and have ultimately affected the outcome of the research presented. With the bench tests that were conducted, the lessons that have been learned are:

- Pressure ranges of the PEMFC

- Temperature control of the MH tank

- Gas content within the MH tank

- Venting system connection lines

- Timing of applying a load to the PEMFC

When using the hydrogen gas cylinder with the fuel cell, the fuel cell was directly connected to the cylinder, and since there was a steady supply of hydrogen gas at the

ready, the fuel cell could startup and provide power immediately. The maximum load that was ever applied to the fuel cell while performing the bench tests was about 800 W as that was the maximum power rating for the electronic load that was used. Most of the challenges came from connecting the MH tank to the system. The first lesson learned was to vent all air that may be trapped within the connection lines of the system. If air is allowed within the MH tank, the overall performance efficiency may be reduced, which is why the lines were first purged of any air. This was done by turning on the electrolyzer and filling hydrogen within the system's connection lines with the MH tank valve closed. Once the hydrogen and air had been ventilated to atmosphere through an open valve for about five minutes, the valve was closed, and only hydrogen remained within the lines.

After making sure the system was connected properly, the first challenge arose after the MH tank was filled with hydrogen gas from the electrolyzer. The input pressure of the MH tank was too high for the fuel cell system to operate. The pressure from the MH tank was set at 170 PSI. However, the maximum pressure that the fuel cell would except was 155 PSI. The solution to the problem was to add an inline regulator that would reduce the input pressure. After adding the regulator, the second challenge occurred which was the timing of when to apply a load to the PEMFC. When a load was applied for the first time to the fuel cell with the MH tank as the supplier of hydrogen fuel, the fuel cell could generate enough power to meet the load, but after a few minutes the system shut down. The pressure within the tank was much lower after the emergency shutdown of the fuel cell, and the system would not start. This scenario led to another challenge, which was the fact that the temperature within the tank needed to be increased to start the desorption process. Because the temperature within the tank was not increased, there was no readily

available supply of hydrogen gas, thus the system shut down. The discovery was made that the MH tank must experience a temperature increase and time must be allowed for the MH tank to desorb the hydrogen into a gas. Initial tests revealed that increasing the temperature by at least 5°C in the MH tank and waiting a half hour before starting the fuel cell system allows the system to operate normally. The last challenge that was discovered was the gas content within the MH tank. For shipping purposes, the MH tank was filled with a small amount of Argon gas, and the discovery was made after the tank had been filled with hydrogen. When the tank is low or close to empty, the fuel cell shuts down. The assumption is made that a mixture of Argon gas and hydrogen gas is leaving the tank, and there are not enough hydrogen molecules reaching the electrode of the fuel cell for the chemical reaction to continue. This challenge is being resolved by slowly purging the Argon from the MH tank.

The MATLAB model revealed that theoretical methodology does not always match the actual results, but the theoretical equations can make close predictions. Some of the lessons learned from this principle were:

- Constant versus varying hydrogen flow rate from the electrolyzer

- Constant versus varying pressure output of the electrolyzer

- Absorption and desorption rates of the $LaNi_5$ MH tank

- Solar radiation capture from the solar PV array

The first three points listed above were some of the critical points within the model. For conducting the simulations, these variables were listed as constants, values that would not change as the simulation progressed, at first to validate that the model worked, but to make the results more accurate actual data recorded need to be added to the model.

Both the hydrogen flow rate and the pressure of the electrolyzer were key variables needed for determining the amount of hydrogen generated within the system, and since these variables change over time, data was needed from the actual bench test. Once this data entered the model, a more accurate analysis was made as to the amount of hydrogen that was being produced over time. One of the remaining challenges of the model is to apply the desorption and absorption theories of the MH tank that are specific to the crystalline structure of $LaNi_5$. The absorption and desorption process, in general, follows the same trend or pattern as an MH tank should, however, to make the model more accurate, real data was needed where the pressure changes with respect to temperature over time could be presented. Since the MH tank contained a mixture of different gasses besides pure hydrogen, the data recorded from the performed bench tests were not completely accurate and were not used with the model. Another area of the model where assumptions were made was the capture of solar radiance from the PV array. Mock weather conditions were used for simulating the model, but to make the model more accurate, real weather data from Arizona would need to be used to better represent the capture of solar radiation in Arizona.

Lessons learned from the HOMER analysis were as follows:

- Unit cost affects sizing of the system

- Components sized to handle extreme operating conditions

- Efficiency of components alters the size of the system

The most important factor for sizing the SH2C system was cost. The most expensive items within the system is the PEMFC, MH tank, and the electrolyzer. Based on the cost of each component, the size of the solar PV array alone was increased when the cost of

the three fuel cell system components was kept at face value. When the cost of the fuel cell system components was reduced to 25% of the original price, the size of the PV array dropped from a 48 kW system to a 36 kW system. The reason for the significant drop in the size of the array was due to the number of operational hours that was designated to the PV system and the fuel cell system. When the cost of the components for the solar PV array is much cheaper than that of the fuel cell components, the PV array was increased to capture more energy during the first and last hours of light during the day. When the fuel cell component's costs were reduced, the fuel cell was used more during the early morning and late evening hours.

Another factor that affected the outcome of the simulation was the efficiency rating of all the components. The two components that had the greatest impact on the generation of energy was the solar PV array and the electrolyzer. The efficiency ratings that are affected by temperature had a tremendous impact on the system and played a major role in sourcing the appropriate solar module to use for the system. By increasing the efficiency rating of the module by just 5%, the size of the PV array was reduced from 100 kW to 60 kW. The same effect was true with the electrolyzer. An initial error in calculating the efficiency of the electrolyzer was made, and the suggested system configuration called for four electrolyzers. After realizing the error in the calculation, an 11% reduction in efficiency was added to the electrolyzer inputs, and the system configuration suggested using a total of six electrolyzers instead of four.

The last observation made with the HOMER analysis was the oversizing of components within the optimized system. HOMER is programmed to present the best system that addresses meeting the energy needs of the load at the lowest cost possible.

The system that was presented as the optimal system for the Arizona load was a 36 kW PV array, six 1.2 kW PEMFC, six 1.2 kW electrolyzers, and two MH7000 storage tanks. This system configuration provides the energy needed for the Arizona home for 99% of the year, and covers the most extreme cases of weather conditions. However, the system has been oversized to accommodate the most extreme conditions, and a smaller system would provide enough energy for the home throughout most of the year. The proposed system has been sized accordingly to meet the energy demand during the evenings of the summer months.

5.2 Future Work

For the second phase of the SH2C project, the MATLAB model will need to be finetuned as the accuracy of the model will increase as more data is gathered from the bench tests. The two subsystems that will need more refining is the MH storage tank system and the solar PV system. The MH tank subsystem representation will become more accurate if the actual data gathered from the bench test is incorporated. What makes the MH tank simulation unique is the reaction process that occurs between the $LaNi_5$ and the hydrogen gas, which makes the absorption and the desorption process unique to the current system configuration. The bench tests with the hydrogen gas cylinder are complete, but further testing with the MH tank regarding desorption needs to be conducted. The Argon gas will need to be completely removed from the system before accurate data can be achieved.

Based on the results of the HOMER and the MATLAB models, several components will need to be upgraded for the system to fully support a 37 kWh/d load in Arizona. The components that should be upgraded are the fuel cell and the electrolyzer.

88

The Hogen GC 600 has an extremely low flow rate of hydrogen, which requires several days to fill the MH tank rather than several hours. If this system is to work effectively by producing and storing hydrogen while the solar PV array is operating, the MH tank will need to be filled within a couple of hours from when the tank is empty. Another component that needs to be upgraded is the PEMFC. Based on the simulations, a 6 kW PEMFC is required to provide enough energy to the home in extreme cases such as the peak load demand during the evening hours of the summer months. Another avenue that is suggested for further research is recapturing energy lost in the system due to heat. About 50% of the energy produced within the system is lost due to heat, which could potentially be reused if a thermal management system is applied. For example, part of the residential load comes from a water heater. The heat that is produced from the system could be captured and redirected to help support the heating process of the water heater.

5.3 Conclusion

Based on the results of the phase one objectives, the hypothesis was proven to be correct. The Solar-H2 Cycle system is a feasible and viable source of energy generation in Arizona. The SH2C system is able to meet the needs of the residential home, however, the cost of the system remains high when compared to the current grid prices. The cost of energy for the average Arizona resident is just under $1,500 per year, and if the grid rates stay the same for the next 25 years, the total NPC would be about $37,500. The total NPC of the proposed SH2C system is $266,000. To make this system more competitive with the current residential grid prices, the cost of the fuel cell components such as the PEMFC, electrolyzer, and the MH tank need to decrease significantly by about 80% or more.

Another factor to consider that was determined by analyzing the system performance was the time of the day (and season) at which the solar PV array and fuel cell system operate. The number of operating hours for the more expensive components was less, which as a result affected the sizing of the system. The optimal system configuration based on the worst-case scenario suggested that the solar PV array be oversized to compensate for the cost and durability of the fuel cell system. Thus, the optimal system was less expensive when the solar PV array operated for a longer period. To decrease the size of the solar PV array, the fuel cell components such as the PEMFC and the electrolyzer would need to become cheaper, more durable, and more efficient. Efficiency of the system can be enhanced by recapturing some of the energy lost through heat, and durability of the system will increase if the system operates in a cleaner environment with less chance for contamination. Nevertheless, the SH2C system would be a viable source of energy generation for Arizona homes.

REFERENCES

"Climate for Phoenix, Arizona." RSS Weather, 2013, http://www.rssweather.com/climate/Arizona/Phoenix/. Accessed 27 Nov. 2016.

"Household Energy Use in Arizona." EIA Residential Energy Consumption Survey, 2009, https://www.eia.gov/consumption/residential/. Accessed 2 Feb. 2017.

"Hybrid Systems." FNQ Solar Solutions, 2017, http://www.fnqsolarsolutions.com/hybrid. Accessed 6 Apr. 2017.

"Hydrogen Stations." Nikola Motor Company, 2017, https://nikolamotor.com/#stations. Accessed 8 Mar. 2017.

"Hydrogen Weight and Volume Equivalents." Air Products, 2017, http://www.airproducts.com/products/Gases/gas-facts/conversion-formulas/weight-and-volume-equivalents/hydrogen.aspx. Accessed 1 Feb. 2017.

"Thaisum TSG72-320P Poly Solar Panel." GoGreenSolar, 2017, https://www.gogreensolar.com/products/thaisun-tsg72-320p-320w-poly-solar-panel. Accessed 25 Feb. 20

Abdallah, M.A.H., Asfour, S.S. "Solar-Hydrogen Energy System for Egypt." *International Journal of Hydrogen Energy*, Vol. 24, 1999, pp. 505–517.

Adametz, P., Muller, K., Arlt, W. "Energetic Evaluation of Hydrogen Storage in Metal Hydrides." *International Journal of Energy Research*, Vol. 40, 2016, pp. 1820-1831.

Agbossou, K., Chahine, R. "Renewable Energy Systems Based on Hydrogen for Remote Applications." *Journal of Power Sources*, Vol. 96, 2001, pp. 168–172.

Andrews, J., Shabani, B. "Re-Envisioning the Role of Hydrogen in a Sustainable Energy Economy." *International Journal of Hydrogen Energy*, Vol. 37, 2012, pp. 1184–1203.

Andújar, J.M., Segura, F. "Fuel Cells: History and Updating. A Walk Along Two Centuries." *Renewable and Sustainable Energy Reviews*, Vol. 13, 2009, pp. 2309–2322.

Askri, F., *et al.* "Optimization of Hydrogen Storage in Metal–Hydride Tanks." *International Journal of Hydrogen Energy*, Vol. 34, 2009, pp. 897–905.

Baharoon, D.A., Rahman, H.A., Omar, W.Z.W., Fadhl, S.O. "Historical Development of Concentrating Solar Power Technologies to Generate Clean Electricity Efficiently – a Review." *Renewable and Sustainable Energy Reviews*, Vol. 41, 2015, pp. 996–1027.

Belmonte, N., Girgenti, V., Florian, P., Peano, C., Luetto, C., Rizzi, P., Baricco, M. "A Comparison of Energy Storage from Renewable Sources Through Batteries and Fuel Cells: A Case Study in Turin, Italy." *International Journal of Hydrogen Energy*, Vol. 41, 2016, pp. 21427 - 21438.

Bouraiou, A., Hamouda, M., Chaker, A. "Analysis and Evaluation of the Impact of Climatic Conditions on the Photovoltaic Modules Performance in the Desert Environment." *Energy Conversation and Management*, Vol. 106, 2015, pp. 1345–1355.

Brown, M., Cohen, M., Gary, K. "American History: Fuel Cell Origins." *Smithsonian Institution*, 2016, http://americanhistory.si.edu/fuelcells/basics.htm. Accessed 15 Feb. 2017.

California ISO. *What the Duck Curve Tells us about Managing a Green Grid*. Calso, 2013.

Cheddie, D., Munroe, N. "Review and Comparison of Approaches to Proton Exchange Membrane Fuel Cell Modeling." *Journal of Power Sources*, Vol. 147, 2005, pp. 72–84.

Cheng, X., Shi, Z., Glass, N., Zhang, L., Zhang, J., Song, D., Liu, Z.S., Wang, H., Shen, J. "A Review of PEM Hydrogen Fuel Cell Contamination: Impacts, Mechanisms, and Mitigation." *Journal of Power Sources*, Vol. 165, 2007, pp. 739–756.

Contreras, A., Posso, F., Guervos, E. "Modelling and Simulation of the Utilization of a PEM Fuel Cell in the Rural Sector of Venezuela." *Applied Energy*, Vol. 87, 2010, pp. 1376–1385.

Cooper, C., Sovacool, B.K. "Miracle or Mirage? The Promise and Peril of Desert Energy Part 1." *Renewable Energy*, Vol. 50, 2013, pp. 628–636.

Darzi, A.A., Afrouzi, H., Alizadeh, E., Shokri, V., Farhadi, M. "Numerical Simulation of Heat and Mass Transfer during Absorption of Hydrogen in Metal Hydride Tank." *Heat Transfer Asian Research*, Vol. 46, 2017, pp. 75-90.

Dubey, S., Sarvaiya, J.N., Seshadri, B. "Temperature Dependent Photovoltaic (PV) Efficiency and its Effect on PV Production in the World – a Review." *Energy Procedia*, 33, 2013, pp. 311–321.

Elgowainy, A., Gaines, L., Wang, M. "Fuel-Cycle Analysis of Early Market Applications of Fuel Cells: Forklift Propulsion Systems and Distributed Power Generation." *International Journal of Hydrogen Energy*, Vol. 34, 2009, pp. 3557–3570.

El-Nashar, A.M. "The Effect of Dust Accumulation on the Performance of Evacuated Tube Collectors." *Solar Energy*, Vol. 53, No. 1, 1994, pp. 105–115.

El-Sharkh, M.Y., Rahman, A., Alam, M.S., Byrne, P.C., Sakla, A.A., Thomas, T. "A Dynamic Model for a Stand-Alone PEM Fuel Fell Power Plant for Residential Applications." *Journal of Power Sources*, Vol. 138, 2004, pp. 199–204.

Galli, S., Stephanoni, M. "Development of a Solar-Hydrogen Cycle in Italy." *International Journal of Hydrogen Energy*, Vol. 22, 1997, pp. 453–458.

Gencoglu, M., Ural, Z. "Design of a PEM Fuel Cell System for Residential Application." *International Journal of Hydrogen Energy*, Vol. 34, 2009, pp. 5242–5248.

Gkanas, E., Grant, D., Khzouz, M., Stuart, A., Manickam, K., Walker, G. "Efficient Hydrogen Storage in Up Scale Metal Hydride Tanks as Possible Metal Hydride Compression Agents Equipped with Aluminum Extended Surfaces." *International Journal of Hydrogen Energy*, Vol. 41, 2016, pp. 10795-10810.

Gray, E.M., Webb, C.J., Andrews, J., Shabani, B., Tsai, P.J., Chan, S.L.I. "Hydrogen Storage for Off-Grid Power Supply." *International Journal of Hydrogen Energy*, Vol. 36, 2011, pp. 654–663.

Hamada, Y., Takeda, K., Goto, R., Kubota, H. "Hybrid Utilization of Renewable Energy and Fuel Cells for Residential Energy Systems." *Energy and Buildings*, Vol. 43, 2011, pp. 3680–3684.

Ho, J., Saw, E., Lu, L., Liu, J. "Technological Barriers and Research Trends in Fuel Cell Technologies: A Citation Network Analysis." *Technological Forecasting & Social Change*, Vol. 82, 2014, pp. 66-79.

Kajikawa, Y., Yoshikawa, J., Takeda, Y., Matsushima, K. "Tracking Emerging Technologies in Energy Research: Toward a Roadmap for Sustainable Energy." *Technology Forecasting & Social Change*, Vol. 75, 2008, pp. 771–782.

Kalinci, Y., Hepbasli, A., Dincer, I. "Techno-Economic Analysis of a Stand-Alone Hybrid Renewable Energy System with Hydrogen Production and Storage Options." *International Journal of Hydrogen Energy*, Vol. 40, 2015, pp. 7652–7664.

Khan, M.J., Iqbal, M.T. "Pre-feasibility Study of Stand-alone Hybrid Energy Systems for Applications in Newfoundland." *Renewable Energy*, Vol. 30, 2005, pp. 835–854.

Kirubakaran, A., Jain, S., Nema, RK. "A Review on Fuel Cell Technologies and Power Electronic Interface." *Renewable and Sustainable Energy Reviews*, Vol. 13, 2009, pp. 2430–2440.

Lototskyy, M., Yartys, V.A. "Comparative Analysis of the Efficiencies of Hydrogen Storage Systems Utilising Solid State H Storage Materials." *Journal of Alloys and Compounds*, Vol. 645, 2015, pp. 365-373.

Lucia, U. "Overview of Fuel Cells." *International Journal of Hydrogen Energy*, Vol. 30, 2014, pp. 164-169.

Mahlia, T.M.I., Chan, P.L. "Life Cycle Cost Analysis of Fuel Cell Based Cogeneration System for Residential Application in Malaysia." *Renewable and Sustainable Energy Reviews*, Vol. 15, 2011, pp. 416–426.

Makridis, S.S., Gkanas, E.I., Stubos, A.K. "Modeling and Simulation for Absorption-Desorption Cyclic Process on a Three-Stage Metal Hydride Hydrogen Compressor." *Elsevier B.V.*, Vol. 23, 2013, pp. 379–384

Mann, R.F., Amphlett, J.C., Hooper, M.A., Jensen, H.M., Peppley, B.A., Roberge, P.R. "Development and Application of a Generalized Steady-state Electrochemical Model for a PEM Fuel Cell." *Journal of Power Sources*, Vol. 86, 2000, pp. 173–180.

Mehta, V., Cooper, J.S. "Review and Analysis of PEM Fuel Cell Design and Manufacturing." *Journal of Power Sources*, Vol. 114, 2003, pp. 32–53.

Mekhilef, S., Saidur, R., Safari, A. "Comparative Study of Different Fuel Cell Technologies." *Renewable and Sustainable Energy Reviews*, Vol. 16, 2012, pp. 981–989.

Mohamed, B., Ali, B., Ahmed, B., Ahmed, B., Salah, L., Rachid, D. "Study of Hydrogen Production by Solar Energy as Tool of Storing and Utilization Renewable Energy for the Desert Areas." *International Journal of Hydrogen Energy*, Vol. 41, 2016, pp. 20788-20806.

Motalleb, M., Đukic, A., Firak, M. "Solar Hydrogen Power System for Isolated Passive House." *International Journal of Hydrogen Energy*, Vol. 40, 2015, pp. 16001-16009.

Ni, J., Liu, H. "Experimental Research on Refrigeration Characteristics of a Metal Hydride Heat Pump in Auto Air-Conditioning." *International Journal of Hydrogen Energy*, Vol. 32, 2007, pp. 2567–2572.

O'Malley K, Ordaz G, Adams J, Randolph K, Ahn CC, Stetson NT. "Applied Hydrogen Storage Research and Development: A Perspective from the US Department of Energy." *Journal of Alloys and Compounds*, Vol. 645, 2015, pp. 419-422.

Ou, K., Wang, Y., Kim, Y. "Modeling and Experimental Validation of Hybrid Proton Exchange Membrane Fuel Cell/Battery System for Power Management Control." *International Journal of Hydrogen Energy*, Vol. 40, 2015, pp. 11713–11721.

Rekioua, D., Samia, B., Nabila, B. "Development of Hybrid Photovoltaic-Fuel Cell System for Stand-alone Application." *International Journal of Hydrogen Energy*, Vol. 39, 2014, pp. 1604–1611.

Renquist, J.V., Dickman, B., Bradley, T.H. "Economic Comparison of Fuel Cell Powered Forklifts to Battery Powered Forklifts." *International Journal of Hydrogen Energy*, Vol. 37, 2012, pp. 12054–12059.

Santarelli, M., Cali, M., Macagno, S. "Design and Analysis of Stand-Alone Hydrogen Energy Systems with Different Renewable Sources." *International Journal of Hydrogen Energy*, Vol. 29, 2004, pp. 1571–1586.

Sarver, T., Al-Qaraghuli, A., Kazmerski, L.L. "A Comprehensive Review of the Impact of Dust on the Use of Solar Energy: History, Investigations, Results Literature, and Mitigation Approaches." *Renewable and Sustainable Energy Reviews*, Vol. 22, 2013, pp. 698–733.

Schmittinger, W., Vahidi, A. "A Review of the Main Parameters Influencing Long-Term Performance and Durability of PEM Fuel Cells." *Journal of Power Sources*, Vol. 180, 2008, pp. 1–14.

Shabani, B., Andrews, J. "An Experimental Investigation of a PEM Fuel Cell to Supply Both Heat and Power in a Solar-Hydrogen RAPS System." *International Journal of Hydrogen Energy*, Vol. 36, 2011, pp. 5442–5452.

Sharaf, O., Orphan, M. "An Overview of Fuel Cell Technology: Fundamentals and Applications." *Renewable and Sustainable Energy Reviews*, Vol. 32, 2014, pp. 810-853.

Simbolotti, G. "IEA Energy Technology Essentials: Fuel Cells." OECD/IEA, 2007, https://www.iea.org/publications/freepublications/publication/iea-energy-technology-essentials-fuel-cells.html. Accessed 17 Feb. 2017.

Spakovsky, M.R. von, Olsommer, B. "Fuel Cell Systems and System Modeling and Analysis Perspectives for Fuel Cell Development." *Energy Conversion and Management*, Vol. 43, 2002, pp. 1249–1257.

Stumper, J., Stone, C. "Recent Advances in Fuel Cell Technology at Ballard." *Journal of Power Sources*, Vol. 176, 2008, pp. 468–476.

Tolj, I., Lototskyy, M., Davids, M., Klochko, Y., Parsons, A., Swanepoel, D., Ehlers, R., Louw, G., Westhuizen, B., Smith, F., Pollet, B., Sita, C., Linkov, V. "Metal Hydride Hydrogen Storage and Supply Systems for Electric Forklift with Low Temperature Proton Exchange Membrane Fuel Cell Power Module." *International Journal of Hydrogen Energy*, Vol. 41, 2016, pp. 13831-13842.

Torres, L.A., Rodrigez, F.J. "Simulation of a Solar-Hydrogen-Fuel Cell System: Results for Different Locations in Mexico." *International Journal of Hydrogen Energy*, Vol. 23, 1998, pp. 1005–1009.

U.S. Department of Energy. *Fuel Cell Handbook*. 7th ed., EG&G Technical Services, Inc., 2004.

U.S. Department of Energy. *Fuel Cell Technologies Program*. Energy Efficiency & Renewable Energy, 2010.

Vanhanen, J.P., Lund, P.D. "Electrolyser-Metal Hydride-Fuel Cell System for Seasonal Energy Storage." *International Journal of Hydrogen Energy*, Vol. 23, 1998, pp. 267–271.

Varkaraki, E., Lymberopoulos, N., Zachariou, A. "Hydrogen Based Emergency Back-Up System for Telecommunication Applications." *Journal of Power Sources*, Vol. 118, 2003, pp. 14–22.

Viebahn, P., Lechon, Y., Trieb, F. "The Potential Role of Concentrated Solar Power (CSP) in Africa and Europe − a Dynamic Assessment of Technology Development, Cost Development and Life Cycle Inventories Until 2050." *Energy Policy*, Vol. 39, 2011, pp. 4420–4430.
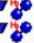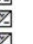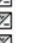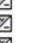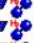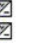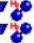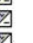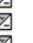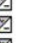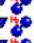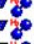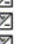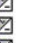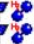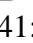
Vosen, S.R., Keller, J.O. "Hybrid Energy Storage for Stand-Alone Electric Power Systems: Optimization of System Performance and Cost through Control Strategies." *International Journal of Hydrogen Energy*, Vol. 24, 1999, pp. 1139–1156.

Wang, Y., Chen, K.S., Mishler, J., Cho, S.C., Adroher, X.C. "A Review of Polymer Electrolyte Membrane Fuel Cells: Technology, Applications, and Needs on Fundamental Research." Applied Energy, Vol. 88, 2011, pp. 981–1007.

Yilanci, A., Dincer, I., Ozturk, H.K. "A Review on Solar-Hydrogen/Fuel Cell Hybrid Energy Systems for Stationary Applications." *Progress in Energy and Combustion Science*, Vol. 35, 2009, pp. 231–244.

Zoulias, E.I., Lymberopoulos, N. "Techno-Economic Analysis of the Integration of Hydrogen Energy Technologies in Renewable Energy-Based Stand-Alone Power Systems." *Renewable Energy*, Vol. 32, 2007, pp. 680–696.

APPENDIX A

HOMER SENSITIVITY RESULTS

FC Cap. Mult.	Elec. Cap. Mult.	2 Tank Ca Mult.	(icons)	PV (kW)	FC (kW)	Conv. (kW)	Elec. (kW)	H2 Tank (kg)	Initial Capital	Operating Cost ($/yr)	Total NPC	COE ($/kWh)	Ren. Frac.	Capacity Shortage	FC (hrs)
1.00	1.00	1.00		48	6	4.8	4.8	1.00	$ 181,535	14,745	$ 370,028	2.130	1.00	0.02	4,777
1.00	1.00	0.75		48	6	4.8	4.8	1.00	$ 176,376	14,745	$ 364,870	2.100	1.00	0.02	4,777
1.00	1.00	0.50		48	6	4.8	4.8	1.00	$ 171,217	14,745	$ 359,711	2.071	1.00	0.02	4,777
1.00	1.00	0.25		36	6	4.8	4.8	1.63	$ 156,184	15,446	$ 353,636	2.039	1.00	0.02	4,859
1.00	0.75	1.00		36	6	4.8	6.0	1.00	$ 165,410	14,969	$ 356,766	2.060	1.00	0.02	4,839
1.00	0.75	0.75		36	6	4.8	6.0	1.00	$ 160,251	14,969	$ 351,607	2.030	1.00	0.02	4,839
1.00	0.75	0.50		36	6	4.8	6.0	1.00	$ 155,092	14,969	$ 346,449	2.000	1.00	0.02	4,839
1.00	0.75	0.25		36	6	4.8	6.0	1.00	$ 149,934	14,969	$ 341,290	1.970	1.00	0.02	4,839
1.00	0.50	1.00		36	6	4.8	6.0	1.00	$ 150,410	14,969	$ 341,766	1.973	1.00	0.02	4,839
1.00	0.50	0.75		36	6	4.8	6.0	1.00	$ 145,251	14,969	$ 336,607	1.943	1.00	0.02	4,839
1.00	0.50	0.50		36	6	4.8	6.0	1.00	$ 140,092	14,969	$ 331,449	1.914	1.00	0.02	4,839
1.00	0.50	0.25		36	6	4.8	6.0	1.00	$ 134,934	14,969	$ 326,290	1.884	1.00	0.02	4,839
1.00	0.25	1.00		36	6	4.8	6.0	1.00	$ 135,410	14,969	$ 326,766	1.887	1.00	0.02	4,839
1.00	0.25	0.75		36	6	4.8	6.0	1.00	$ 130,251	14,969	$ 321,607	1.857	1.00	0.02	4,839
1.00	0.25	0.50		36	6	4.8	6.0	1.00	$ 125,092	14,969	$ 316,449	1.827	1.00	0.02	4,839
1.00	0.25	0.25		36	6	4.8	6.0	1.00	$ 119,934	14,969	$ 311,290	1.797	1.00	0.02	4,839
0.75	1.00	1.00		48	6	4.8	4.8	1.00	$ 166,535	14,745	$ 355,028	2.044	1.00	0.02	4,777
0.75	1.00	0.75		48	6	4.8	4.8	1.00	$ 161,376	14,745	$ 349,870	2.014	1.00	0.02	4,777
0.75	1.00	0.50		48	6	4.8	4.8	1.00	$ 156,217	14,745	$ 344,711	1.984	1.00	0.02	4,777
0.75	1.00	0.25		36	6	4.8	4.8	1.63	$ 141,184	15,446	$ 338,636	1.953	1.00	0.02	4,859
0.75	0.75	1.00		36	6	4.8	6.0	1.00	$ 150,410	14,969	$ 341,766	1.973	1.00	0.02	4,839
0.75	0.75	0.75		36	6	4.8	6.0	1.00	$ 145,251	14,969	$ 336,607	1.943	1.00	0.02	4,839
0.75	0.75	0.50		36	6	4.8	6.0	1.00	$ 140,092	14,969	$ 331,449	1.914	1.00	0.02	4,839
0.75	0.75	0.25		36	6	4.8	6.0	1.00	$ 134,934	14,969	$ 326,290	1.884	1.00	0.02	4,839
0.75	0.50	1.00		36	6	4.8	6.0	1.00	$ 135,410	14,969	$ 326,766	1.887	1.00	0.02	4,839
0.75	0.50	0.75		36	6	4.8	6.0	1.00	$ 130,251	14,969	$ 321,607	1.857	1.00	0.02	4,839
0.75	0.50	0.50		36	6	4.8	6.0	1.00	$ 125,092	14,969	$ 316,449	1.827	1.00	0.02	4,839
0.75	0.50	0.25		36	6	4.8	6.0	1.00	$ 119,934	14,969	$ 311,290	1.797	1.00	0.02	4,839
0.75	0.25	1.00		36	6	4.8	6.0	1.00	$ 120,410	14,969	$ 311,766	1.800	1.00	0.02	4,839
0.75	0.25	0.75		36	6	4.8	6.0	1.00	$ 115,251	14,969	$ 306,607	1.770	1.00	0.02	4,839
0.75	0.25	0.50		36	6	4.8	6.0	1.00	$ 110,092	14,969	$ 301,449	1.740	1.00	0.02	4,839
0.75	0.25	0.25		36	6	4.8	6.0	1.00	$ 104,934	14,969	$ 296,290	1.711	1.00	0.02	4,839
0.50	1.00	1.00		48	6	4.8	4.8	1.00	$ 151,535	14,745	$ 340,028	1.957	1.00	0.02	4,777
0.50	1.00	0.75		48	6	4.8	4.8	1.00	$ 146,376	14,745	$ 334,870	1.928	1.00	0.02	4,777
0.50	1.00	0.50		48	6	4.8	4.8	1.00	$ 141,217	14,745	$ 329,711	1.898	1.00	0.02	4,777
0.50	1.00	0.25		36	6	4.8	4.8	1.63	$ 126,184	15,446	$ 323,636	1.866	1.00	0.02	4,859
0.50	0.75	1.00		36	6	4.8	6.0	1.00	$ 135,410	14,969	$ 326,766	1.887	1.00	0.02	4,839
0.50	0.75	0.75		36	6	4.8	6.0	1.00	$ 130,251	14,969	$ 321,607	1.857	1.00	0.02	4,839
0.50	0.75	0.50		36	6	4.8	6.0	1.00	$ 125,092	14,969	$ 316,449	1.827	1.00	0.02	4,839
0.50	0.75	0.25		36	6	4.8	6.0	1.00	$ 119,934	14,969	$ 311,290	1.797	1.00	0.02	4,839
0.50	0.50	1.00		36	6	4.8	6.0	1.00	$ 120,410	14,969	$ 311,766	1.800	1.00	0.02	4,839
0.50	0.50	0.75		36	6	4.8	6.0	1.00	$ 115,251	14,969	$ 306,607	1.770	1.00	0.02	4,839
0.50	0.50	0.50		36	6	4.8	6.0	1.00	$ 110,092	14,969	$ 301,449	1.740	1.00	0.02	4,839
0.50	0.50	0.25		36	6	4.8	6.0	1.00	$ 104,934	14,969	$ 296,290	1.711	1.00	0.02	4,839
0.50	0.25	1.00		36	6	4.8	6.0	1.00	$ 105,410	14,969	$ 296,766	1.713	1.00	0.02	4,839
0.50	0.25	0.75		36	6	4.8	6.0	1.00	$ 100,251	14,969	$ 291,607	1.684	1.00	0.02	4,839
0.50	0.25	0.50		36	6	4.8	6.0	1.00	$ 95,092	14,969	$ 286,449	1.654	1.00	0.02	4,839
0.50	0.25	0.25		36	6	4.8	6.0	1.00	$ 89,934	14,969	$ 281,290	1.624	1.00	0.02	4,839
0.25	1.00	1.00		48	6	4.8	4.8	1.00	$ 136,535	14,745	$ 325,028	1.871	1.00	0.02	4,777
0.25	1.00	0.75		48	6	4.8	4.8	1.00	$ 131,376	14,745	$ 319,870	1.841	1.00	0.02	4,777
0.25	1.00	0.50		48	6	4.8	4.8	1.00	$ 126,217	14,745	$ 314,711	1.812	1.00	0.02	4,777
0.25	1.00	0.25		36	6	4.8	4.8	1.63	$ 111,184	15,446	$ 308,636	1.780	1.00	0.02	4,859
0.25	0.75	1.00		36	6	4.8	6.0	1.00	$ 120,410	14,969	$ 311,766	1.800	1.00	0.02	4,839
0.25	0.75	0.75		36	6	4.8	6.0	1.00	$ 115,251	14,969	$ 306,607	1.770	1.00	0.02	4,839
0.25	0.75	0.50		36	6	4.8	6.0	1.00	$ 110,092	14,969	$ 301,449	1.740	1.00	0.02	4,839
0.25	0.75	0.25		36	6	4.8	6.0	1.00	$ 104,934	14,969	$ 296,290	1.711	1.00	0.02	4,839
0.25	0.50	1.00		36	6	4.8	6.0	1.00	$ 105,410	14,969	$ 296,766	1.713	1.00	0.02	4,839
0.25	0.50	0.75		36	6	4.8	6.0	1.00	$ 100,251	14,969	$ 291,607	1.684	1.00	0.02	4,839
0.25	0.50	0.50		36	6	4.8	6.0	1.00	$ 95,092	14,969	$ 286,449	1.654	1.00	0.02	4,839
0.25	0.50	0.25		36	6	4.8	6.0	1.00	$ 89,934	14,969	$ 281,290	1.624	1.00	0.02	4,839
0.25	0.25	1.00		36	6	4.8	6.0	1.00	$ 90,410	14,969	$ 281,766	1.627	1.00	0.02	4,839
0.25	0.25	0.75		36	6	4.8	6.0	1.00	$ 85,251	14,969	$ 276,607	1.597	1.00	0.02	4,839
0.25	0.25	0.50		36	6	4.8	6.0	1.00	$ 80,092	14,969	$ 271,449	1.567	1.00	0.02	4,839
0.25	0.25	0.25		36	6	4.8	6.0	1.00	$ 74,934	14,969	$ 266,290	1.537	1.00	0.02	4,839

Figure 41: Sensitivity Results from the HOMER Model

APPENDIX B

MATLAB SCRIPT FOR SOLAR PV ARRAY

```matlab
close all

clear all

clc


filename = input('To input weather data input the filename including
the extension: ','s');

[X,Y] = xlsread('WeatherTest.xlsx');

%data imported from weather file includes

% temp

% solar azimuth and zenith

% normal solar irradiation

Ta = X(:,1); % Ta is ambient temp

Tref = 298.15; % Tref is standard testing temp 25 deg. C

SAdeg = X(:,3);

SArad = SAdeg*pi/180;

SZdeg = X(:,2);

SZrad = SZdeg*pi/180;

Gt = X(:,4); %solar irradiation

%dust deposition for now will remain constant at 0 for now

Aj = 0.06; %Aj is coefficient related to local dust type

DD = 0; %DD is amount of dust deposited on panel in [g/m^2]


%Entering Data on Solar Panel

TC = input('From the data sheet for your solar panel\nenter the
temperature coefficient: ');

uref = input('\nenter the reference efficiency: ');

PA = input('\nenter the effective area of 1 solar panel in meters
squared: ');
```

```matlab
NP = input('\nenter the number of solar panels used: ');

% k is related to mounting of solar panel

k = input('\nBased on the below table enter a value\nfor the mounting
coefficient\nwell cooled k = 0.02\nfree standing k = 0.0208\nflat on
roof k = 0.026\nnot so well cooled k = 0.0342\ntransparent PV k =
0.0455\nFacade Integrated k = 0.0538\non sloped roof k = 0.0563\n');

PAdeg = input('\nEnter the Azimuth Angle of the panel in degrees: ');

PArad = PAdeg*pi/180;

PZdeg = input('\nEnter the Zenith angle of the panel in degrees: ');

PZrad = PZdeg*pi/180;

upc = 1; %power conditioner efficiency set to 1 for now

%Enter data for load, electrolyzer, and fuel cell

Load = input('\nEnter the load expected in watts: ');

Current= Load*0.045-0.332;

Elec_power = input('\nFrom the data sheet for the electrolyzer\nEnter
the power requirement for the electrolyzer in watts: ');

Elec_Flow = input('\Enter the flow rate for the electrolyzer in cc/min:
');

simOut = sim('SolarFLux2'); %calculate solar flux vector

simOut = sim('SolarModel3'); %calculate solar power generated vector

simOut = sim('loadcalc'); %calculate FC truth table, and electrolyzer
flow rate vectors

H2_storage = []; %initialize hydrogen stor{age vector

H2_pressure = []; %initialize hydrogen pressure vector

FC_flow_rate = []; %initialize FC flow rate vector

i = 1;

H2_pressure(:,i) = 0; %initial pressure in tank is 0

H2_storage(:,i) = 0; %initial amount of H2 stored is 0
```

```matlab
simOut = sim('pressure2'); %run simulink model

FC_flow_rate(:,i) = e; %save new flow rate for fuel cell

H2_storage(:,i+1) = d; %save new amount of H2 stored

H2_pressure(:,i+1) = f; %save new H2 pressure

x = length(powerout);

for i = 2:x-1

    simOut = sim('flowrate'); %run flow rate simulink model

    FC_flow_rate(:,i) = e; %save new flow rate for fuel cell

    H2_storage(:,i+1) = d; %save new amount of H2 stored

end

for i = 2:x

    simOut = sim('pressure3'); %run pressure simulink model

    H2_pressure(:,i) = f; %save new H2 pressure

end
```

APPENDIX C

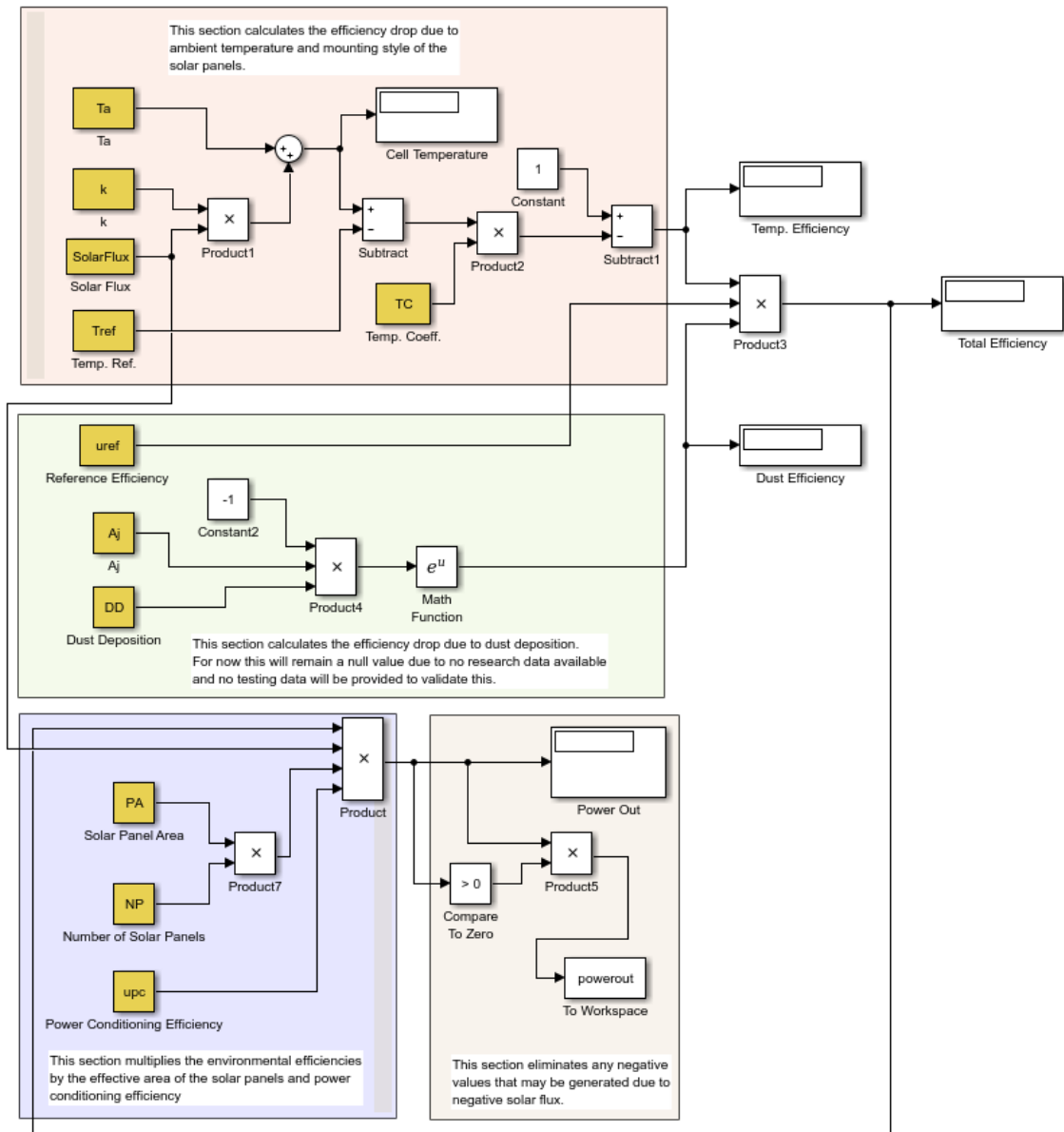SIMULINK MODEL OF THE SOLAR PV ARRAY

Figure 42: Simulink Solar Model
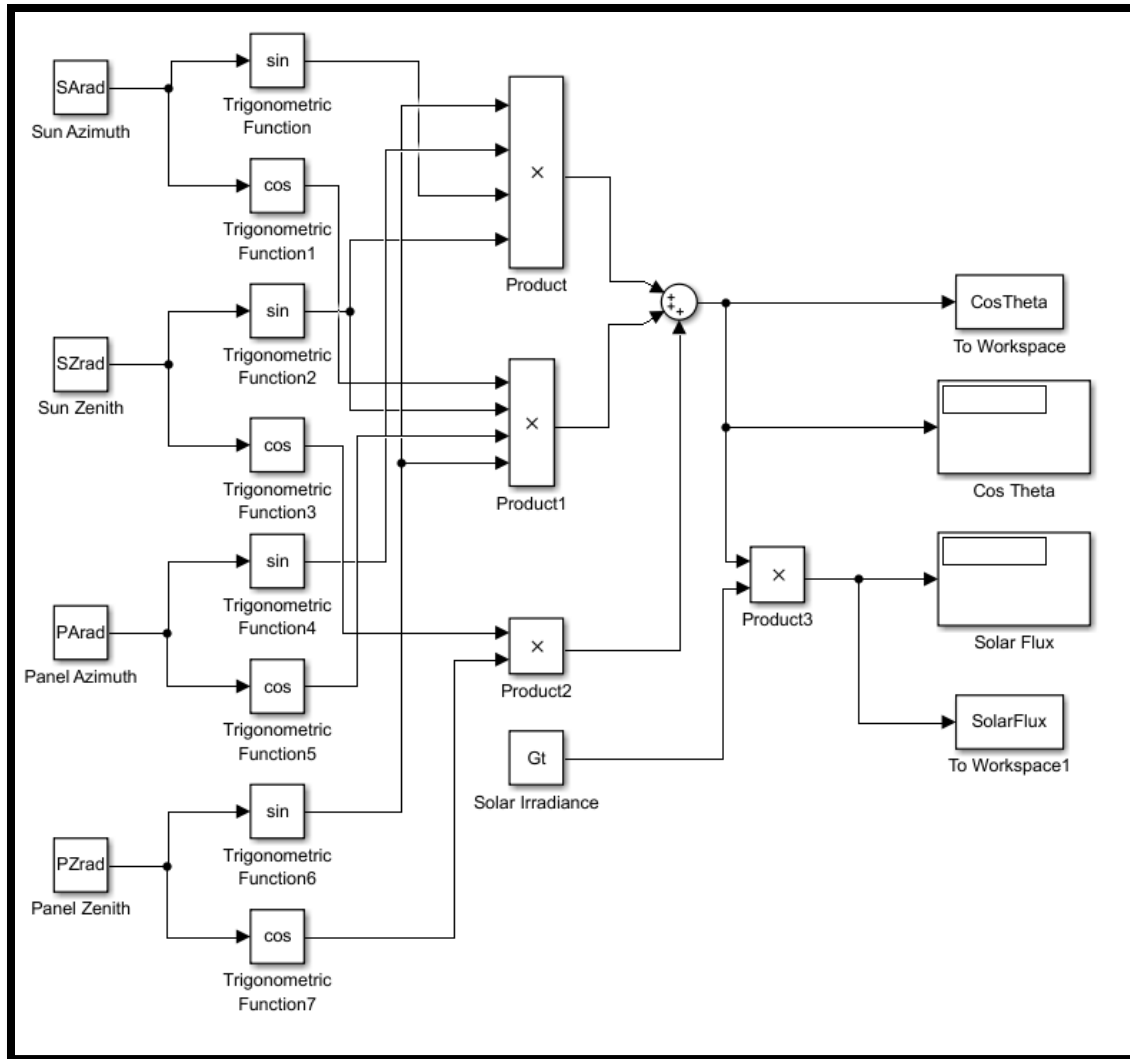
APPENDIX D

SIMULINK MODEL OF THE SOLAR FLUX

Figure 43: Simulink Solar Flux Model

APPENDIX E

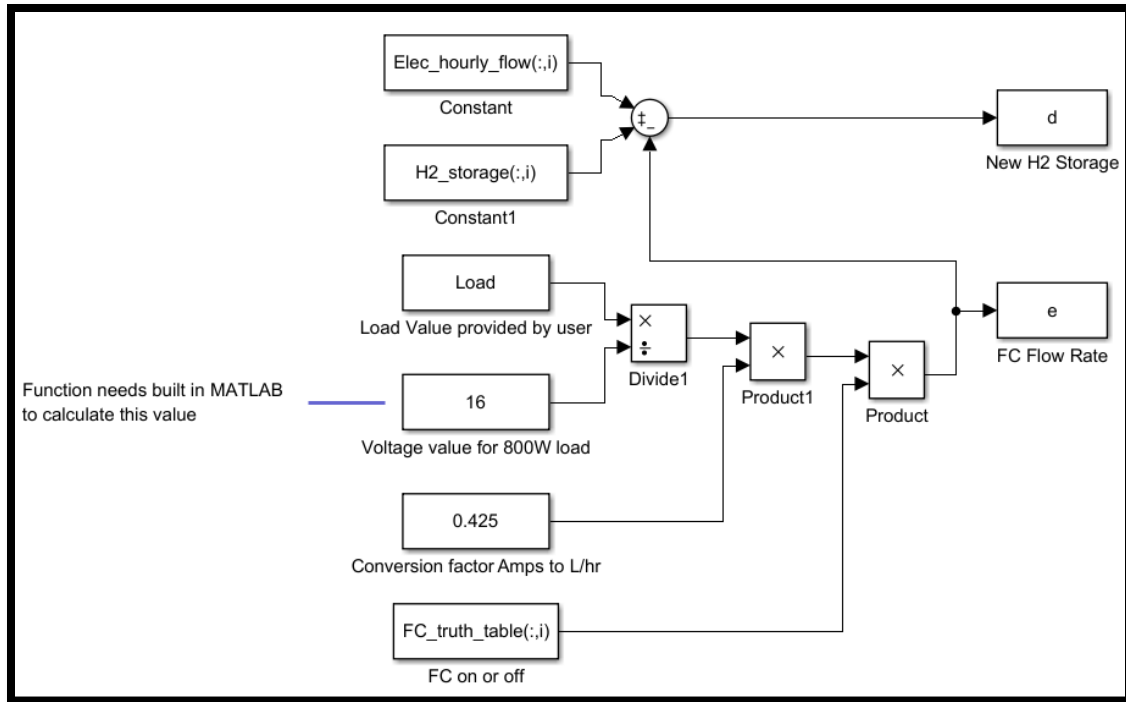SIMULINK MODEL OF THE HYDROGEN FLOW RATE

Figure 44: Hydrogen Flow Rate of the System

APPENDIX F

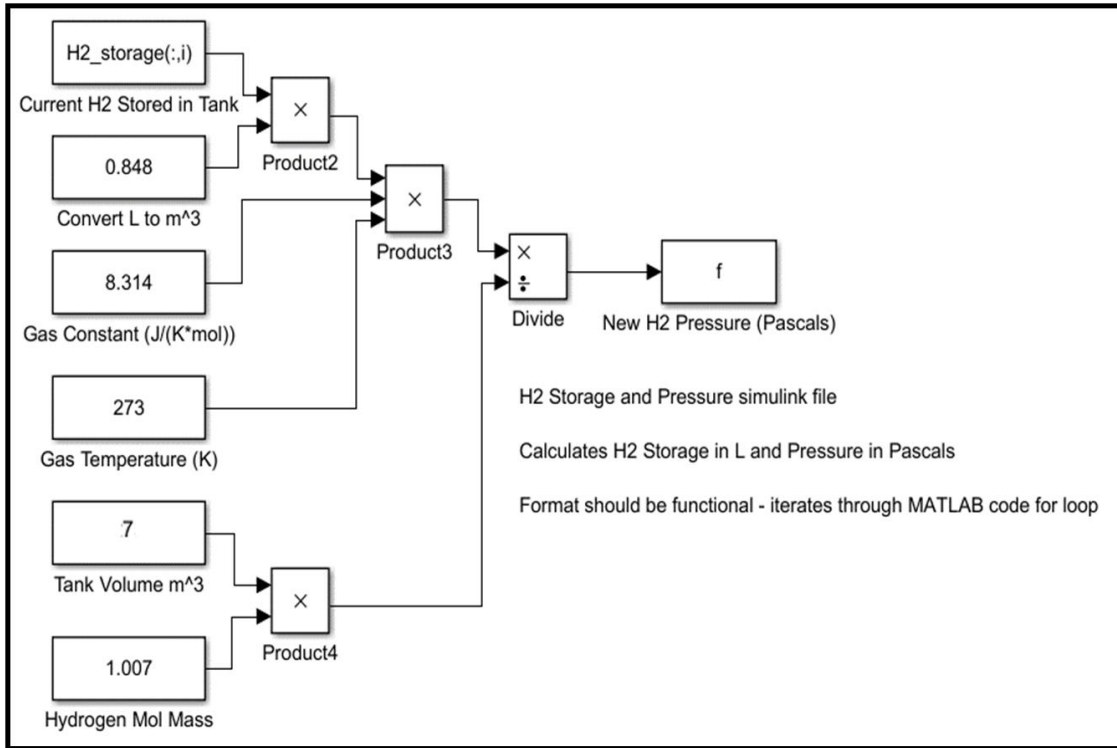SIMULINK MODEL OF THE PRESSURE SUB-MODEL

Figure 45: MH Storage and Pressure Sub-model

BIOGRAPHICAL SKETCH

The author of the work presented above has concluded his educational experience with the publication of this thesis. He attended Arizona State University, Polytechnic Campus, for both his four-year Bachelors of Science degree in Electrical Systems Engineering and Masters of Science degree in General Engineering. In combination with the required courses for the university degrees, he was involved in two additional projects which were the ASU EcoCAR3 project, sponsored by General Motors, the US Department of Energy, and Argonne National Laboratories, and the Solar H2 Cycle Energy project sponsored by the Salt River Project. The four-year ASU EcoCAR3 project was tasked with developing a Hybrid 2016 Chevrolet Camaro, and he was the Lead Electrical Engineer for one and a half years during the project. After graduating from ASU, he was hired by General Motors as a Power Systems Engineer.